THE CONSTITUTION OF THE GOLD-CADMIUM SYSTEM.

A thesis submitted for the degree of Doctor of Philosophy.

by

V.G. Rivlin, B.A.,

Balliol College.



OXFORD,

August, 1961.

C O N T E N T S

		PAGE
ABSTRACT	.....	(i)
INTRODUCTION		
1.	OBJECT OF WORK	1
2.	SUMMARY OF THE DIAGRAM	1
3.	PHASES IN THE RANGE 0-50 ATOMIC % CADMIUM	
	(a) The β'-Phase	7
	(b) The β'-Phase Boundaries	7
	(c) The β'-Phase Transformation	8
	(d) The α_2-Phase	10
	(e) The α_1-Phase	11
	(f) The α-Phase	13
EXPERIMENTAL METHODS		
1.	THERMAL ANALYSIS	15
2.	PREPARATION OF INGOTS	
	(a) Melting	17
	(b) Heat-Treatment	20
3.	METALLOGRAPHY	
	(a) Chemical Etching	21
	(b) Electrolytic Polishing And Etching	21
4.	X-RAY METHODS	
	(a) Preparation of Powders	22
	(b) Room-Temperature X-Ray Photographs	24
	(c) High-Temperature X-Ray Specimens	24
	(d) The High-Temperature Camera	26
	(e) Calibration Of The High-Temperature Camera ...	28
	(f) High-Temperature X-Ray Films	30
RESULTS		
1.	THE LIQUIDUS	32
2.	MICROSTRUCTURES OF COOLING CURVE INGOTS	40
3.	THE α-SOLIDUS	44
4.	INTERMEDIATE PHASES	
	The β'-Phase	51
	(a) The α_3-Phase And The β'-Phase Transformations	51
	(b) The $\alpha_2 + \beta'$ Region	54
	(c) The $(\alpha_2 + \beta')\beta'$ Boundary	54
	(d) The $\beta'(\beta' + \gamma)$ Boundary	56
	(e) High-Temperature Films Of The β'-Phase ...	57
	The α'_2-Phase	61
	(a) The $\alpha_2(\alpha_2 + \beta')$ Boundary	61
	(b) The $\alpha + \alpha_2$ Boundaries	64
	(c) Sharp And Diffuse Reflections In α_2 Films ...	70
	The α_1-Phase	72
	(a) The Boundaries Of The α_1-Phase	75
	(b) The α'-Phase	75
	(c) Ordering In The α_1-Phase	79

PAGE

DISCUSSION

1. THE LIQUIDUS AND SOLIDUS
   (a) The Electrochemical Factor 80
   (b) The Liquidus In Systems of Ag and Au ... 82
   (c) The α-Liquidus In Some Au Systems ... 84
   (d) α-Solidus : α-Liquidus Equilibria ... 88

2. INTERMEDIATE PHASES
   (a) The Au-Cd β'-Phase 90
   (b) The α_2-Phase 93
      (i) Stacking Faults 93
      (ii) Energy Considerations and Stacking Faults 96
      (iii) The Peritectic-Eutectic Reaction ... 98
      (iv) Stacking Faults And The $(\alpha + \alpha_2)/\alpha_2$ Boundary 100
      (v) Cavities In α_2-Alloys 101
   (c) 3/2 Electron Compounds In Gold Alloys ... 104
      (i) Ordering In The b.c.c. Phase ... 104
      (ii) ζ-Phases 105
      (iii) The Occurrence Of The α_2-Phase ... 107
3. SOLID SOLUBILITY IN GOLD ALLOYS 109

APPENDIX 118

PURITY OF MATERIALS 126

REFERENCES 127

LIST OF FIGURES 130

LIST OF PLATES 131

LIST OF TABLES 132

ACKNOWLEDGMENTS 133

ABSTRACT

The constitution of the gold-rich region of the gold-cadmium diagram has been studied by means of thermal analysis, optical microscopy and Debye-Scherrer X-ray films of high-temperature and quenched specimens. Five phases have been identified, α face-centred cubic, α_2 close-packed hexagonal, β' ordered body-centred cubic as well as two phases at low temperatures, α_1 face-centred tetragonal and α' face-centred cubic.

The liquidus and solidus relationships have been found for the α, α_2 and β -phases by thermal analysis, the results being in good agreement with the X-ray and microscopical results. A eutectic horisontal representing the reaction $\alpha_2 + \beta' \rightleftharpoons$ liquid is found at 626.5°C. The β' -phase maximum is only just detectable, rising to 629°C. From the X-ray evidence a peritectic horizontal, corresponding to the reaction α + liquid $\rightleftharpoons \alpha_2$, is believed to exist between 633°C and the eutectic temperature; the thermal arrests place it at 627°C.

The $\alpha_2(\alpha_2 + \beta')$ and $(\alpha_2 + \beta')\beta'$ boundaries have been determined microscopically. Only a few experimental points have been obtained for the $\alpha + \alpha_2$ boundaries but the high-temperature X-ray films indicate that the boundaries of previous workers are in need of revision. The maximum solid solubility of cadmium in gold is 34 atomic % at 620°C to 630°C.

The β' -phase narrows in composition range as temperature falls. The high-temperature X-ray films showed superlattice lines up to 624°C and an estimate of the degree of ordering at 620°C suggests the β' -phase to be about 90% ordered at this temperature.

The α_1-phase at 23 atomic % cadmium is disordered face-centred tetragonal when photographed at elevated temperatures. The

absence of superlattice lines is contrary to previous work which describes the unit cell in quenched α_1 specimens as ordered (an anti-phase domain structure based on four fundamental tetragonal cells). It is conjectured that quenched α_1 specimens may be ordered but as temperature is increased the long-range order is broken down, producing small domains each highly ordered.

At about 25 atomic % cadmium the structure is face-centred cubic. A new phase α' is proposed at this composition. A tentative diagram of the Au_3Cd region, linking the four phases α, α_1, α' and α_2 is suggested with peritectoid horizontals at 412°C and 407°C.

Factors affecting the behaviour of the liquidus and solidus of the gold-cadmium system are revealed by comparing with other systems of copper, silver and gold. The comparisons show the influence of the electron concentration, modified by lattice distortions and the electrochemical factor.

The α_2-phase (close-packed hexagonal) is shown to contain numerous stacking faults; this may be a consequence of the α (face-centred cubic) and α_2-phases having nearly equal free energies. The occurrence of the 3/2 electron compounds in gold is discussed and suggestions are given for their bearing on maximum solid solubilities in gold.

INTRODUCTION.

1. OBJECT OF WORK.

The work has been concerned with the gold-cadmium system in the range 0-55 atomic % cadmium. This system has attracted a good deal of attention in the past. The main features of the diagram are produced from Hansen (1) in fig.1. Conflicting claims based mainly on X-ray work have been put forward for the gold-rich part of the diagram and, as can be seen from fig.1., not all the boundaries have been determined in this region. The present work on the diagram was undertaken with the aim of clearing up existing uncertainties.

2. SUMMARY OF THE DIAGRAM.

From the point of view of previous work the diagram can be divided in two parts separated by the phase centred about 50 atomic % cadmium, i.e. the β-phase: 1. The range 0-62 atomic % and 2. The range 52-100 atomic %. The latter part was dealt with by P.J. Durrant (2) who, by means of thermal analysis and optical microscopy, produced a complete diagram that has remained almost unaltered to this day and is incorporated in fig.1. This shows the solid solubility of gold in cadmium to be limited, extending to a maximum of 3.5 atomic % gold. The intermediate phases γ and ϵ separate the primary solid solution from the β-phase. Durrant demonstrated the existence of high temperature modifications of the γ-phase, δ' and δ. The ϵ-phase was later suspected as a result of E.M.F. investigations by Ölander (3) of having a low temperature modification, ϵ'. The transition temperature 269°C for the change $\epsilon' \longrightarrow \epsilon$ possibly represents a change from an ordered to a disordered structure (4). Durrant found two eutectic horizontals, one at 309°C for the reaction ϵ + primary solid solution $\rightleftharpoons$ liquid and one at 496°C where the reaction is $\epsilon + \delta \rightleftharpoons$ liquid. The ϵ-liquidus rises to a

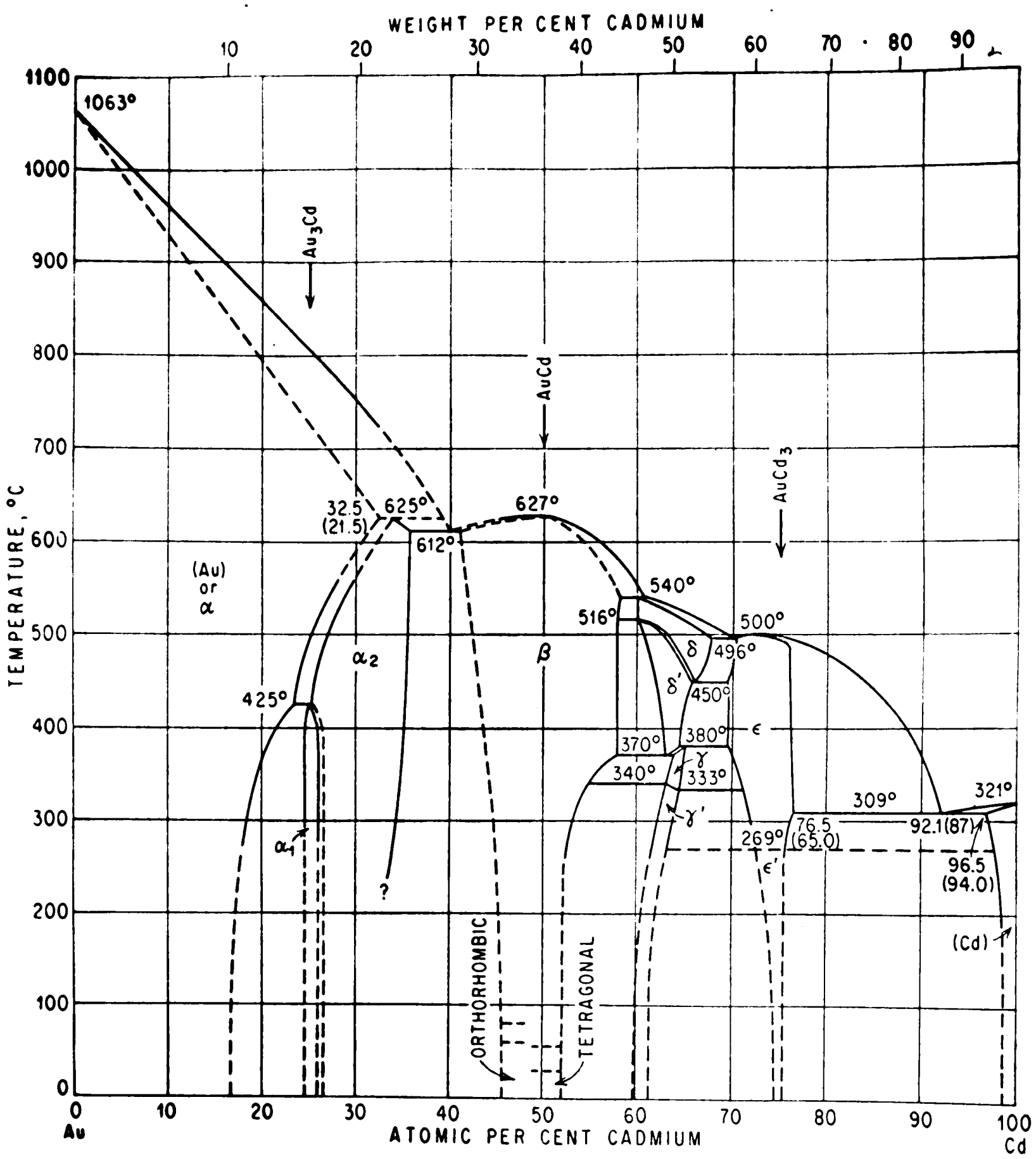

Au-Cd

Fig.1. Hansen, 1958.

flat maximum at 500°C, only 4° above the 496°C eutectic horizontal. The δ -liquidus rises to a peritectic horizontal at 540°C.

Previous investigators have reported six phases altogether in the range 0-55 atomic % cadmium. For reference they are listed below and a detailed discussion follows. All atomic percentages refer to cadmium unless otherwise stated.

α : Face-centred cubic (f.c.c.) Primary solid solution of cadmium in gold.

α_1 : Ordered face-centred tetragonal (f.c.tetragonal or f.c.t.) Narrow composition limits, centred about 25 atomic %.

α'' : Ordered face-centred cubic, between α and α_2, a high-temperature phase.

α_2 : Close-packed hexagonal (c.p.h.) c/a ratio about 1.64, centred about the composition Au_2Cd. Analogous to the ζ -phases in other IB systems but the designation α_2 is retained in this thesis.

α_3 : Provisionally allotted the structure hexagonal rhombohedral. Between 41 and 47 atomic % at 600°C and 45 and 49 atomic % at 260°C.

β' : Ordered body-centred cubic (b.c.c.) In the equi-atomic region, undergoing a transformation to an orthorhombic or tetragonal structure below 100°C.

In the remainder of the thesis the above structures are referred to by their abbreviations, e.g. f.c.c. for face-centred cubic.

Early work on the gold-cadmium system is summarised in a diagram by Ölander (3), fig.2. The α-liquidus, the β'-liquidus and the 612° eutectic horizontal shown in this diagram are due to Saldau (5) who relied on thermal analysis and resistivity experiments. The α - and β'-phases are regarded as being in equilibrium with each other at all temperatures. The eutectic point is at 43 atomic % and the β'-liquidus has a maximum at 627°C. Ölander, like Saldau, found the α-phase to have a low-temperature modification at the composition Au_3Cd, but unlike Saldau he gave it an upper temperature limit of 420°C whereas Saldau claimed two modifications, one below 135°C and one between 430° and 135°C. Ölander's electrolytic measurements also gave values for the $\alpha + \beta'$ boundaries. His X-ray experiments (6) had already shown that the β'-phase transforms to a low-temperature modification with an orthorhombic structure. The electrochemical results (3) showed an effect in the β'-phase at 267°C and this temperature was believed to be the transition temperature for the change b.c.c. $\rightleftharpoons$ orthorhombic.

F.A. Owen et al. (7, 8) made a careful survey of the gold-cadmium system in the range 0–62 atomic % by means of room temperature X-ray photographs of quenched powder specimens. Their final results are summarised in fig.3. They show 1, The α- and α_1- phase boundaries. 2, Two new phases α_2 and α_3 with corresponding boundaries. The α_1 phase was found to be f.c. tetragonal but no superlattice lines were observed. The β'-phase is drawn with a much narrower range than in previous diagrams. Superlattice lines were found for this phase.

The determination of the boundaries by Owen was carried out where possible by the lattice parameter method otherwise by bracketing.

The α_2-phase was found by Owen to be c.p.h. The lines attributed to an α_3-phase gave some difficulty but it was eventually decided that because a large number of lines fitted a hexagonal rhombohedral chart, the unit cell could be regarded as a special case of a face centred rhombohedron. Apparently Owen and Roberts were unaware of Öländer's work on the β'-phase transformation (6) and the bearing it could have on their α_3-phase. They did find however that after annealing and quenching, some β'-phase alloys were unstable at room temperature. This led Owen (8) to remark that a high-temperature X-ray investigation would be desirable before accepting the new boundaries.

Such an investigation was soon carried out by Bystrőm and Almin (9). They produced a new diagram (fig. 1). Besides high temperature work on the β'-phase, they repeated Owen's work on the α-phases using quenched X-ray powders and carried out dilatometric experiments.

The high-temperature work gave no evidence of the α_3-phase. Instead it showed that the β'-phase underwent a transformation at $85 \pm 15^{\circ}C$ to the low-temperature orthorhombic structure, a conclusion subsequently confirmed in the numerous investigations carried out on the β'-phase. Bystrőm and Almin therefore considered the β'-phase to be in equilibrium with the α_2-phase.

The dilatometric experiments gave a value of $64 \pm 6^{\circ}C$ for the β'-phase transformation b.c.c. $\rightleftharpoons$ orthorhombic. They also showed a slight effect at $290^{\circ}C$ which is to be compared with the effect reported at $269^{\circ}C$ by Öländer. But the X-ray photographs taken at elevated temperatures failed to reveal any structural change corresponding to this effect and its significance is unknown. Work on the modulus of elasticity (4) gave the temperature as $275^{\circ}C$; on the other hand electrical resistivity measurements (10) showed no effects at these temperatures.

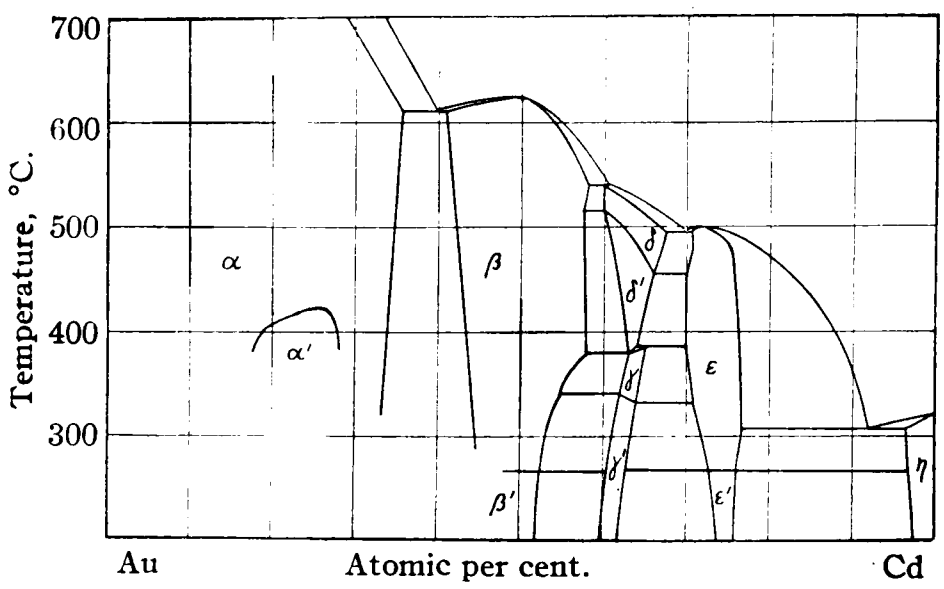

Phase diagram of the gold–cadmium system.

Fig.2. Ölander, 1932.

the Gold–Cadmium Alloy System

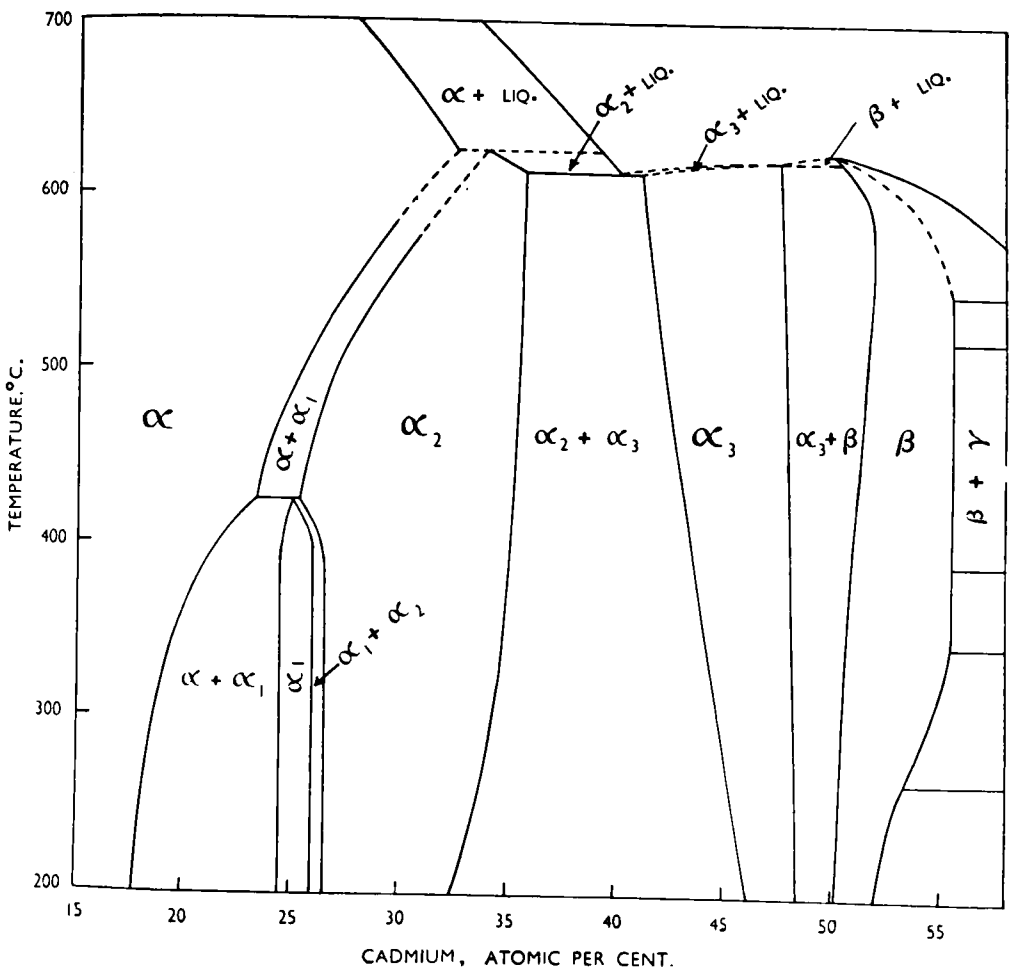

FIG. 2.—Phase Diagram of the Gold–Cadmium Alloy System, up to Approx. 60 Atomic Per Cent. Cadmium, According to Owen, Roberts, and Rees.

Fig.3. Owen et.al. 1940, 1941.

Bystrom and Almin did not take high-temperature photographs of the α -phases to check their results with quenched specimens. They slightly altered the positions of the boundaries (fig.4) and introduced another α -phase labelled α " and described as ordered f.c.c.

The intermediate phases on the gold-rich side of the diagram are now described below in detail.

3. PHASES IN THE RANGE 0-50 ATOMIC % CADMIUM

(a) The β' -phase

The β' -phase is ordered body-centred cubic. Gold atoms are regarded as being at the corners of the unit cell and cadmium atoms at the centre or vice-versa. It is not known whether the ordered structure persists in the adjacent two-phase regions but the results available from scanning experiments with a Norelco diffractometer (15 ii) suggests that the structure becomes less ordered, the further one gets from the composition 50 atomic %. No high temperature X-ray data are available for the upper limit of the ordered form of β. Bystrom and Almin (9) were unable to take films above 400°C because their specimens were in wire form and not enclosed in capsules and this gave rise to excessive cadmium evaporation above 400°C. Kubaschewski (11) obtained some calorimetric data on the heat content of the β -phase before and after melting and concluded that the β -phase was disordered below the melting point.

(b) The β' -Phase Boundaries

The β' ($\beta' + \gamma$) boundary in fig.1 is due to Owen (8). It was measured below 310°C by the lattice parameter method and between 310°C and 590°C by bracketing because the $\beta' + \gamma$ alloys did not give X-ray lines at high angles sufficiently sharp for measurement between 310° and 590°C. The boundary

is placed between 55 and 56 atomic % from 570° to 320°C and bends towards the gold-rich axis below 310°C. This is at a rather lower cadmium content than Durrant's boundary; Durrant however had based his boundary solely on the evidence of the absence of thermal arrests below 60 atomic % cadmium.

Byström and Almin redetermined the $(\alpha_2 + \beta')\beta'$ boundary after they disproved the α_3-phase of Owen. They used the dimensions of the β' (orthorhombic) phase in quenched $\alpha_2 + \beta'$ alloys to fix this boundary parametrically. Results given are

°C	at.% Cd
200	47.5
400	44.8
550	44.8

A bend is revealed between 200° and 400°C. Ölander (3) had given two points for this boundary.

°C	at.% Cd
300	44.7
550	41.2

(c) The β'-Phase Transformation

A large amount of work has been done on the mechanism and products of this transformation (4, 9, 12, 13, 14, 15). The present position on the transformation is as follows.

On the gold-rich side of the β'-phase, at 47.5 atomic %, the ordered (CsCl) structure transforms on cooling to orthorhombic while at 50 atomic % a change to tetragonal structure occurs. The mechanism of transformation is a diffusionless process (12 iii) and the products are probably metastable.

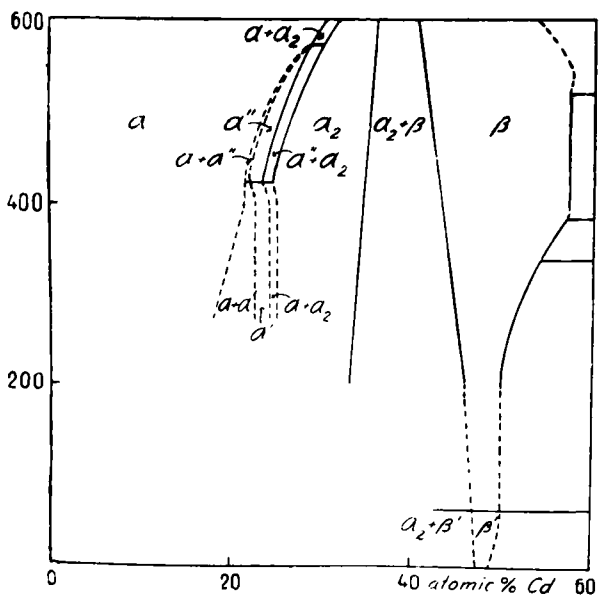

Phase diagram of the gold-rich part of the gold-cadmium system.

Fig.4. Byström and Almin, 1947.

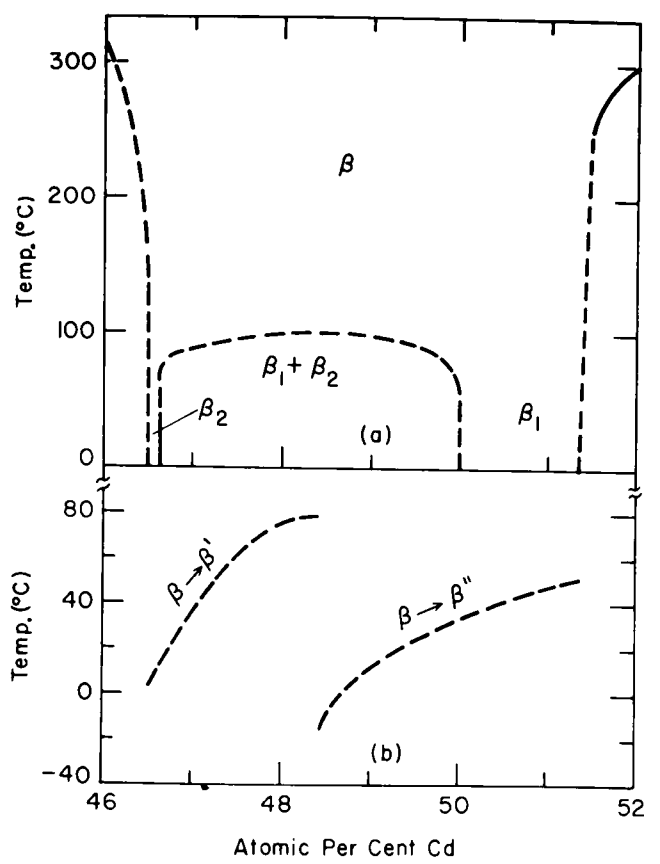

Fig. 5(*a*)—Proposed phase diagram in β-phase region. (*b*) Proposed transformation temperature dependence on the cadmium content.

Fig.5. The Au-Cd β -phase below 100°C, Birnbaum, 1959.

All changes have been recorded as taking place below 100°C. The change b.c.c. ⟶ orthorhombic occurs at about 60°C and the change b.c.c. ⟶ tetragonal at 30°C. Hysteresis has been observed. The transition temperatures and products have been shown to depend on the thermal history of the specimens (15). Specimens of composition 47.5 and 50 atomic % cadmium were given prolonged anneals at temperatures of 100°C or less in a Norelco diffractometer prior to cooling (15 ii). At 47.5 atomic % β' was found to give tetragonal as well as orthorhombic but at 50 atomic % β' never gives orthorhombic. A tentative diagram (fig.5) was drawn to account for the results. The two phases β_1 and β_2 have the CsCl structure but differ slightly in spacing.

(d) The α_2-Phase.

The existence of this c.p.h. phase was first noted by Owen et.al (7, 8) who made a careful determination of its composition limits between 574° and 220°C. In his diagram, Fig.3, which, apart from the α_3-phase, is the diagram accepted by Hansen in Fig.1., the α_2-phase is shown to extend from between 26 and 27 atomic % to 32 atomic % at low temperatures. The α_2 ($\alpha_2 + \beta'$) boundary (which Owen called the α_2 ($\alpha_2 + \alpha_3$)boundary) was determined twice by the lattice spacing method, the second determination being slightly to gold-rich side of the first but agreeing closely. It is nearly vertical. Owen extrapolated it to meet Baldau's 612° horizontal at 35.7 atomic %. The narrow $\alpha + \alpha_2$ region, also determined parametrically, slopes to the cadmium axis above 425°C. Above 574°C no data were obtained but the $\alpha + \alpha_2$ boundaries were extrapolated to meet a hypothetical peritectic at 625°C.

Bystrom and Almin (9) gave parameters for the c.p.h. cell which differ somewhat from Owen's. They attributed diffuse and weakened lines obeerved in films on the gold-rich

side of the α_2-phase to stacking faults. Owen makes no mention of diffuse lines in this part of the diagram.

Massalski (23) obtained lattice parameters for the α_2-phase in a diffractometer which suggest that while both c and a initially increase with increase in cadmium content, there is a decrease in c/a from a value greater than 1.633 to a value smaller than ideal. Massalski has also reported that some α_2-alloys appear, under the microscope, to be two-phase contrary to previous work. However, his published photograph suggests that the second phase was in fact a series of cavities. These cavities were encountered in the present work (Plate 6). Their occurrence is dealt with in the Discussion, Section 2b(iv).

(c) The α_1-Phase

That a low-temperature modification of the α-solid solution exists at Au_3Cd has been demonstrated several times. The high electrical conductivity observed by Haldau (5) suggested it was an ordered structure.

Köster and Schneider carried out damping and elastic moduli measurements on alloys of composition Au_3Cd, AuCd and $AuCd_3$. They report changes for Au_3Cd as follows

$$\alpha \xrightarrow{475^\circ C} \alpha_1 \qquad \xrightarrow{415^\circ C} \alpha_1'$$

The symbols used are those of Köster and Schneider. The transition at 415°C is marked by a pronounced effect in the curve relating elastic modulus with temperature. No such effect is seen at 475° but the change in the temperature coefficient is taken as evidence for it. The alloy was slowly cooled to room-temperature for the modulus experiments.

Alloys quenched from above 475°C were found microscopically to be extensively twinned. Those quenched from between 415 and 475°C showed martensitic markings. The same markings were observed in slow-cooled alloys.

It was possible to retain disordered α_1 and α_1' on quenching but a change to ordering on annealing between 75° and 325°C is observed. X-rays showed a slightly distorted f.c.tetragonal for the α_1-phase. Quench films of the α_1'-phase were ordered.

Owen and Roberts (7) made a careful survey of the gold-rich region, using quenched powders examined by means of X-rays. The ingots were made in steps of ½ atomic %. Three phases α, α_1 and α_2 emerge as a result of their work, with the structures and compositions given in the list on a previous page. The α_2-phase has been described already. According to Owen and Roberts there is only one modification of the α-phase with a disordered f.c.tetragonal structure. Its boundaries are as in fig.3. From their diagram it will be seen that they regard the upper limit of the α_1-phase as 425°C (and not 475°C as claimed by Köster and Schneider). This limit was determined by temperature bracketing with quenched powders. Their α_1'-phase is f.c. tetragonal with the c/a ratio in one-phase alloys changing from 1.0039 at 24.77 atomic % cadmium to 1.0029 at 25.5 atomic % cadmium. The $\alpha(\alpha+\alpha_1)$, $(\alpha+\alpha_1)\alpha_1$ and $\alpha_1(\alpha_1+\alpha_2)$ boundaries were boundaries were obtained by the lattice parameter method. An accurate determination of the $(\alpha_1+\alpha_2)\alpha_2$ boundary was not achieved in spite of a good deal of work being devoted to the problem. The results place it by bracketing between 26 and 27 atomic % and 400° and 350°C.

Bystrŏm and Almin (9) from quenching experiments made the α_1 region a little wider than did Owen and the $\alpha+\alpha_1$ region a little narrower. At 350°C their results are as follows.

At.% Cd.	20.2	22.8	24.6	25.3	25.9
	α	α_1	α_1	$\alpha_1+\alpha_2$	$\alpha_1+\alpha_2$

Their $\alpha(\alpha+\alpha_1)$ boundary extrapolates into the α one-phase region, contrary to thermodynamic prediction (16).

Unlike Owen and Roberts they discovered superlattice lines in their α_1-films. Their value for the c/a ratio is 1.008 at 22.8 atomic % cadmium, decreasing to 1.005 at 24.6 atomic % cadmium, a larger distortion than reported previously. From visual comparison of the X-ray lines they calculated the atom positions to be as follows.

1	Cd	000.
1	Au	$\frac{1}{2}\frac{1}{2}$0.
2	Au	0$\frac{1}{2}\frac{1}{2}$, $\frac{1}{2}$0$\frac{1}{2}$.

The appearance of superlattice lines in some alloys quenched from the α -region at about the composition Au_3Cd led Byström and Almin to postulate a new phase restricted to high temperatures (fig.4) denoted α".

The work of Hirabayashi and Ogawa (24), which has recently appeared, postulates a modified form of the diagram of Owen and Roberts (fig.15) based on resistometric and calorimetric measurements of slowly cooled alloys. The peritectoid is drawn at 412 $\pm$ 1°C and the α (α + α_1) boundary is found at a lower temperature than expected from Owen's diagram. Marked specific heat peaks at 26.9 and 28 atomic % cadmium are interpreted as showing that the (α_1 + α_2)α_2 boundary is not vertical as drawn by Owen. Their single crystal work gave a unit cell for Au_3Cd, based on four fundamental f.c.tetragonal cells, which is reproduced in fig.16. This cell was originally derived by Wegst and Schubert (25). According to Hirabayashi and Ogawa the disorder-order reaction is difficult to supress on quenching since faint superlattice reflections (110) are seen.

(f) The α-Phase

Lattice spacings were determined as in refs. 7 and 9, the results agreeing very well. The solid solubility limit was determined parametrically by Owen and Roberts using α + α_1, and α + α_2 alloys. The extrapolation of the α + α_2 boundaries to

meet a solidus boundary from the 612° horizontal suggested that there was a 625°C peritectic horizontal. No experimental evidence for the peritectic was available; it had to be assumed in order to accommodate the α_2-phase.

1. THERMAL ANALYSIS.

A simple crucible assembly, described below, was used for the thermal analysis of the system in the range 0 to 55 atomic % cadmium.

The crucible and lid were of graphite to minimise oxidation of cadmium. They were made by drilling solid graphite rods. The approximate dimensions of the crucible were 3 inches length and one inch diameter, inner diameter half an inch. The lid fitting tightly in the crucible was drilled centrally to take a stirrer and thermocouple sheath. The shape of the drill used to hollow out the crucible formed a conical depression at the bottom and fitting the sheath into the tip of the depression ensured that the hot junction of the thermocouple would be in the centre of the ingot (fig.6).

The stirrer and sheath were made of silica, the latter being 1/8 inch in diameter. A shallow depression was drilled round the hole admitting the stirrer to the crucible and a silica tube, $\frac{1}{4}$ inch in diameter fitted in the depression. This prevented asbestos wool from slipping into the crucible when the whole assembly was lagged with wool in the furnace.

Heating and cooling were obtained in a nichrome-wound electric resistance furnace, the power supply of which was controlled by a Variac transformer with an ammeter in circuit. The thermocouple, platinum-platinum/13% rhodium with the cold junction immersed in crushed ice and water in a Dewar flask, was calibrated by determining the freezing points of aluminium, zinc and tin. The calibration curve was checked regularly. Millivolt readings were obtained with a Tinsley potentiometer graduated in 0.5 mv steps. A mirror-and-scale galvanometer gave off-balance readings, the sensitivity being about 0.5 mv/25.0 cm. Tables published by the British Standards Institution for conversion of millivolt readings to temperatures gave a sensitivity of about 2°/cm. i.e. readings should be accurate to about 0.2°C.

For each cooling-curve the pure metals were weighed out in lump form. Prior to weighing both metals were pickled in dilute nitric

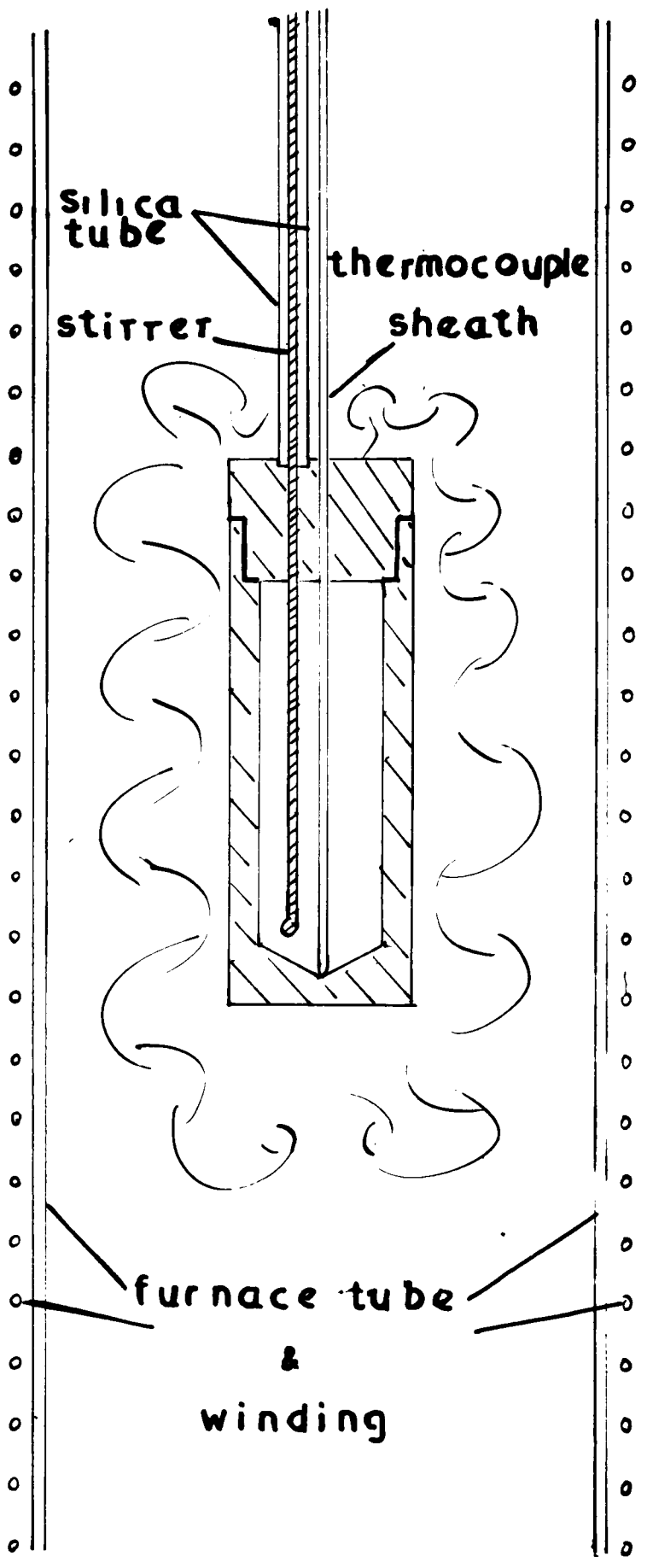

Fig.6. Thermal analysis crucible assembly.

acid, washed in water, ethyl alcohol, ether and dried. The weighed samples were placed in the crucible and covered with graphite powder. All ingots weighed about twenty grams. After microscopic examination all were analysed for gold and in some cases for cadmium as well. Analysis results together with details of thermal arrests, etc., are tabulated in Table 1. page 33.

One would expect that the reactivity and volatility of cadmium to be the main problem encountered. The analysis results show (i) only a slight cadmium loss, nearly always less than one atomic %. (ii) that where analyses were obtained for both metals the analysis totals varied between 99.90 and 100.23, i.e. very little graphite or other impurity was present. As a rule only cooling curves were tried for each ingot. This minimised cadmium loss, giving analytic compositions corresponding as closely as possible to the thermal arrests obtained on cooling. In a few cases cooling curves were checked by heating and gave good agreement (fig.7a). Supercooling was hardly ever observed.

2. PREPARATION OF INGOTS

(a) Melting

Ingots for microscopical and X-ray work were prepared in the range 10–55 atomic % cadmium. Each ingot was made in a sealed silica tube, 5 mm. bore, from which air had been evacuated. In most cases argon was admitted to a pressure of 20 cm.Hg before sealing, to reduce cadmium loss. Each sealed tube was held vertically for two or three hours in a vertical platinum-wound resistance furnace at temperatures of 100° to 200°C above the liquidus. A simple wire grip supported the tube in the furnace. By means of this grip it was possible to remove the tube, invert it and replace it in the furnace within a few seconds. This was carried out every fifteen to thirty minutes and was intended to prevent denser parts of the molten alloy from settling out at the bottom of the tube. The melt was quenched by removing the tube from the furnace and plunging it, still vertical, into ice-water.

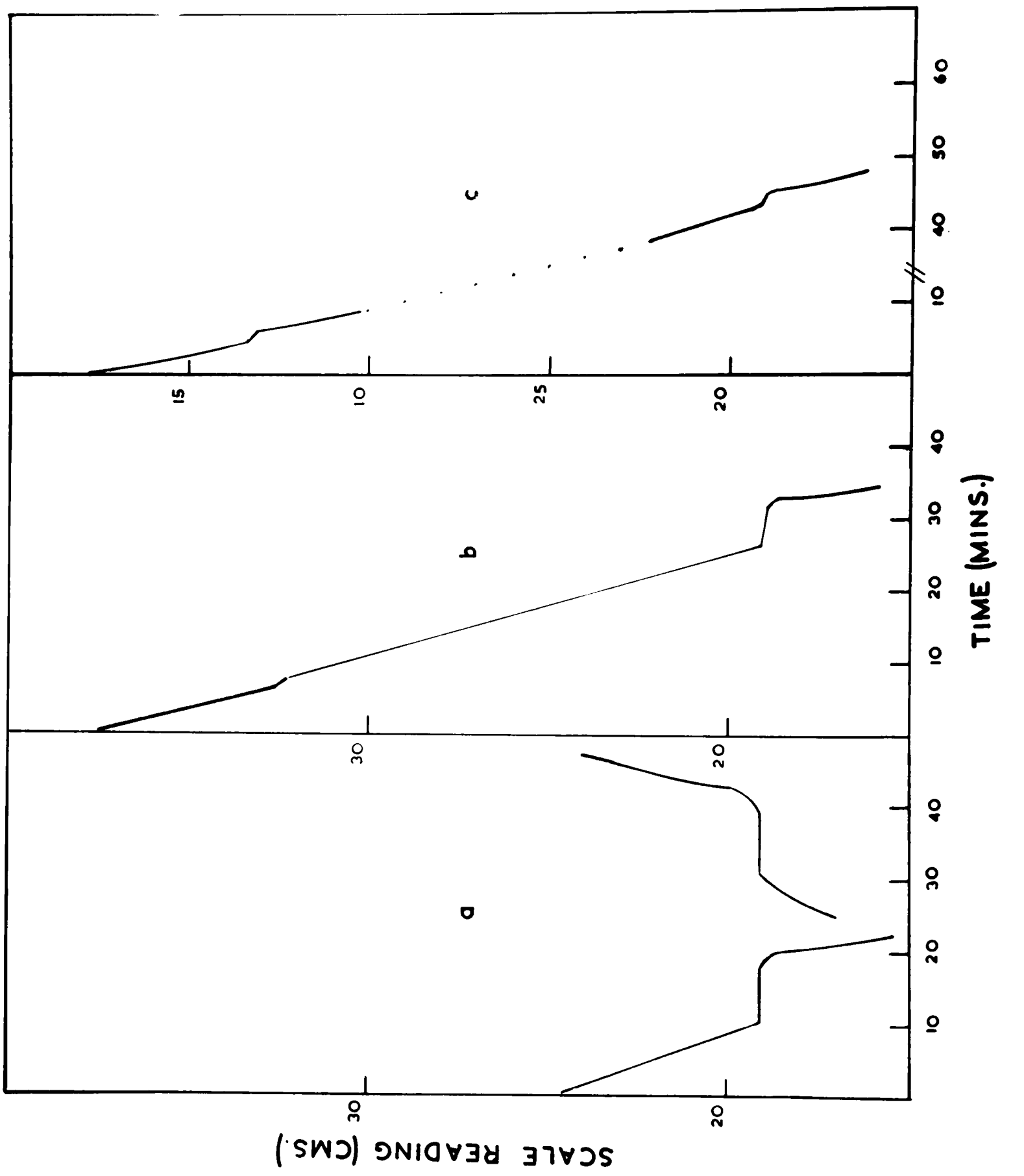

Fig.7. Examples of cooling and heating curves.

Most ingots weighed about 5 grams, with diameter 5 mm and length about 2 cm. A few ingots 10 grams in weight were made. From a survey of twenty ingots the average weight % loss after quenching was found to be 0.07. In most cases it was much less. In five other ingots a weight gain was recorded, being about 0.1%.

The weight loss was assumed to represent loss in cadmium and synthetic compositions were calculated accordingly. The silica tubes were sometimes observed to have faint yellowish streaks after quenching. This suggests that slight cadmium oxidation took place which might also account for the weight gains. The possibility of reaction between molten gold and silica was never contemplated at the beginning. Recent work on the effect of oxygen on the bonding of gold in fused silica is of interest (17). Au^{198} used as a tracer showed that molten gold diffused into silica when oxygen was present. The amount of diffusion decreases with decreasing oxygen pressure, becoming zero in vacuo. The analysis of microscopical specimens in the present work gave rise to the suspicion that gold might have been lost since the results were frequently too high in cadmium and too low in gold. But it was found (see Appendix) that this only occurred when the specimens were very small, and that the analysis of reasonably large samples (1 gm. or more) gave values very close to the synthetic compositions.

Another possible explanation of the analysis discrepancies is that the ingots may contain some silica because the melting in sealed silica tubes was carried out for long periods. According to the analytic procedure described in the Appendix, the silica might be found in colloidal form when alloy samples are dissolved and would be weighed together with cadmium sulphate. Consequently cadmium values would be too high and gold values too low. In answer to this it may be pointed out that such an effect is independent of specimen weight but the discrepancies were only observed in small samples. An appreciable gain in weight should also be observed in the quenched melts but some of the worst discrepancies appeared in ingots which showed no change in weight.

After quenching the ingots were homogenised under argon in sealed glass tubes at temperatures from 480°C to 571°C. The homogenising period varied from about seven days for the cadmium-rich ingots to about nineteen days for the gold-rich ingots. Microscopical examination after quenching and after homogenising gave satisfactory results in most cases.

The question of ingot homogeneity is dealt with further in the Appendix.

(b) Heat-Treatment.

Electric-resistance furnaces with a standard arrangement of power supply, lagging and temperature control were used for homogenising ingots and annealing specimens. Three furnaces (nichrome-wound) were each fitted with an expansion temperature controller and were used at temperatures from 350°C downwards. Three other furnaces, one platinum-wound and two nichrome-wound, were each fitted with an Ether Wheelco controller and used for high temperatures. A pen-and-ink temperature recorder was attached to the three latter furnaces and acted as a check on their behaviour over long periods.

The temperature gradient of each furnace was found to be practically zero for a distance of 2.5 cm in the middle of the furnace tube. The tubes containing the specimens were of length 2.5 to 4 cm and were placed in the constant-temperature region. Temperatures were measured with a platinum-platinum 13% rhodium thermocouple, calibrated as described in Section 1. The maximum temperature fluctuation observed during anneals is estimated as $\pm$ 3°C. For the determination of the α-solidus each specimen was annealed for half an hour in a hand-controlled furnace. The accuracy of temperature control is estimated as $\pm$ 0.7°C in most cases.

All specimens, whether powders or lumps, were sealed in vacuo or under 20 cm.Hg pressure of argon. The tubes were of glass or silica. The annealing period of lumps intended for microscopical examination varied from one day at 620°C to eight months at 150°C.

All specimens were quenched by plunging the tubes into ice-water or iced brine. In all cases where lumps were weighed before and after heat-treatment the weight change, if any, was negligible.

3. METALLOGRAPHY

The lumps were thin slices about 1 to 2 mm thick and 5 mm diameter. For easy handling each lump was mounted in a plastic disc with a hole drilled from the top of the disc to the specimen so that electrical contact for electropolishing could be made. Surfaces were made by grinding on silicon carbide wheels in a stream of water and polished on a diamond wheel (selvyt cloth with 1 to 2μ diamond paste). The results were then satisfactory for etching which was carried out chemically or electrolytically.

(a) Chemical Etching

As would be expected the gold alloys did not etch easily. Dilute hydrochloric acid or ferric chloride in methyl alcohol worked well with alloys containing 55 atomic % cadmium or more but for the chemical etching of the gold-rich alloys of lower cadmium content acqua regia, to which water has been added, was used. The technique was to cover the specimen in water and add the aqua regia in small amounts. One minute was usually sufficient to produce an etch.

(b) Electrolytic Polishing and Etching

In general the electrolytic method was preferred to aqua regia since it gave polished and etched surfaces very rapidly. Chemical etching was used to confirm the electrolytic results when necessary.

A very dilute solution of hydrochloric acid ($\frac{1}{1000}$ M) made a satisfactory electrolyte. The polishing and etching was carried out on a Shandon electrolytic machine. The cathode was of copper. The solution was stirred by a motor at controlled speed. It was a matter of trial and error to find suitable conditions. Thirty seconds was

usually sufficient to produce a polished surface almost free of scratches. It should be noted, however, that the ideal volts/amperes curve with a plateau was never found; the current increased continuously with applied voltage. Alloys containing β'-phase material were found to have been etched under these conditions but to etch α-material (i.e. gold-rich), about 5 seconds with a lower current density was necessary.

4. X-RAY METHODS

All photographs were taken by the Debye-Scherrer method for powder specimens. The exposures were made either at room temperature in a Hilger 9 cm. camera, or at elevated temperatures using a special high-temperature Unicam 19 cm. camera.

(a) Preparation of Powders

Portions of microscopical specimens or ingots were filed down on glazed papers. Sieving of powders was unnecessary and was only carried out with some of the first samples used for room-temperature X-ray photographs. The powders were treated with a magnet to remove iron particles from the file, washed with carbon tetrachloride, alcohol, ether and dried by warming the container in a hot air-stream. Strain-annealing was carried out in glass under argon or in vacuo.

The room-temperature X-ray photographs were taken in order to identify the structures of the phases found in quenched microscopical specimens. Accordingly the powders, prepared as described from the microscopic specimens, were strain-annealed at the temperatures at which the microscopical specimens had been annealed. Strain-anneal periods varied from one hour at 620° to two weeks at 240°C. To quench a powder the tube was plunged into a clean beaker of ice-water, the powder was retrieved, washed and dried as before.

Powders for the high-temperature work were prepared in the same way. Rather larger amounts were made by filing down ingot portions. In some cases lumps were given prolonged anneals followed

Section of modified Unicam High temperature Camera

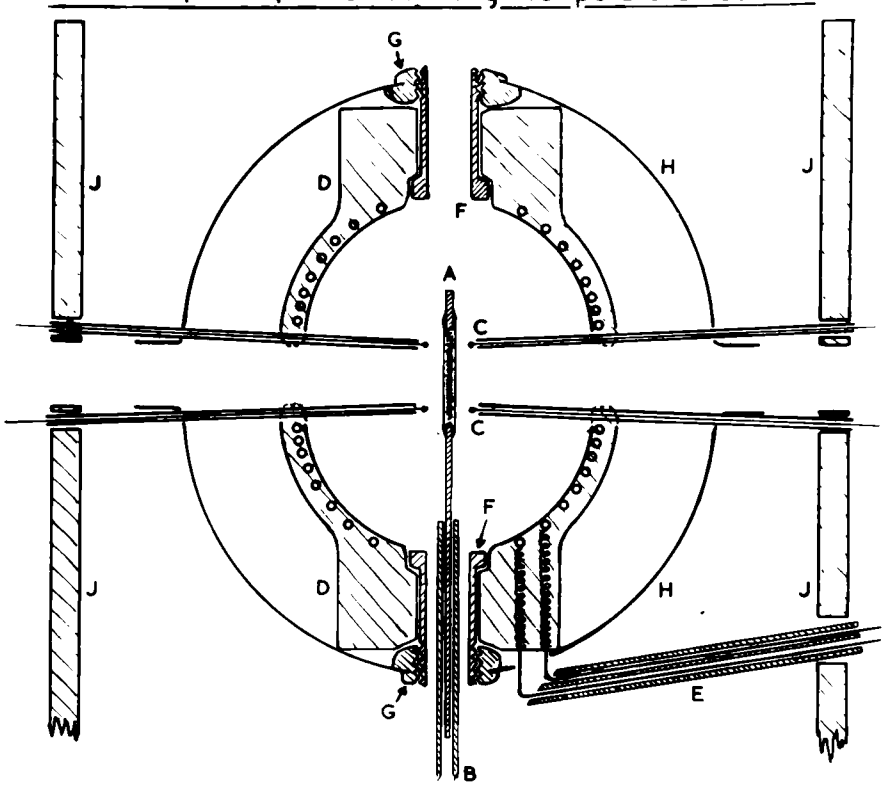

A specimen
B refractory tube supporting specimen
C ring thermocouple
D furnace
E leads
F stainless steel tubular bolt
G bush
H hemispherical nickel dome
J stainless steel tube

Scale : 0 1/2 1 in.

Fig.8.

by strain-anneals of the powders at the same temperature. All powders were given a preliminary anneal of a week or more before preparing the high-temperature specimens.

(b) Room-Temperature X-Ray Photographs

The specimens were made by rolling glass fibres, smeared lightly with Canada Balsam, in the powder on a watch-glass. Each exposure was carried out with copper radiation using nickel filters to absorb β-radiation. Exposure periods were between one and two hours. Emission conditions were 36 kilovolts and 10 milliamperes or 40 kilovolts and 12 milliamperes. Films were loaded in the Hilger camera in the asymmetric Ievinš-Straumanis arrangement so that diffraction angles could be measured without camera constants being needed.

(c) High-Temperature X-Ray Specimens

The procedure described by Hume-Rothery, Christian and Pearson (18) was used in the preparation of high-temperature X-ray specimens. Each specimen consisted of a transparent silica capillary containing alloy powder. The capillary was fitted with a solid silica rod to which it was sealed. The powder rested on the top of the rod while the capillary was closed with a plug of silica rod which rested on top of the powder. After evacuating the capillary with a rotary-diffusion pump unit, it was sealed off. A specimen is illustrated in fig.8.

Before sealing the powder in its capsule the specimen was degassed for at least one hour. A gentle heat was applied for a few seconds to assist degassing. Sometimes the specimen was allowed to pump out for about fifteen hours before sealing. The pressure was zero with the Pirani vacuum gauge used and was probably close to the pressure of the diffusion pump oil (5×10^{-6} mm.). It is not possible to be certain that this represented the actual pressure in the specimen even after pumping for 15 hours owing to the very small diameter of the capillary.

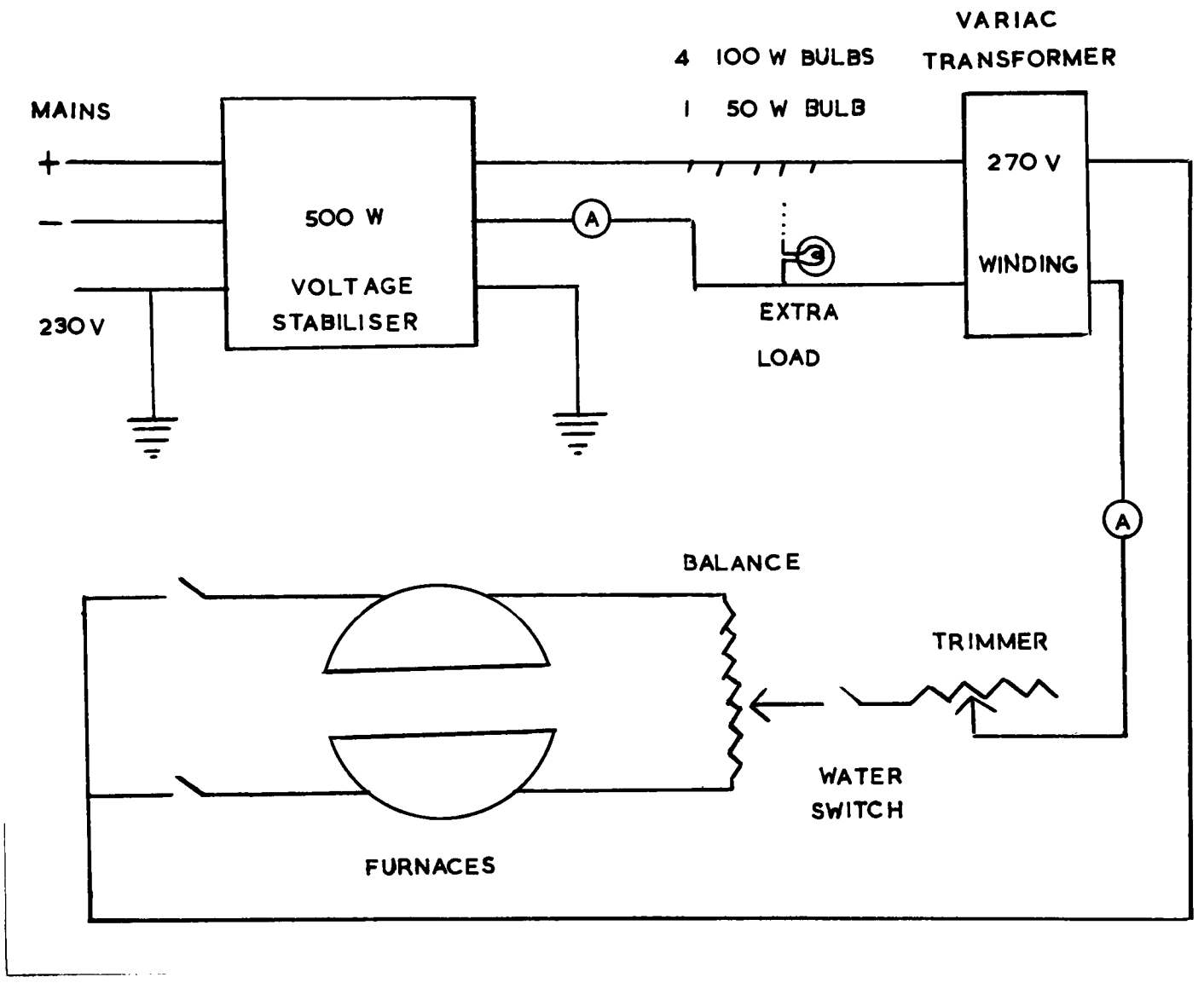

Fig.9. Temperature control unit of the Unicam camera.

Silver specimens for the calibration of the Unicam camera were prepared in the same way but preliminary strain-anneals of the silver powder, prior to making the specimens, were omitted, a strain-anneal period of one hour in the camera itself being considered sufficient.

The wall thickness of the capsules was usually about 0.07 mm. The rule was to use thick specimens with thin walls for the gold-cadmium powders and thin specimens with thick walls for silver where lattice parameters were required. The X-ray films showed satisfactory sharp reflections for all specimens.

Specimens were between 5 and 6 cm in length, with capsule length about 2 cm.

(d) The High-Temperature Camera

The Unicam 19 cm. camera was used as developed by other workers (19, 20). The apparatus can be considered in four parts. 1. A water-cooled vacuum chamber with a transparent plastic window permitting the emergence of the diffracted X-ray beam. 2. A rotary-diffusion pumping unit. 3. Temperature control unit (fig.9). 4. A detachable furnace frame which, when in position, is fixed to the floor of the vacuum chamber.

The furnace frame is illustrated in vertical section in fig.8., reproduced from ref.19. Two hemispherical furnaces are fixed so that when both specimen and frame are in position the furnaces surround the specimen. Two ring thermocouples, platinum-platinum 13% rhodium, encircle the specimen just above and below the section exposed to the X-ray beam. The two furnaces and the two thermocouples are connected to the temperature control unit via the floor of the vacuum chamber. The pumping unit also is connected to the chamber through the floor. Figs.9 and 10 are schematic diagrams of the temperature control unit and of the thermocouple arrangement.

For the mounting of each specimen the following procedure was used. The specimen was wedged into the specimen holder on the vacuum chamber floor with one or more molybdenum strips and centred accurately with a telescope and scale using two centering screws

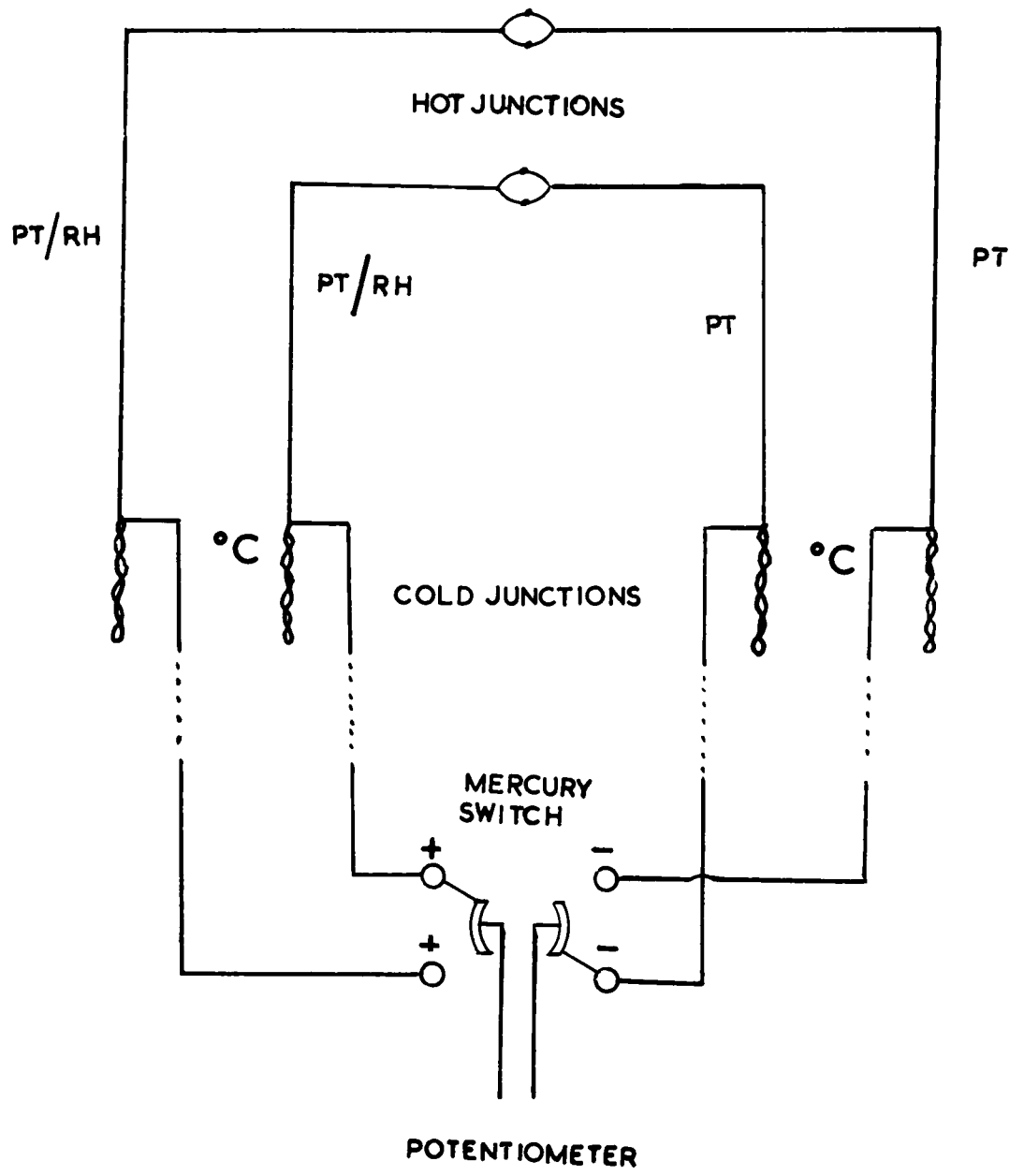

Fig.10. Thermocouple circuit.

placed at right angles to each other. The next step was to mount the furnace frame in position on the chamber floor without disturbing the specimen, usually a troublesome process. The chamber was then closed and the system pumped out at room temperature to less than 0.1 μ . After flushing out several times with hydrogen the camera was filled to a pressure of 15 cm hydrogen at room temperature in order to ensure that thermal equilibrium would be reached more readily.

Power supply to the camera was controlled by a Variac transformer with a trimmer and balance in circuit (fig.9). The first exposures were made before a voltage stabiliser was fitted in circuit and continuous control by hand was necessary. With the stabiliser in circuit (fig.9) a periodic check sufficed. The temperature fluctuation could then be controlled to $\pm$ 3° or less. Temperatures were read with a Tinsley potentiometer using a mirror-and-scale galvanometer. The sensitivity was 0.5 mv/10 cm or 5°C to 1 cm.

(e) Calibration Of The High-Temperature Camera

The observed temperature in the camera was that of the thermocouples. The specimen temperature (corrected temperature) was estimated as follows. A silver specimen was photographed at various temperatures between 640° and 300°C and the lattice spacings measured. Data in refs 21 and 22 give a lattice parameter/temperature curve for silver. From the spacings obtained in the present work the corresponding temperatures could be read off using this curve. The lattice spacing of silver was determined by measuring the doublets $\left.\begin{matrix}511\\333\end{matrix}\right)$, 422, 420 and sometimes the 331. A plot of the measured spacing against the Nelson-Riley function gave in all cases a smooth nearly linear curve. The parameter obtained by extrapolation was to the fourth place. A comparison reveals that temperatures observed on the potentiometer were usually 7 to 10° higher than the corrected temperature. A calibration curve relating observed and corrected temperatures was plotted, fig.11. It is seen that with two exceptions, nos.7 and 31, the points fall on a straight line. The numbers refer to the order in which the silver films were taken.

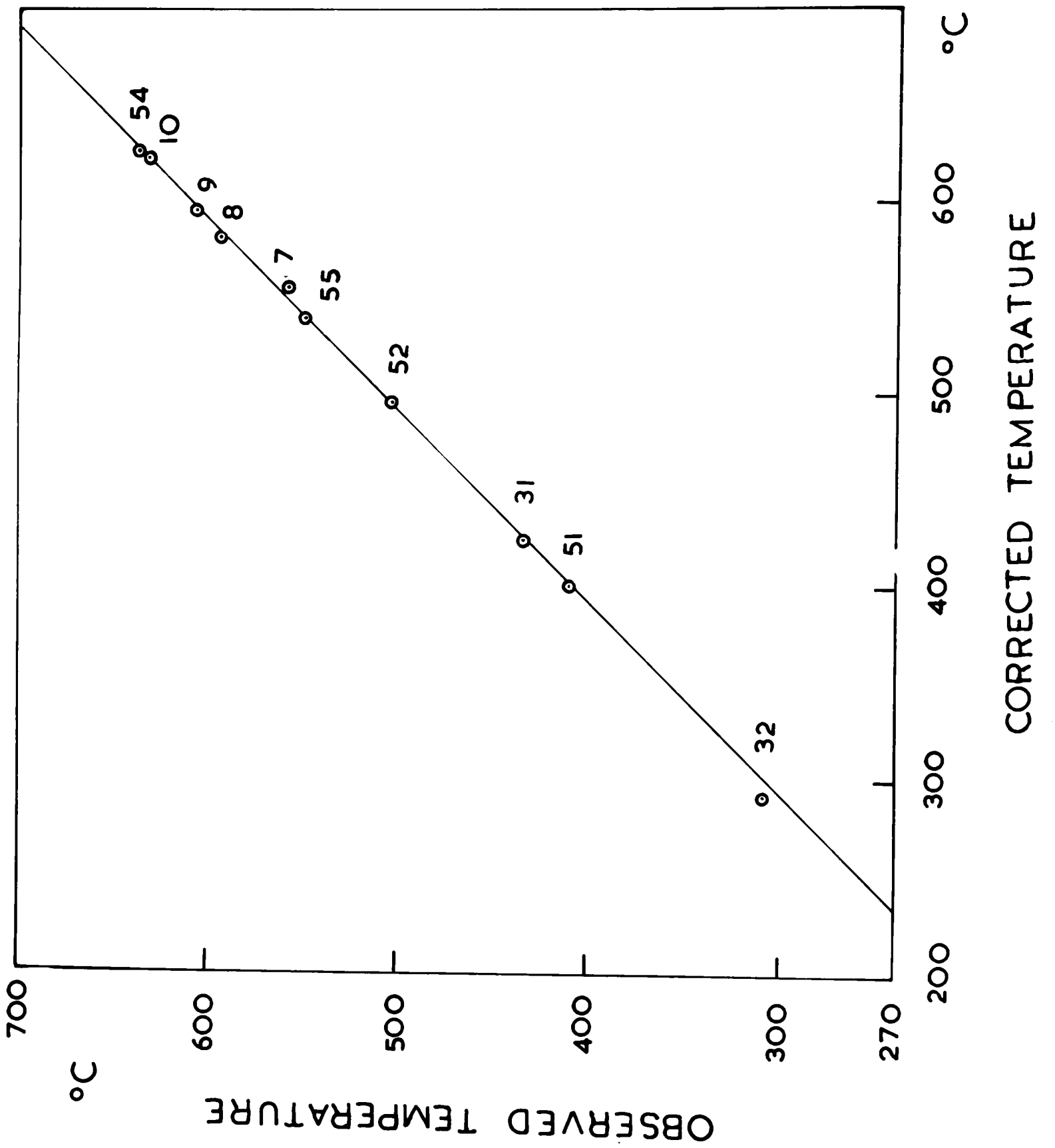

Fig.11. High-temperature camera calibration curve.

Altogether 117 films were taken and the silver films were obtained in three batches, nos.7 to 10, 31 and 32, 51 to 55 over a period of several months. It appears that during this period the correction for a given temperature has remained almost constant. Any change is regarded as within the experimental error in temperature measurements. This is estimated as follows. The temperature fluctuation in the exposures of silver observed on the potentiometer was, at most, $\pm 3^{\circ}$ and often $\pm 1^{\circ}C$. It is considered that the temperature measurements from the silver films were accurate to about $1^{\circ}C$. The points on the calibration curve have therefore been drawn as representing temperature values accurate to $\pm 3^{\circ}C$ or less. There is very little room for uncertainty as to the choice of 'best' straight line for the calibration curve. This adds $\pm 1^{\circ}C$ to the estimate of the experimental error in the measured temperatures for the gold-cadmium alloys. Therefore the estimates noted on subsequent pages include both the observed fluctuations and the estimated calibration error of $\pm 1^{\circ}C$.

(f) High-Temperature X-Ray Films.

At the beginning of a run the specimen was allowed to anneal for an hour or more at the exposure temperature before actually taking the film. The camera was protected against a possible failure in the water supply to the chamber by a water switch in the heating circuit. As far as possible cooling the camera to room temperature between successive exposures was avoided. In order to save the furnaces unnecessary thermal stress heating and cooling rates were kept low, about 10° or $20^{\circ}C$ a minute.

Emission conditions during exposure were as described in 4(b). Exposure times were usually 6 hours, though, where necessary, periods of up to 10 hours were tried. For silver, using unfiltered copper radiation, a two-hour period was enough.

The films were enclosed in a detachable cassette surrounding the vacuum chamber. The camera constants, determined by a previous worker, (20), are as follows :

High angle knife edge : 85.039°

Low angle knife edge : 39.944 mm.

The following wave-lengths were taken for copper radiation.

Cu $K\alpha_1$: 1.537 39 kX

α_2 : 1.541 226 kX

(From 'Data for X-Ray analysis'; Vol II, Phillips Technical Library).

RESULTS.

RESULTS.

1. THE LIQUIDUS.

Thermal analysis gave results for the liquidus in the range 0-55 atomic % cadmium. As explained in the experimental section all cooling curve ingots were analysed showing in most cases only a slight cadmium loss. Heating curves were usually omitted so that the thermal arrests should correspond as closely as possible to the analytic compositions. Further, the volatility of cadmium would be especially serious at the higher temperatures, 1000-750°C where the freezing-range is quite wide. Therefore to ensure that the analytic compositions should correspond as closely as possible to the thermal arrests in this temperature range, the crucible was rapidly cooled by withdrawing from the furnace as soon as the liquidus arrest was completed. Cooling curves at 10, 20 and 30 atomic % cadmium were carried out in this way, giving satisfactory results: a small but distinct arrest was observed in each case, and the loss in cadmium was less than one atomic per cent. Half a dozen cooling curves were tried on the cadmium-rich side of the diagram and, except in the equiatomic region, were in good agreement with Durrant's results.

Fig. 7 shows some typical thermal arrests. Most of those observed were well-marked, even when of short duration. The arrests obtained for the eutectic horizontal at 626.5 (fig.7a) were almost ideally horizontal: in the curve recorded in fig.7a it lasted for eight minutes on cooling. Supercooling was hardly ever observed in the range 0-55 atomic %. Table 1 gives the details for each cooling curve. In what follows each alloy is referred to by its analytic composition in atomic % cadmium, e.g. alloy 41.79.

In Table 1 it can be seen that a series of horizontal or nearly horizontal arrests were observed in all the alloys from 47.34 atomic % to 35.29 atomic %. Of alloys 42.76, 41.79, 41.08 and 40.19, the last gave an ideally horizontal arrest at 626.3°C while the remainder gave ideally horizontal arrests at 626.5°C or 626.6.

Table 1. Thermal Analysis Results.

L = Liquidus
S = Solidus
E = Eutectic
P = Peritectic

Composition in % Cadmium				Temp. Range °C	Rate of Change °C/min	Arrests °C	Type of Arrest
Synthetic At.%	Synthetic wt.%	Analytic At.%	Analytic wt.%				
55.04	41.1	54.22	40.3	625-460	cooling <2	603.9	L.
					heating 1.6	575.8 605.9	L. } Doubtful
53.00	39.13	51.53	37.74	713-530	cooling 1.7	621.4 619.9	L. (Heated up twice S. before reading taken)
50.00	36.33	51.02	37.26	650-580	cooling 1.8	627.6 621.9	L. ? Horizontal
47.8	34.3	47.34	33.88	650-580	cooling 1 to 1.1	628.7	L. Horizontal
				580-650	heating 1.4-0.5	628.3 to 629.5	S. Sloped
47.00	35.05	46.80	33.40	640-580	cooling 0.7-1.4	628.9	L. Horizontal
46.5	33.13	45.78	32.49	715-590	cooling 1.7	628.8 to 628.7	L. Almost horizontal from beginning to end of arrest.
				603-630	heating 1.0	628.8 to 629.4	L. Sloped
45.00	31.81	44.54	31.40	713-560	cooling 1.4	627.6 to 627.4	L. Almost horizontal
				611-637	heating 1.2	627.1 to 628.4	Sloped
Heating curve preceded by 2 hr. anneal at 550°C then 1 hr. anneal at 623°C.							
44.00	30.95	43.93	30.87	654-594	cooling 1.2	627.3 (uncorrected)	L. Horizontal
43.00	30.07	42.76	29.88	660-590	cooling 1.1	626.6	L. Horizontal
42.00	29.24	41.79	29.04	650-580	cooling<1	626.5	E. Horizontal
				620-635	heating 0.6	626.6	E. Horizontal
Heating curve preceded by ½-hr. anneal of ingot at 610-616, see fig.7a.							

Cont'd .....

Table 1 (Cont'd)

Composition in % Cadmium				Temp. Range °C	Rate of Change °C/min	Arrests °C	Type of Arrest
Synthetic At.%	Synthetic wt.%	Analytic At.%	Analytic wt.%				
41.42	28.73	41.08	28.44	680-616	cooling 1.2-1.0	626.6	E. Horizontal
40.23	27.73	40.19	27.70	671-615	cooling	626.3	E. Horizontal
40.00	27.54	39.14	26.83	730-593	cooling 1.5-1.1	650 627.1 to 626.6	L. Primary F. Slightly sloped E. (see fig. 7b)
39.00	26.74	40.10	27.60	670-600	cooling 1.7	626.4 to 625.7	Sloped } not plotted
				600-637	heating 1.7	626.2 to 627.7	Sloped } not plotted
37.02	25.10	35.29	23.72	890-593	cooling 2.7-1.1	702.4 627.0	L. Primary F. Almost horizontal (see Fig. 7c)
35.00	23.49	34.64	23.20	740-600	cooling 1.3	709.3 627.3	L. Arrests very slight F.
29.99	19.62	29.61	19.34	800-767	cooling 1.9	768.2 (uncorrected)	L. Rapid cooling at 765°C
20.67	12.93	19.86	12.38	887-871	cooling 1.7	873.1 (uncorrected)	L. Rapid cooling at 870°C
11.38	6.83	10.40	6.21	1014-963	cooling 2.7	971.5 (uncorrected)	L. Rapid cooling at 960°C. Alloy prepared by melting 40 at.% Cd ingot with gold.

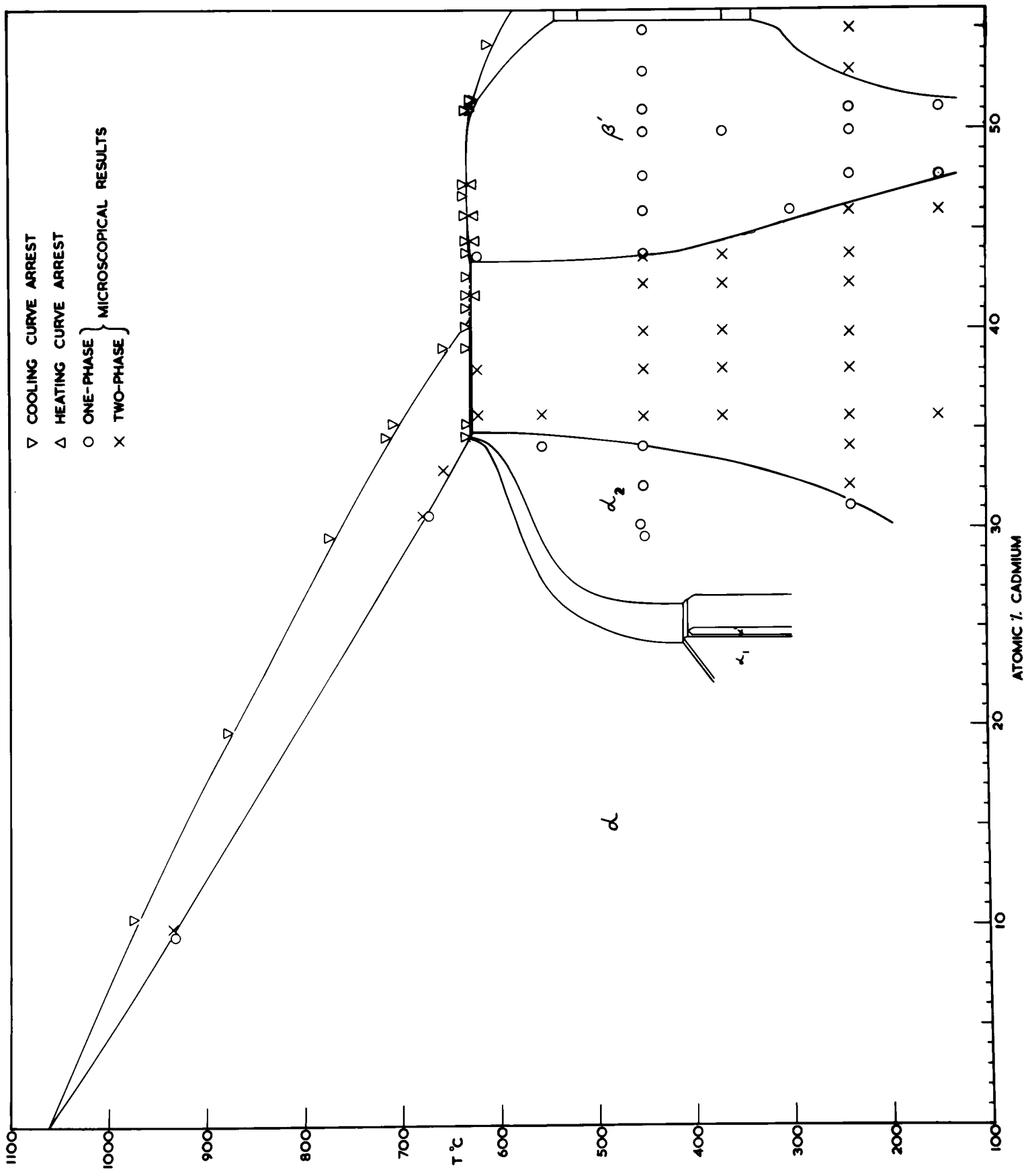

Fig.12. The gold-cadmium system. Results of present work.

This was checked by a heating-curve in alloy 41.79 which showed an ideal arrest at 626.6°C (fig.7a). It is worth noting that cooling curves with alloys 41.08 and 40.19 were carried out a year after the main batch of thermal analyses, using the same crucible assembly but with a new potentiometer of twice the sensitivity and a new galvanometer. Results were a confirmation of the arrest temperature.

It is clear that the arrests at 626.5 were due to a horizontal. That it is eutectic is indicated (i) by the appearance of primary arrests in alloys 39.14, 35.29 and 34.64 where slight arrests were also recorded at about 627°C (figs. 7b and c). (ii) By the gradual increase of the arrest temperature to a maximum of 629°C in alloys 43.93 to 47.34.

The series of arrests corresponding to the eutectic horizontal extend from between 34 and 35 atomic % to between 43 and 44 atomic % cadmium. Thus it is concluded that the eutectic horizontal extends between those limits, a conclusion which is confirmed by the microstructure of the ingots.

The maximum observed on the cadmium-rich side of the horizontal was very broad and flat, but it drops sharply beyond 50 atomic %. It was difficult to distinguish between liquidus and solidus in the maximum because arrests were very nearly horizontal. However, the use of heating curves with alloys 47.34 to 44.54 did show a distinction between liquidus and solidus, though the difference is only about half a degree.

In Fig.12 the thermal analysis results can be viewed as a whole. Fig.13 summarises the results in the range 33 to 47 atomic % drawn on a large scale. It will be recalled that arrests at

about 40 atomic % were almost exactly 626.5°C and ideally horizontal or very nearly so (to within 1 mm scale reading on the potentiometer). Now alloys 39.14 to 34.64 (Table 1) gave arrests at temperatures slightly higher than 626.5°C. Also in alloys 39.14 and 35.29 the arrests are now sloped while alloy 34.64 gives a slight arrest at 627°C in addition to the primary arrest. Fig. 7b and c give the cooling curves for alloys 39.14 and 35.29. It is therefore possible that there is another horizontal half a degree above the eutectic horizontal, forming a peritectic.

Fig.13 shows the thermal analysis results with a peritectic at 627°C. The extrapolation of the α-liquidus meets the peritectic between 40 and 41 atomic per cent cadmium. It is not clear where the eutectic point should be but the evidence from the microstructures of the cooling-curve ingots, discussed below, favours placing it between 43 and 44 atomic per cent, and not between 40 and 41 atomic %.

As described in the introduction two horizontals were postulated by previous workers. One was the eutectic horizontal at 612°C, originally supposed to represent the reaction $\alpha + \beta' \rightleftharpoons$ liquid, but later when Owen discovered the α_2 phase, drawn to represent the reaction $\alpha_2 + \beta' \rightleftharpoons$ liquid. The other horizontal, a peritectic, was placed at 625°C by Owen (7). He had no experimental evidence for this horizontal which was deduced by extrapolation of the α ($\alpha + \alpha_2$) and ($\alpha + \alpha_2$)α_2 boundaries from 550°C to meet a boundary from the 612°C horizontal at 625°C. There has been no evidence of any kind in the present work for the 612°C horizontal. If the 626.5 horizontal be taken as the eutectic, corresponding to the reaction $\alpha_2 + \beta' \rightleftharpoons$ liquid, then there must be some other horizontal above this temperature if

the phase rule is to be obeyed. Another interpretation would be to make the 626.5 horizontal correspond to the reaction $\alpha + \beta' \rightleftharpoons$ liquid, and to postulate a peritectoid below this temperature, but high-temperature X-ray work has given no evidence of this. All the evidence obtained in the present work does suggest the existence of a peritectic horizontal quite close to 626.5, corresponding to the reaction α + liq. $\rightleftharpoons \alpha_2$, as drawn in fig.13. If there is no peritectic at 627°C there must be one at some higher temperature. Alloy 35.67, photographed at high temperatures, gave the following sequence of films:

$629 \pm 4^{\circ}C$: c.p.h., α_2 + several faint lines.
(melting observed)

$634 \pm 2^{\circ}C$: f.c.c., α, + several faint lines.

(see also p. 54.)

The extra lines have not been accounted for. From the two films it is concluded that the peritectic cannot be higher than about 633°C. Attempts to identify the extra lines by means of the A.S.T.M. X-ray file (1960) gave no result and it seems unlikely they were due to impurities.

Saldau used graphite crucibles with a layer of powdered carbon. Temperatures were recorded on an automatic pyrometer and ingots were analysed (5(i)). The primary arrests in alloys of composition 15.44 and 34.60 atomic % cadmium are respectively 24° and 44°C lower than the present work suggests. From 35 to 52 atomic % Saldau's arrest temperature is smaller by 3° to 15°C than would be expected, the difference being least at the liquidus maximum. Reasons for disagreement between Saldau's work and the present work may include : (i) Apparently no stirrer for the melt (ii) Alloys were presumably slow-cooled to room-temperature and so, because of cadmium evaporation, analytic compositions may not correspond to the composition at the arrest temperature.

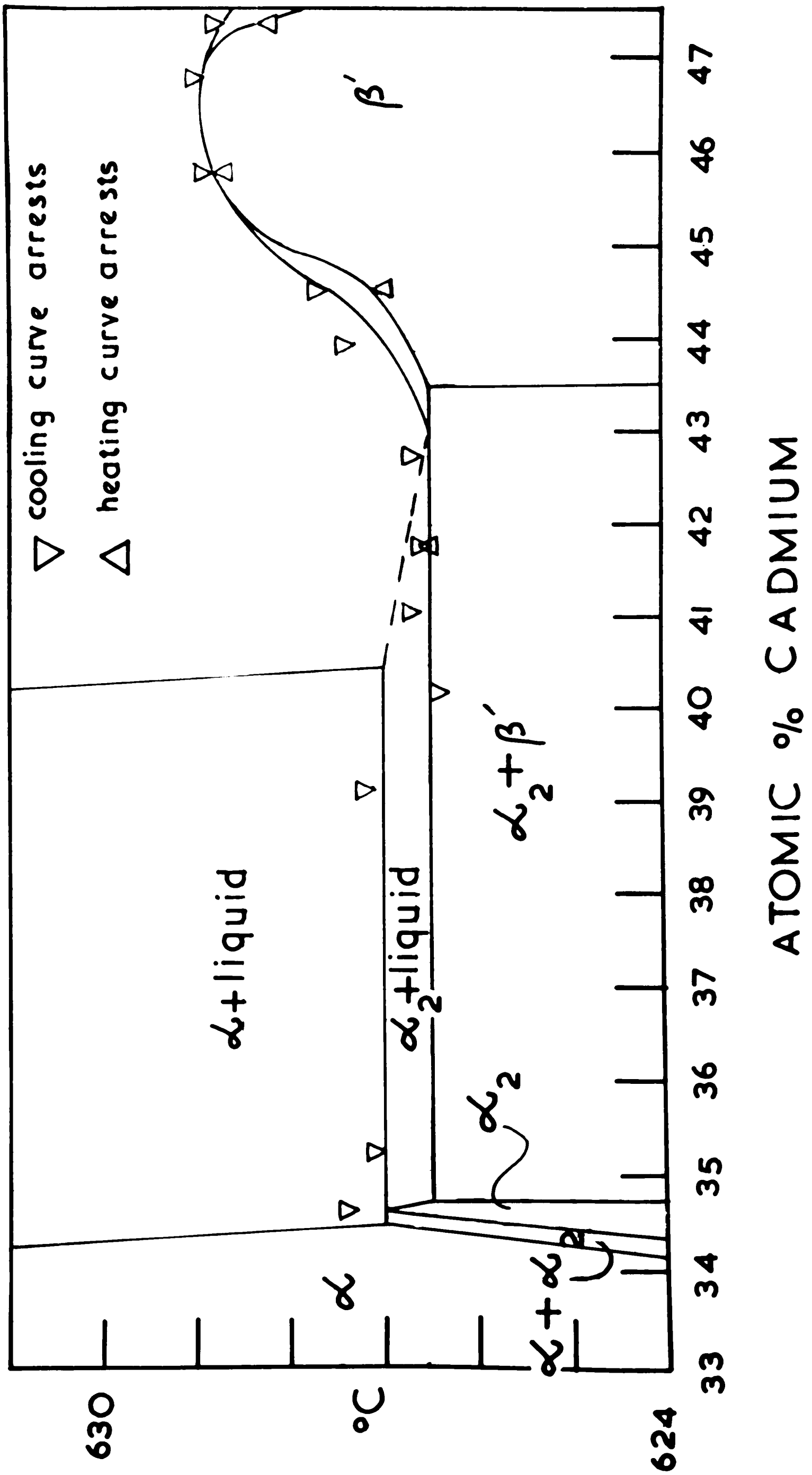

Fig.13. Results of present work in range 33-47 atomic % cadmium.

2. MICROSTRUCTURES OF THE COOLING CURVE INGOTS

The ingots, when examined in vertical section, are in good agreement with the interpretation of the thermal arrests. Details are listed in Table 2.

Alloys 46.80 to 51.53 are one-phase, corresponding to the liquidus maximum observed in this composition range at about 629°C. This phase is the β'-phase. Alloy 54.22 has cooled from the one-phase β' region across the $\beta'(\beta' + \gamma)$ boundary (Plate 1). On the other side of the β-region alloys 43.93 to 44.54 45.78 all show signs of a light precipitate in a dark matrix of β'-material. The inference is that the light precipitate is a phase richer in gold than the β'-phase, and therefore less easily etched. The evidence from the microscopic work with annealed and quenched specimens, as well as from X-ray work, showed this phase to be the α_2-phase and that ingots 43.93 to 45.78 had cooled across the $\beta'(\beta' + \alpha_2)$ boundary.

Alloys 42.76 to 34.64 were all two-phase. A fine structure of light and dark material is found together with lumps of light material. The lumps were found to have plane faces (Plates 2, 3 and 4). From the thermal analysis results a eutectic structure would be expected and it is probable that the observed fine structure is eutectic material. Primary solid solution material with plane faces (Plate 2) is not a common phenomenon. Hence the lumps appear to be some intermediate phase; this phase has been identified as the α_2-phase.

From the diagram (figs.12 and 13) it would be expected that a micrograph of alloy 39.14 would show primary α. But Plate 2 indicates the material is all α_2. It therefore seems likely that alloy 39.14, and other alloys close to it in composition, first gave α on cooling. α_2 then appeared surrounding the α precipitate. This would give rise to the characteristic plane faces recorded in Plate 2. It was found in the microscopical work with quenched specimens that α and α_2 could not be distinguished on etching and consequently one would not expect to distinguish primary α from the surrounding α_2 material in the micrographs of cooling curve alloys.

Table 2. Microscopic Results with Cooling Curve Ingots.

	Analytic at.% Cd.	No. of Phases	Microscopic Results
1.	54.22	2	The only alloy in the range studied to etch with N/10 hydrochloric acid. Dark material appeared as precipitate in light matrix. This is consistent with cooling from the β-phase field across the β′(β′ + γ) boundary. Plate 1.
2.	51.53	1	Grain boundaries clear. β-phase.
3.	51.03	1	As in 2.
4.	47.34	1	Banded structure recalling martensitic transformation.
5.	46.80	1	As in 4.
6.	45.78	1	As in 4.
7.	44.54	2	Grain-boundaries show signs of precipitation of light material on dark matrix. α_2 precipitate in β′-phase.
8.	43.93	2	As in 7.
9.	42.76	2	Lumps of light material plus a fine structure of light and dark material, α_2 + β′.
10.	41.79	2	As 9.
11.	41.08	2	As 9.
12.	40.19	2	As 9.
13.	39.14	2	Nos. 13, 14 & 15 show as cadmium content decreases, a trend towards an increasing amount of α_2 and diminishing amount of eutectic, α_2 + β′. Plate 2.
14.	35.29	2	
15.	34.64	2	

The proportion of α_2 to eutectic material increases with decrease in cadmium content. Thus the eutectic material is found only in small amounts in alloy 34.64, confirming the conclusion that the series of arrests observed at 626.5 to 627°C must terminate close to this point. Similarly eutectic material appears in alloy 42.76 but not alloy 43.93, where the series of thermal arrests now rise towards the maximum at 629°C.

Another point of interest is that all the ingots in the range 42.76 to 34.64 atomic % cadmium show white α_2 plus eutectic. Now if the α-liquidus be extrapolated as a smooth curve it would cut the 626.5° eutectic horizontal between 40 and 41 atomic %. In that case one would expect primary β′ material plus eutectic in alloys 41.08 to 42.76, but they are the same as alloys 40.19 and 39.14. This suggests that the eutectic point should be placed somewhere close to the cadmium-rich end of the horizontal, i.e. near the point where the series of eutectic arrests terminates between 42.76 and 43.93.

To summarise. The liquidus has been determined in the range 0-55 atomic %. A series of arrests has been found in the range 34 to 44 atomic % between 626.5 and 627°C. The arrests rise to about 629° in the range 45 to 47 atomic %, forming a very broad, flat maximum which, however, drops sharply to lower temperatures beyond 50 atomic %. The arrests observed between 34 and 44 atomic % and the microstructures of the ingots show a eutectic horizontal is present at 626.5°C. The evidence suggests that it extends from between 34 and 35 atomic % to between 44 and 45 atomic %. The primary arrests obtained in alloys 10.40 to 39.14 form a smooth curve for the α-liquidus. The exact position of the eutectic point is in doubt. An extrapolation of the α-liquidus cuts the 626.5° horizontal between 40 and 41 atomic %; the microstructures suggest that the eutectic point be placed between 43 and 44 atomic % instead, as drawn in figs. 12 and 13. The reaction at the eutectic temperature appears to be $\alpha_2 + \beta' \rightleftharpoons$ liquid.

Then from the number of phases observed in the present work at about this temperature, α, α_2, β' as well as liquid there must be some peritectic horizontal above 626.5°C. If the eutectic reaction were $\alpha + \beta' \rightleftharpoons$ liquid, then a peritectoid would be present below 626.5°. The evidence from high-temperature X-ray work indicates that there is no peritectoid. Hence the missing horizontal must be above 626.5°C. There has been almost no evidence of it apart from the form of arrests observed in alloys 34.64 to 39.14. Therefore a peritectic horizontal has been drawn at 627°C.

3. THE α - SOLIDUS

Specimens were annealed for half-hour periods in a hand-controlled furnace as described in the experimental section. For a given composition the temperature of anneal was raised in steps of about 5° until melting was observed (Plate 5). The accuracy of temperature control was estimated as $\pm$ 1·0°C in most cases.

Analysis of critical specimens on the solidus gave points which fell on a smooth curve. This curve could be extrapolated to meet the 627°C horizontal at about 34 to 35 atomic % cadmium. But, in common with other small specimens, the cadmium content was found to be always higher than expected and as explained in the Appendix the analysis results had to be abandoned. The solidus has not been fully re-investigated using large microscopical specimens. Table 3 gives points for ingots at about 10, 24, 30 and 33 atomic %. Synthetic compositions are used for the last two. Weights of over 1 gm were used in alloys 10 and 24. The results would suggest a point of inflexion at about 24 atomic %. But this ingot was prepared in a different way from the other alloys: by melting gold and cadmium in an induction coil and casting in a copper mould. Accordingly a smooth curve has been drawn with the other points as in fig.12, but it is possible that further experiments may be needed. It is of interest that alloy 24 also gave higher cadmium content than expected although large lumps were used. This was never found to be the case for alloys prepared by the sealed-tube method.

TABLE 3

Synthetic % at. Cd	Au	Analytic at. % Cd	Au	Temperatures °C	Results
9.98	90.02	9.49	90.47	931 ± 1	Solid
"	"	9.90	89.99	934 ± 1	Solid + liquid
23.90	76.09	23.99	76.02	774 ± 0.7	Solid +? liquid
"	"	24.03	75.83	781.0 ± 1.5	Solid + liquid
30.64	69.36	-	-	671 ± 1	Solid +? liquid
"	"	-	-	676 ± 1	Solid + liquid
33	67	-	-	655 ± 0.7	Solid + liquid

In addition the synthetic composition of alloy 24 given in Table 3 is based on the weights of metals taken. If allowance is made for loss of weight on melting, assuming it to be all cadmium, the composition is 23.59 atomic %.

PLATES.

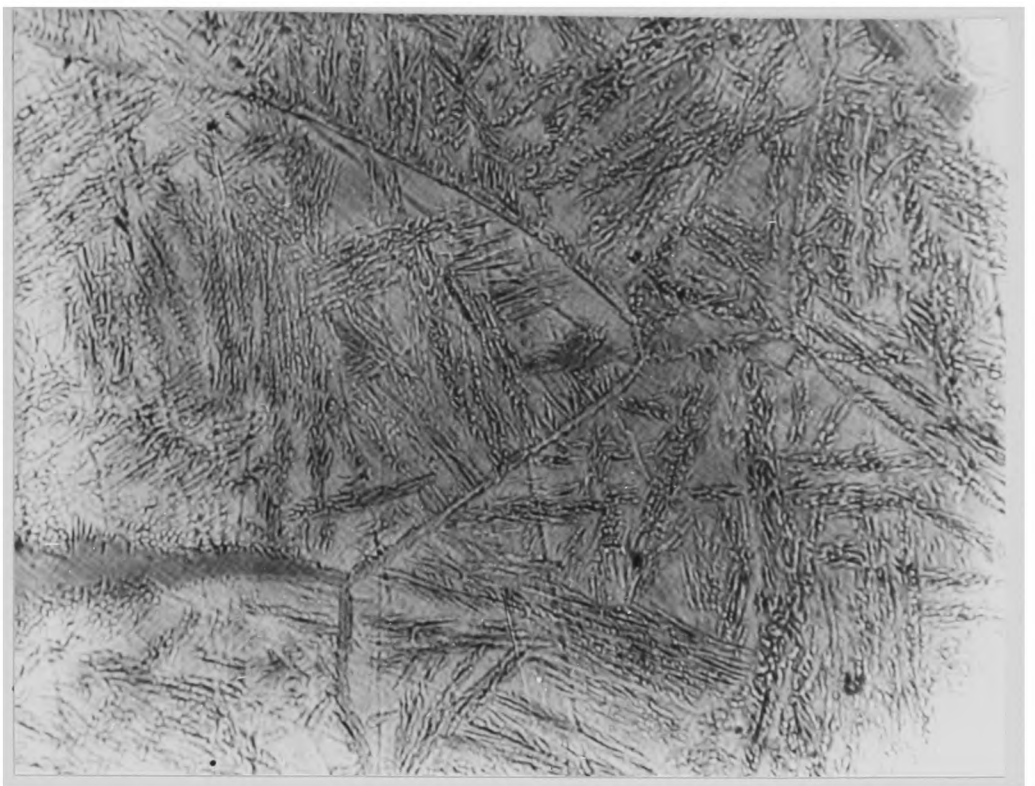

Plate 1. 54.22 at.% Cd. Cooling curve ingot. Widmanstätten precipitation of γ -phase in β' matrix. Electropolish. X 100.

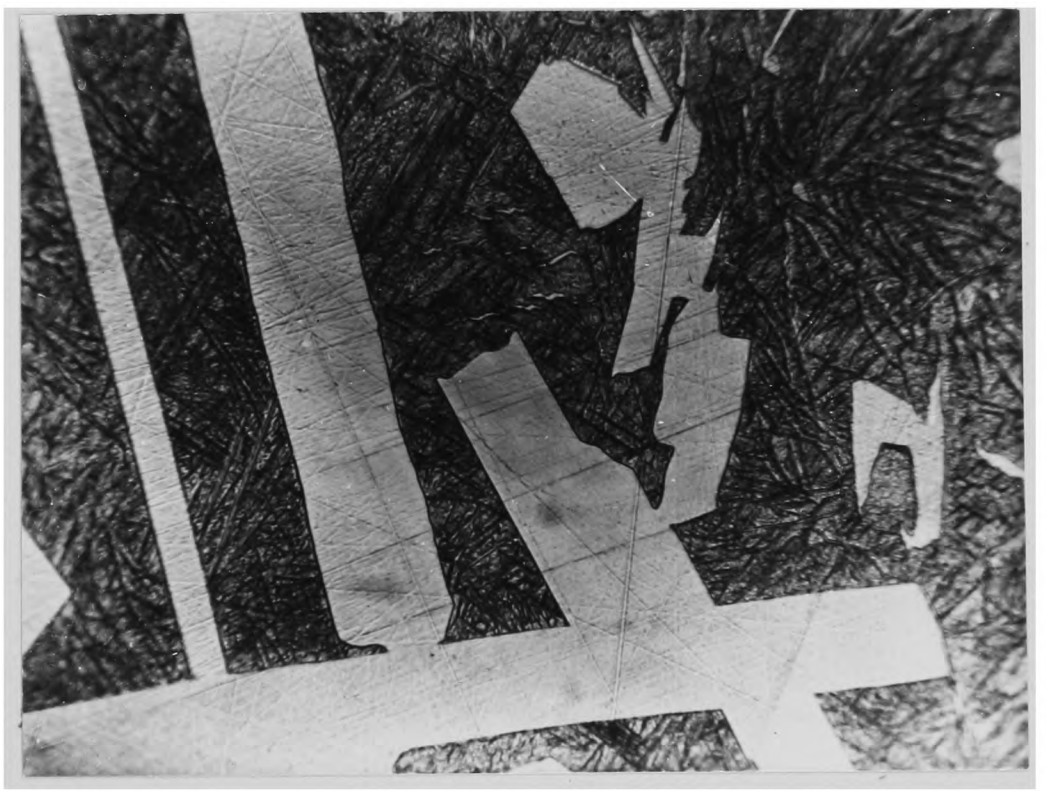

Plate 2. 39.14 at.% Cd. Cooling curve ingot. α_2 + eutectic. Mechanical polish. Etch in aqua regia. X 385.

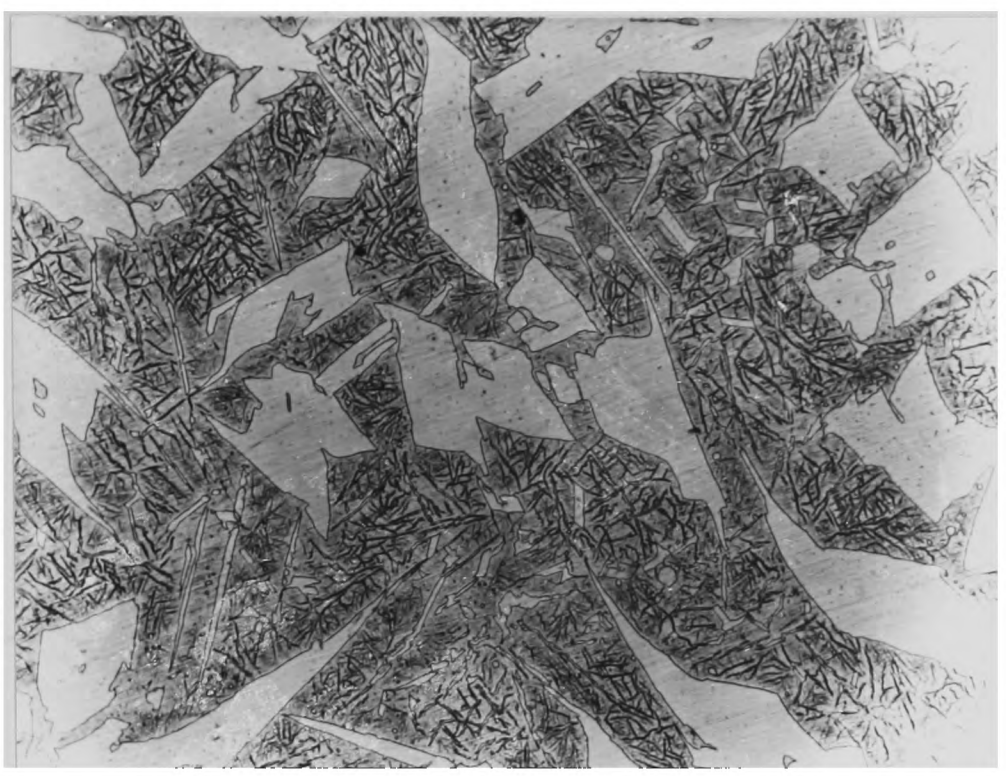

Plate 3. 41.79 at.% Cd. Cooling curve ingot. α_2 + eutect
Mechanical polish, etch in aqua regia. X 200.

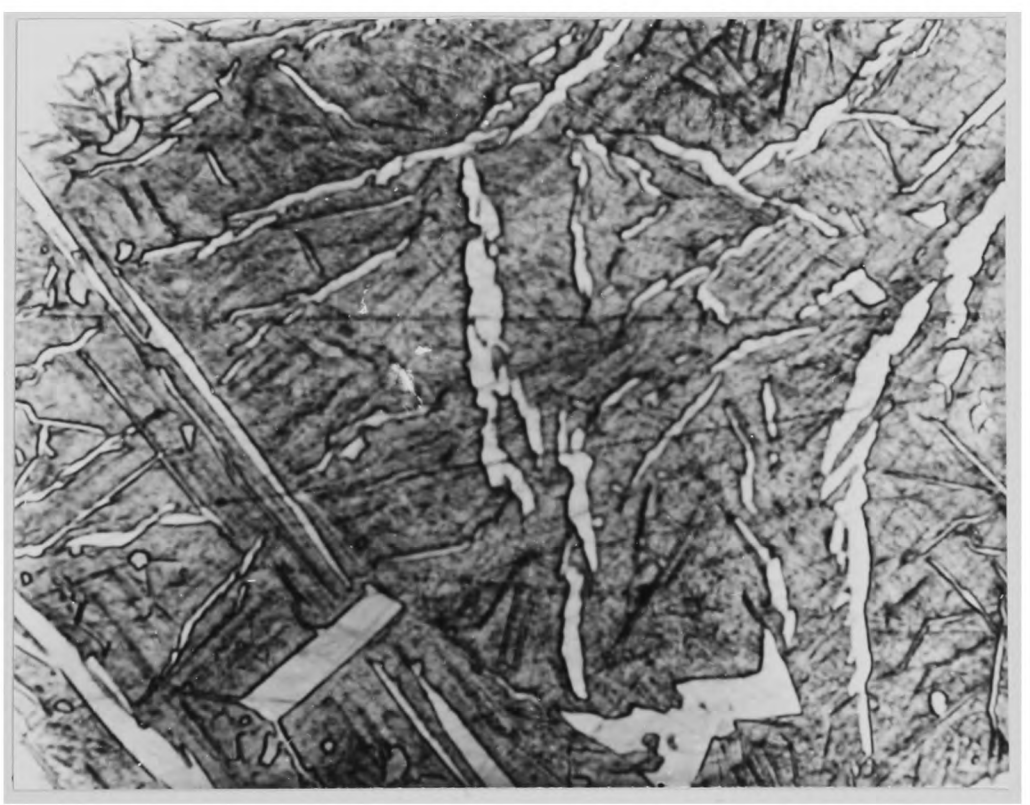

Plate 4. As 3. Electropolish. X 2500.

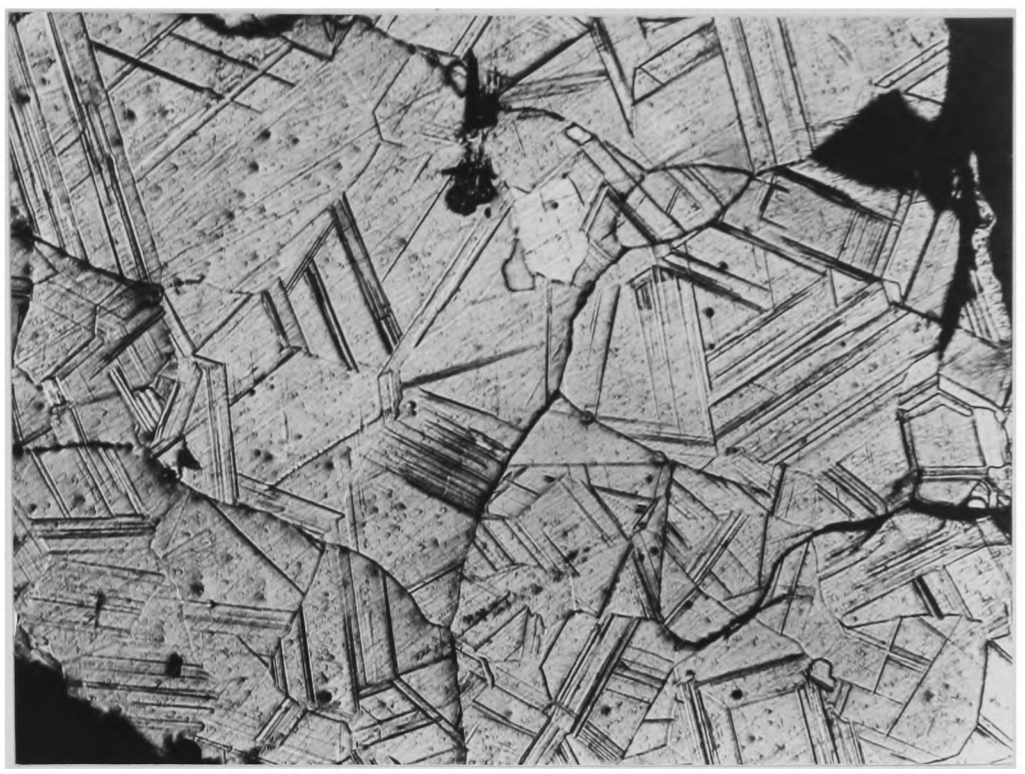

Plate 5. 30.64 at.% Cd. Solidus specimen, annealed at 676 ± 1°C. Traces of liquid at boundaries of f.c.c. α matrix. Heavy twinning. X 100.



Plate 6. 32.14 atomic % Cd. Annealed seven weeks at 240°C. α_2-phase, possibly with traces of β'. Cavities in α_2 due to segregation. Electropolish.

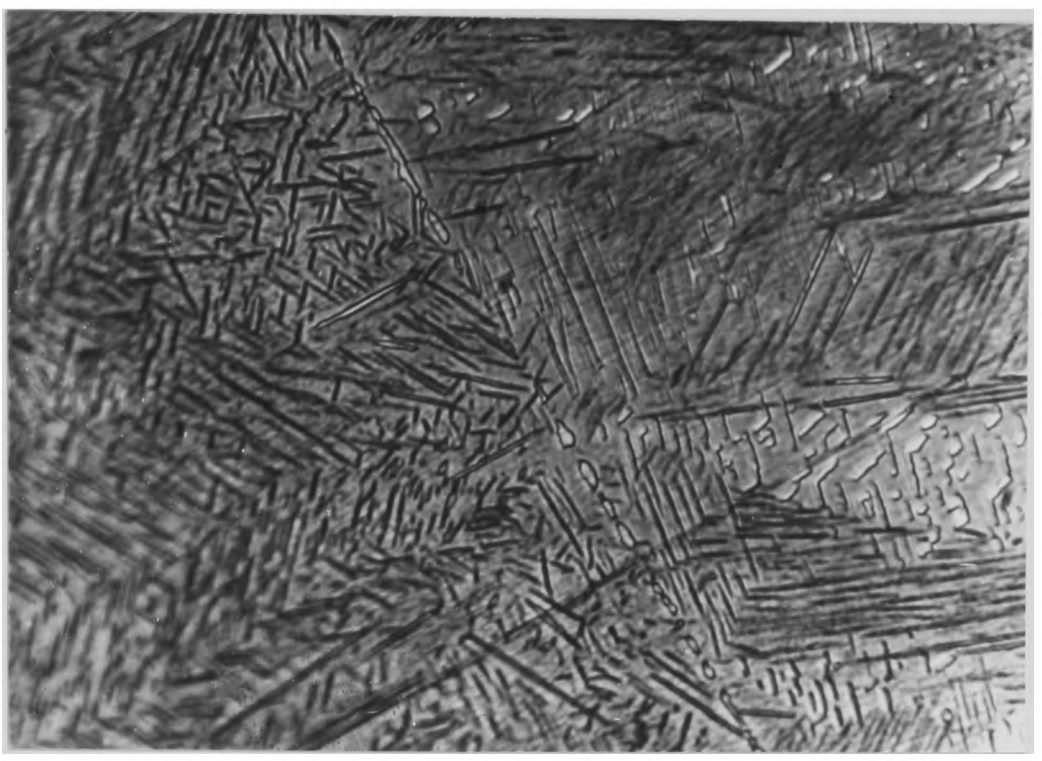

Plate 7. 45.97 at.% Cd. Annealed eight months at 150°C. β' matrix with traces of α_2 at grain boundaries. Fine structure in grains. X 1100.

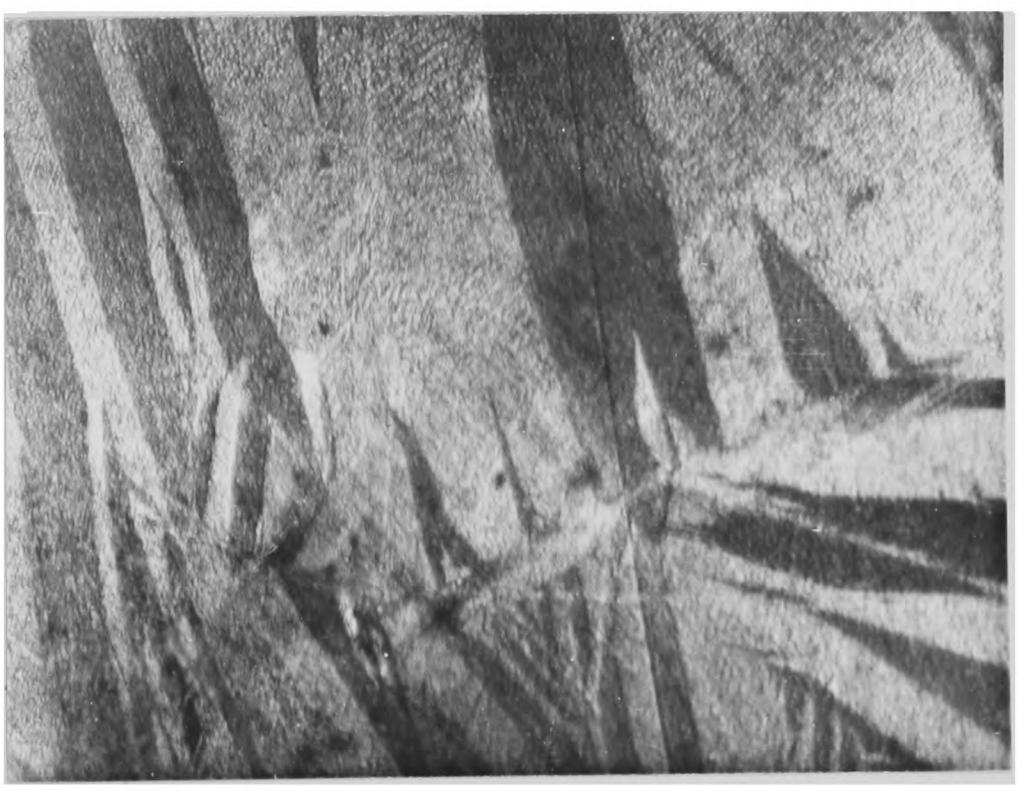

Plate 8. 47.71 at.% Cd. Annealed eight months at 150°C. β'-phase with markings due to b.c.c. $\longrightarrow$ orthorhombic transformation on quenching. Electropolish. X 550.

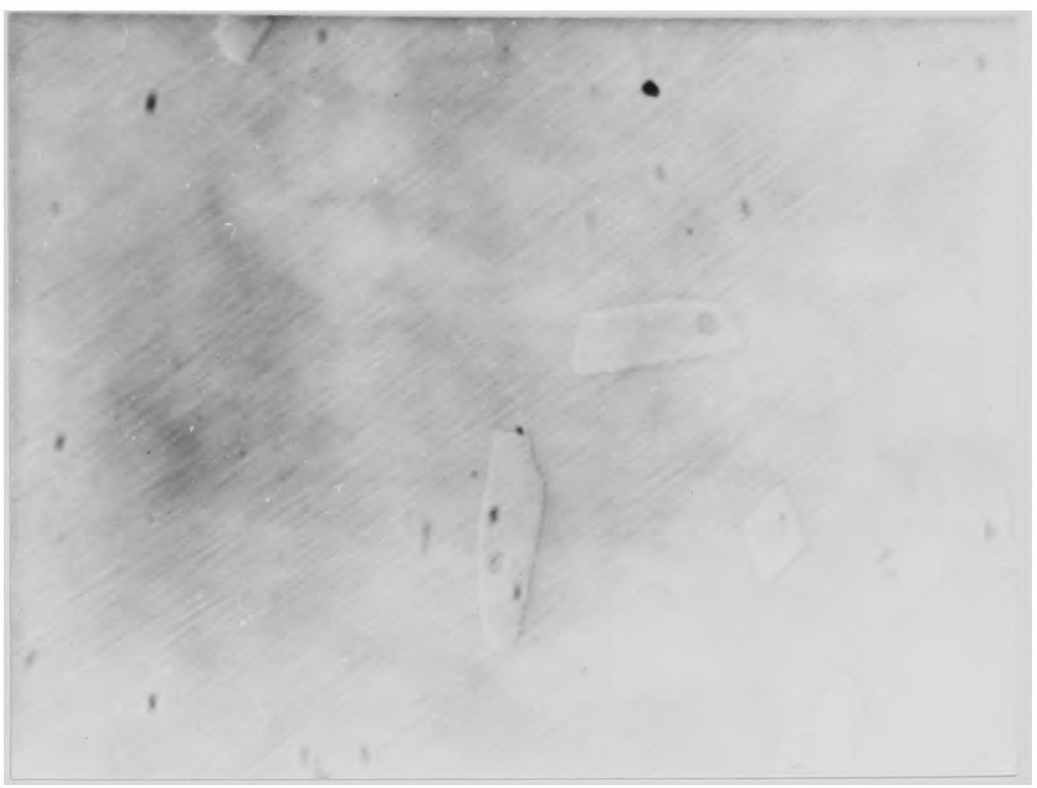

Plate 9. 35.67 at.% Cd. Annealed eight months at 150°C. Mainly α_2 with islands of β'. No etch. Mechanical polish. X 1100.

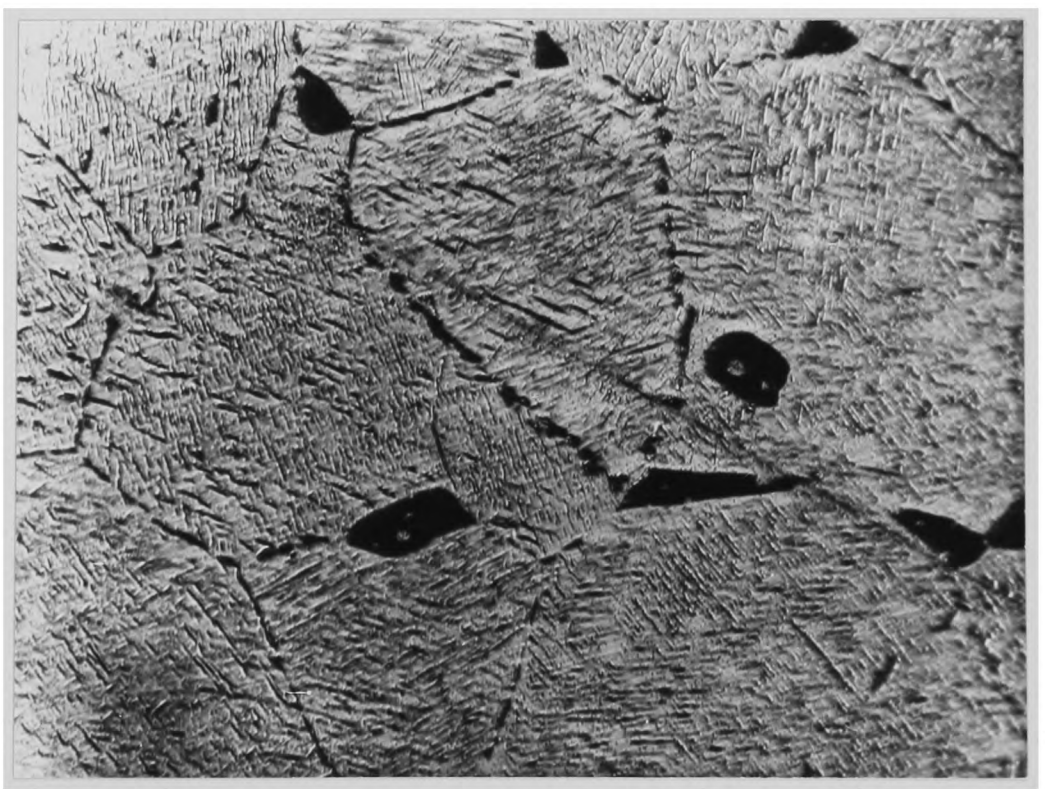

Plate 10. As 9. Annealed seven weeks at 240°C. α_2 with a little β'. Fine structure in grains. Electropolish. X 550.

4. INTERMEDIATE PHASES

The thermal analysis results and the microstructures of the cooling curve ingots gave a clear outline of the diagram in the range 0–55 atomic %. The combined results of microscopic and X-ray work, discussed below, are consistent with this outline.

The β'-Phase.

The work on the β'-phase had three main objectives. One was to identify the phase or phases in equilibrium with the β'-phase on the gold-rich side. The second was the determination of the gold-rich boundary. The third objective was to find by high-temperature X-ray photographs whether the phase was ordered up to the melting point.

(a) The α_3-Phase and the β'-Phase Transformation

With regard to the first objective it is concluded that the β'-phase is in equilibrium with the α_2-phase between 240°C and the eutectic temperature 626.5°C. The results of thermal analysis gave no evidence of an α_3-phase but did indicate that the β'-phase must be in equilibrium with an intermediate phase and not with the primary solid solution of cadmium in gold. They showed a two-phase region between 34 and 44 atomic %. This region was also found from the quenching experiments (fig.12). The X-ray films showed the two phases present to be α_2 and β', a conclusion supported by the high-temperature results obtained up to the eutectic temperature.

It appears that the α_3-phase claimed by Owen was based on the numerous reflections due to the β'-phase transformation, b.c.c. to orthorhombic or b.c.c. to tetragonal,

described in the Introduction. Evidence of this transformation in the present work included the banded structure found in some quenched microscopic specimens and in the microstructures of some cooling curve ingots. Some microscopic specimens showed a fine structure but it was not ascertained whether they represented a structural change or were only due to etching effects. Photographs of specimens in the range 38–50 atomic % quenched from several different temperatures showed numerous lines. Thus a film of alloy 45.97, quenched from 451°C, was indexed as orthorhombic using the spacings of previous workers. Similarly alloy 49.90, quenched from 570°C was ordered b.c.c. plus extra lines. Furnace-cooling of the same alloy from 445°C gave a film with many extra lines. These lines however were not accounted for as satisfactorily as in alloy 45.97. Most of them, but not all, fitted the tetragonal Bunn chart at $c/a = 0.84$. Previous workers reported somewhat different spacings and a c/a ratio of 0.88 (4).

High temperature X-ray films of alloys 45.97 and 47.71 showed conclusively that the numerous reflections were due to a structural change on quenching. Thus the following sequence of films were obtained for alloy 45.97.

17.5°C	:	orthorhombic
240 ± 3°C	:	ordered b.c.c.
351 °C	:	ordered b.c.c.

Alloy 47.71 showed an ordered b.c.c. structure between 400°C and 624°C. There is therefore no reason for postulating an α_3-phase

Table 4.

The $(\alpha_2 + \beta')\beta'$ Boundary

At.% Cd	Annealing Temperature °C	Microscopical Results
43.77	621	β'
	451 ± 2	β' + traces α_2 Fine structure
	369	β' + traces α_2.
43.87	621	β'.
	451 ± 2	β'.
45.97	300 ± 5	β'. Banded structure
	240 ± 3	β'. + traces α_2. Fine structure
	150	Similar to 240°C (Plate 7)
47.71	240 ± 3	β'. Banded Structure
	150	Similar to 240°C (Plate 8)

(b) The $\alpha_2 + \beta'$ Region

Microscopical specimens in the range 32–55 atomic % were annealed at temperatures between 620°C and 150°C. The two-phase region appearing between 34 and 44 atomic % agrees almost exactly in extent with the row of thermal arrests obtained at 626.5° to 627°C. A one-phase region was found between 44 and 55 atomic %, this being clearly the β'-phase. In the range 33–44 atomic % it was a straightforward matter to distinguish light, gold-rich material from the dark β'-material under the microscope. X-ray films of quenched powders taken from the microscopic specimens showed the gold-rich material to be α_2. High-temperature photographs were taken as follows.

At.% Cd	Temperature, °C.	Results
35.67	609 ± 3 to 624 ± 3	c.p.h. + trace b.c.c.
	629 ± 3 (melting observed)	c.p.h. + trace b.c.c. + several faint lines.
	634 ± 2	f.c.c. + faint extra lines
38.06	611 ± 3 to 619 ± 2	c.p.h. + b.c.c.
	625 ± 4	c.p.h. + faint extra lines.

There is thus no evidence that the β'-phase is in equilibrium with the α-solid solution and there is no sign of a peritectoid just below the eutectic temperature 626.5°C. One interpretation of the extra lines is that their appearance is associated in some way with the peritectic–eutectic equilibria, though it is not clear how previously forbidden reflections might become legitimate.

(c) The $(\alpha_2 + \beta')\beta$ Boundary

The boundary was easily determined microscopically

by bracketing. Inspection of a row of specimens for any one temperature showed at which composition the last traces of α_2 material were in equilibrium with β' as one moved from low to high cadmium content. The results, fig.12, where only synthetic compositions of microscopic specimens have been plotted, shows the boundary to run between 43 and 44 atomic % cadmium at about 620°C to about 47.5 atomic % below 240°C. It can be extrapolated to meet the 626.5°C eutectic horizontal at the expected composition, 43 atomic %. Thus the β'-phase narrows in range with decreasing temperature. Some β'-phase cooling curve ingots showed precipitation of α_2 material in agreement with this (Table 2, p.41.).

Critical specimens were analysed. The results put the boundary at a slightly higher atomic % (less than 1%) cadmium but otherwise do not alter its shape. As explained in the Appendix the analyses had to be rejected and synthetic compositions are used.

The behaviour of the β'-phase below 100°C is of great interest owing to the transformation phenomena and an attempt was made to get some data on the course of the boundary at low temperatures. Specimens from ingots 45.97, 47.71 and 51.04 were annealed at 150°C for eight months. On two occasions the furnace cooled accidentally to room temperature. It is estimated, however, that for the main part of the time the specimens were at temperatures between 150°C and 170°C. The microscopic results for all three specimens were the same as those for the specimens of the same compositions annealed seven weeks at 240°C. Alloy 45.97 was two-phase and the others were one-phase. The boundary therefore appears to become nearly vertical below 240°C and is probably at about 47 atomic % at 100°C.

The result for the gold-rich boundary of the β'-phase should be compared with those of previous workers. Owen claimed an $(\alpha_3 + \beta')\beta'$ boundary running from 48 atomic % at 600°C to 49 atomic % at 280°C (fig.3.) No evidence of any kind was found for the α_3-phase and from the present work the extent of the β'-phase is certainly wider than fig.3 indicates. The results of Ölander and of Byström and Almin are given in the Introduction (p.8.). Ölander's boundary cannot be regarded as consistent with the present work as the boundary is placed at about 41 atomic % at 600°C. The boundary of Byström and Almin is in good agreement with the present work but is at slightly higher cadmium content. Table 4 gives figures for the present work.

(d) The $\beta'(\beta' + \gamma)$ Boundary

No attempt was made to determine this boundary and in fig.12 the data plotted are taken from Owen's paper (8). The β'-phase becomes narrower below 300°C and as Plate 1 shows, alloy 54.22 has cooled across the boundary. Microscopical specimens from the present work annealed in the range 50-55 are also in agreement with the boundary (fig.12)

(e) High-Temperature Films of the β′-Phase

High-temperature X-ray films were taken of alloy 47.71 to determine if the alloy was ordered up to the melting point. All the films were found to be b.c.c. with superlattice lines observed as below.

T°C	Superlattice lines			
399 ± 5	(100)	(111)	(210)	
490 ± 2	(100)	(111)	(210)	
599	(100)		(210)	
609	(100)	(111)	(210)	
620 ± 2	(100)	(111)	(210)	
624	(100)	(111)	(210)	(some lines ill defined)
631 ± 4	No reflections. Powder observed to melt.			

It is concluded that alloy 47.71 is ordered up to the melting point. As mentioned previously alloy 45.97 is ordered b.c.c. at 240 ± 3°C and at 351°C.

The degree of ordering in alloy 47.71 at 620°C was measured by taking photometer traces of the film. Intensity charts were recorded on a double-beam microdensitometer and the (100) and (110) reflections selected for measurement. Relative integrated intensities were obtained by counting the squares under the diffraction peaks on the charts, ruled on the centimetre scale. The average of several counts for each half of a film A or B was taken.

A		B		Average	
(110)	(100)	(110)	(100)	(110)	(100)
865 ± 5	50 ± 3	879 ± 8	47 ± 2	872	48

The structure factor for the disordered b.c.c. cell where atom positions are 0 0 0 and $\frac{1}{2}\ \frac{1}{2}\ \frac{1}{2}$ is given by

$$F = f\left[1 + e^{\pi i (h+k+\ell)}\right] \qquad 1.$$

f is the average scattering factor for a completely disordered lattice. If the atomic ratio is 1 : 1 then in the case of β'-Au-Cd

$$f = \tfrac{1}{2}f_{Au} + \tfrac{1}{2} f_{Cd}$$

In the actual case the composition is 47.71 atomic % cadmium.

$$\therefore \quad f = 0.5229f_{Au} + 0.4771f_{Cd}$$

For reflection 110 $F_{110} = 2f$ (h + k + 1 even)

$$\therefore \quad F = 2\,(0.5229f_{Au} + 0.4771f_{Cd}) \qquad 2.$$

If a simple model of long-range order is assumed, then using the unit cell found by previous investigators, i.e. a CsCl lattice with gold atoms in the 0 0 0 positions and cadmium atoms in the $\frac{1}{2}\ \frac{1}{2}\ \frac{1}{2}$ positions, the structure factor for the ordered b.c.c. unit cell is

$$F = f_{Au} + f_{Cd}\, e^{\pi i (h+k+\ell)} \qquad 3.$$

For the (110) reflection equation 3 becomes

$$F_{110} = f_{Au} + f_{Cd}$$

For the (100) reflection equation 3 is

$$F_{100} = f_{Au} - f_{Cd}$$

If the lattice is only partially ordered then for the (100) reflection

$$F_{100} = S\,(f_{Au} - f_{Cd}) \qquad 4.$$

where S is a measure of the degree of order and is defined as follows

$$S = \frac{X_A - x_A}{1 - x_A}$$

x_A is the atomic fraction of one component A and X_A is the

fraction of A sites in the lattice actually occupied by A atoms. For 100 atoms of a 1 : 1 alloy X_{Au} = a/50. When a = 50, as would be the case for perfect order, S = 1.

The relative integrated intensity of a reflection is given by

$$I_{hkl} = |F_{hkl}|^2 \; p\left(\frac{1 + \cos^2 2\theta}{\sin^2\theta \cos\theta}\right) \qquad 5.$$

p is the multiplicity factor and the term in brackets is the Lorentz polarisation factor. The values of the various quantities for the film at 620°C are collected in the table below. $|F|^2$ values were calculated from equations 2 and 4 and the relative integrated intensities from equation 5.

hkl	θ	sin θ/λ	f_{Au}	f_{Cd}	$\lvert F_{hkl}\rvert^2$	p	$\frac{1 + \cos^2 2\theta}{\sin^2\theta \cos\theta}$
100	13.3	0.15	69.8	41	829.44	6	34.94
110	19.0	0.21	64	37	10451.7	12	16.17

The ratio of the calculated values of the relative integrated intensities is then

$$\frac{I_{100}}{I_{110}} = \frac{17.3 \times 10^4 \times S^2}{20.3 \times 10^5}$$

From the observed intensity ratio S = 0.8. The definition of S gives X_{Au} a value of 0.904 and the number of Au sites actually occupied by gold atoms is 45.2 out of 50.

Similarly X_{Cd} = 0.8954 and 44.7 cadmium sites out of 50 are occupied. Thus the alloy is about 90% ordered at 620°C.

No correction has been made for absorption in the intensity calculations. Nor has the temperature factor been allowed for. It is not clear how far omission of these corrections has affected the accuracy of the calculations. Since the (100) and (110) reflections have θ values fairly close to one another it is assumed that the absorption does

not decrease markedly with change of θ from 13.3° to 19.0° Moreover, the intensity decrease due to the temperature factor is greatest at high θ values and least at low θ values. Therefore one can expect the temperature factor and absorption factor to cancel out, in part. The value 90% at 620°C suggests the β'-phase to have a high degree of ordering quite close to its melting point, 629°C.

The α_2-Phase

(a) The α_2 ($\alpha_2 + \beta'$) Boundary.

The boundary was determined (fig.12) by examining quenched lumps microscopically, the results being tested by X-raying the powders. The microscopic work proved to be more difficult than in the case of the $(\alpha_2 + \beta')\beta'$ boundary where it was a simple matter to detect the disappearance of the last traces of light α_2 in a dark β'-matrix.

Table 5 gives the microscopic and X-ray results. It shows that the boundary must be placed to the gold-rich side of alloy 35.67 since at all temperatures this alloy is definitely two-phase with a substantial amount of β'-material in the α_2-matrix (Plates 9 and 10). But it was not so easy to decide which of the alloys in the series 31.16, 32.14 and 34.14 showed β'-material and which did not. Plate 6 is a photomicrograph of alloy 32.14 annealed at 240°C. It is believed to be mainly α_2 plus a few traces of β' at the grain boundaries and has been plotted as such on the diagram. The decision was made more difficult by the appearance of numerous cavities with no apparent relation to the matrix. Similar cavities were found in quite a wide range of alloys from 25 to 35 atomic % cadmium. An explanation of their occurrence in terms of segregation is offered in the discussion. They could be detected by means of oblique light. Sometimes they appeared after mechanical polishing though usually chemical etching or electropolishing was needed to reveal them. It appears that surface layers, formed on mechanical polishing, will conceal them until removed by etching or electropolishing. Their irregular distribution which did not vary systematically with composition would support the view that they are not due to a new phase easily removed on etching.

Table 5.

The α_2 (α_2 + β') Boundary

Alloy composition At.% Cd	T°C	Microscopical Results	X-Ray Results (quench)
31.16	240	α_2 only	-
32.14	451	α_2 only	c.p.h.
	240	α_2 + traces of β'	c.p.h. + 11 extra lines
34.14	451	α_2 only	c.p.h. + 1 extra line
	240	α_2 + traces of β'	c.p.h. + 7 extra lines
35.67	620	α_2 + β'	-
	554	α_2 + β'	c.p.h. + orthorhombic
	451	α_2 + β'	c.p.h. + orthorhombic
	369	α_2 + β'	-
	240	α_2 + β' (Plate I θ)	-
	150	α_2 + β' (Plate I φ)	-

Alloy 34.14 also annealed at 240° was similar to alloy 32.14. On X-raying both alloys gave the α_2 c.p.h. pattern but with some extra lines. From what has gone before, one would expect the extra lines to be due to transformed β', i.e. that they would be orthorhombic reflections. But though most of the lines fitted the orthorhombic pattern found with alloy 45.97, some did not. Alloy 35.67 and alloys of higher cadmium content, shown microscopically to be $\alpha_2 + \beta'$, gave c.p.h. + orthorhombic X-ray patterns.

Alloys 32.14 and 34.14 annealed at 451° and 554°C were one-phase according to the X-ray films, with one exception, 32.14 alloy at 451°C where there was one unexplained line. Microscopical evidence indicated them to be one-phase. In addition apparent signs of decomposition were observed under the microscope in alloys 34.14 and 35.67 but a comparison of high-temperature and quench films of specimens taken from the same ingots did not confirm this.

Alloy 31.16 was annealed at 240°C for twelve weeks. Microscopical examination showed it to be almost certainly one-phase and in fig.12 the boundary is drawn very close to this point.

To sum up. Relying on the synthetic compositions, the boundary is drawn between 31 and 32 atomic % at 240°C. As the temperature rises it slopes to higher cadmium contents and becomes vertical. High-temperature work on the two-phase alloys, $(\alpha_2 + \beta')$, described previously, shows that the $\alpha_2 + \beta'$ equilibrium is found at temperatures just below the eutectic temperature. The boundary must therefore meet the 626.5°C eutectic and can be extrapolated to meet it between 34 and 35 atomic %. The result puts it at a slightly lower cadmium content than the boundary of Owen et.al (7, 8).

(b) The $\alpha + \alpha_2$ Boundaries

An attempt was made to check the $\alpha + \alpha_2$ boundaries by means of microscopical examination of quenched lumps annealed at 451°, 554° and 620°C in the range 20 to 30 atomic %. The alloys were at intervals of one half to one atomic %. α could not be distinguished from α_2 by etching. The use of polarised light gave uncertain results. The appearance of annealing twins made it possible to distinguish f.c.c. (twinned) from c.p.h. in some cases but the twin test was not conclusive. Twins were not always detected in specimens subsequently found by X-raying to be f.c.c. while the appearance of a few twins in alloys 28 and 29.63 at low temperatures which were originally supposed to be one-phase c.p.h, led to doubts about the exact Au-rich limits of the α_2-phase.

Quench X-ray films of powders taken from some of the lump specimens annealed at 451° and 554°C were consistent with the Owen boundaries, with some exceptions.

High-temperature X-ray films were taken of the whole region with alloys 25, 26, 27, 32 and 34.14. The results are collected in Table 6 and plotted in fig.14. This method of determining phase boundaries is necessarily less accurate than the lattice parameter method, by which the Owen and Roberts boundaries were obtained, and is only justified if decomposition on quenching is suspected. Approach to equilibrium may otherwise be very slow and may require inconveniently long anneals in the high-temperature camera.

To check the reproducibility of the results, a series of exposures were taken, in the following order, for

alloy 34.14.

	Temperature, °C	Results
Run 1.	607 ± 3	f.c.c. + c.p.h.
	617 ± 3	f.c.c.
	594	f.c.c. + c.p.h.
	Room Temperature	c.p.h. (fig.20)
Run 2.	591 ± 4	c.p.h.
	617 ± 3	f.c.c.
	607 ± 2	f.c.c. + ?

During Run 1 the 607°C exposure, which lasted six hours, was preceded by a half-hour anneal. The specimen was then held for thirteen hours at this temperature, then raised to 617°C and annealed for half an hour before exposure for ten hours. The 594°C exposure also lasted ten hours and was preceded by a half-hour anneal.

Run 2 was similar to Run 1 with a preliminary anneal of about three-quarters of an hour. The results show, firstly, that the alloy is certainly f.c.c at 617°C and, secondly, that approach to equilibrium is probably quite slow as indicated by the results at about 590°C. For the exposure at 590°C in Run 1 the specimen had been cooled down from the f.c.c. region; in Run 2 it had been heated up from room temperature. It is probable that one or both of the films at 590°C do not represent equilibrium results. The very narrow $\alpha + \alpha_2$ region at this temperature accounts for the fact that, in spite of this, the reflections are sharp. Reaction, even at temperatures close to the solidus, seems to be slow and an accurate measurement of boundaries by the lattice parameter method may be possible with quenched specimens.

After the above series of films, alloy 34.14 was exposed successively at 631° and 650°C. The specimen was seen to melt at 650°C. Both films were f.c.c. The X-ray of the specimen, after

cooling to room temperature, showed the c.p.h. pattern and no extra lines. The lines were now fainter and slightly irregular.

One criticism of the above experiments is the errors which may be introduced by cadmium evaporation. The boiling point of cadmium is 321°C and therefore some loss of cadmium at 600°C is inevitable. But loss of cadmium is unlikely to be important because of the very small free volume in the silica capillary. One way in which cadmium loss might occur is through a crack in the silica, but again this is improbable because alloy 34.14 after exposure at 650°C, in the α + liquid region, was found to be c.p.h. at room temperature.

Films of alloy 32 were consistent with alloy 34.

Table 6 shows that while alloy 25 is consistent with the $\alpha + \alpha_2$ boundaries of Owen and Roberts, alloy 26 is not. The deviations cannot be attributed to short annealing times in the camera because in some cases the specimens were given prolonged anneals to check the results. Thus alloy 26 should be one-phase f.c.c. at 533°C, according to Owen and Roberts, but was found to be f.c.c. + trace c.p.h. even after forty hours annealing at this temperature. At somewhat higher temperatures the c.p.h. reflections disappeared (Fig.14). At 455°C the appearance of f.c.c. + c.p.h. patterns in alloy 26 again disagrees with Owen and Roberts who predict a pure c.p.h. pattern.

Alloy 27 was found to be one phase, c.p.h., (faulted) as expected between 450° and 355°C.

To accommodate the X-ray results from alloy 26, the $\alpha + \alpha_2$ boundaries have been adjusted as in Fig.14. They bend to the cadmium-rich side with increasing temperature. At ca. 600° to 620°C they must become vertical once more according to the films of alloy 34.14. The boundaries at ca.400°C to 450°C have been adjusted to fit in part alloy 26 and in part the results for the α_1-phase described later.

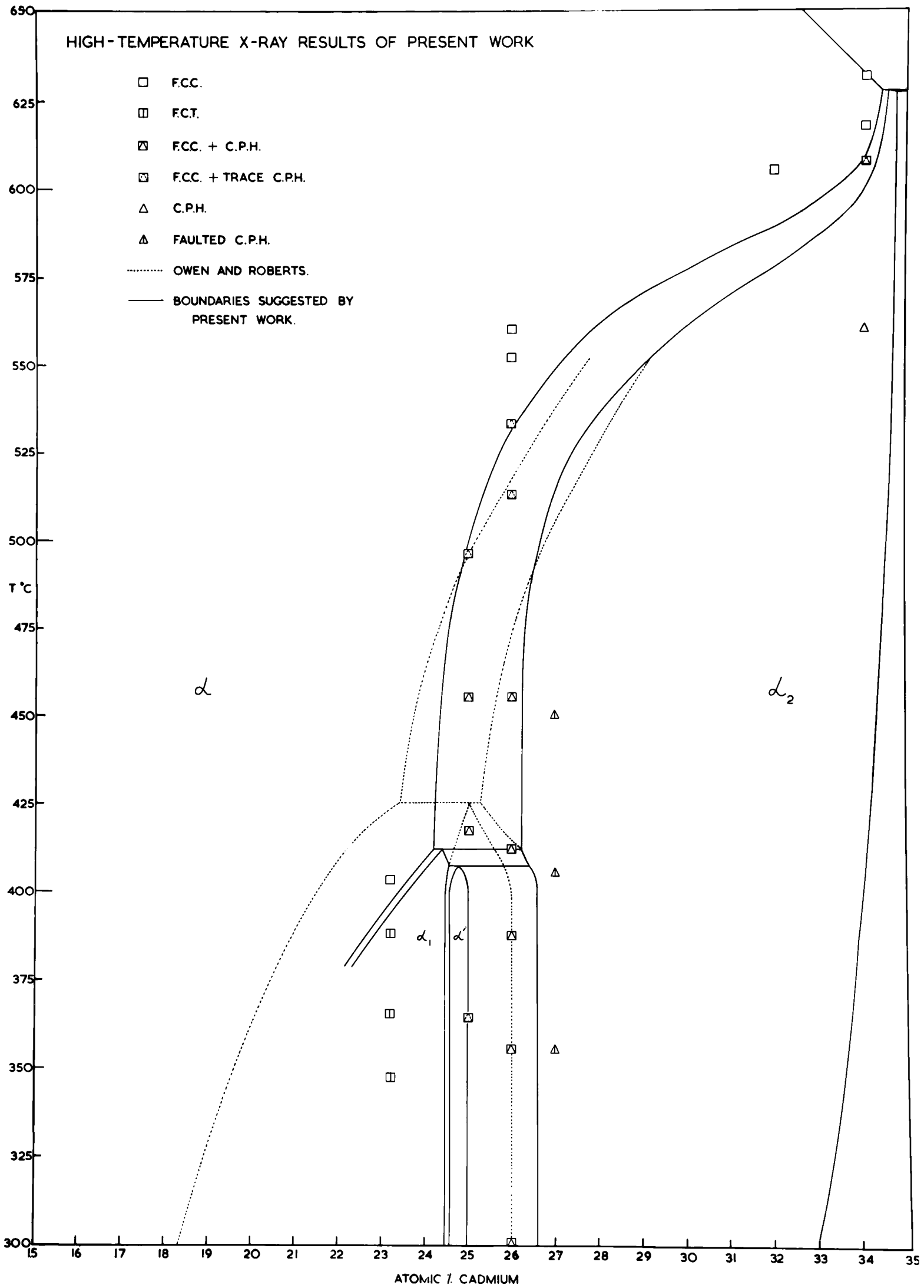

Fig.14. Results of present work in range 22-34 atomic % cadmium.

The answer to the discrepancies between the results of present work and those of Owen and Roberts can perhaps be found from a comparison of the annealing times. For the α ($\alpha + \alpha_2$) boundaries a maximum of twelve hours was used by Owen and Roberts in preparing powders for X-ray measurements. It is stated that widely varying annealing times were used for the ($\alpha + \alpha_2$)α_2 boundary, giving consistent results. But since Owen and Roberts do not appear to have annealed specimens for more than nineteen hours for the ($\alpha + \alpha_2$)α_2 boundary, it is reasonable to infer that disagreement with the present work may have been due to short annealing times. Thus alloy 26 was annealed 40 hours at 333°C whereas Owen and Roberts annealed their powders only about three or four hours at this temperature. The behaviour of alloy 34.14, described above, supports this interpretation. It must be admitted, however, that when specimens were given prolonged anneals at any one temperature in the camera, no change was observed by inspection of the films taken throughout the annealing period.

The X-ray experiments have not been carried far enough to draw a satisfactory α ($\alpha + \alpha_2$) and ($\alpha + \alpha_2$)α_2 boundary. In fig.14 they are only provisional. The survey of the results indicates that approach to equilibrium is slow and that a new X-ray parameter investigation with annealing times of days or weeks rather than hours may give accurate results. The resistometric and calorimetric work of Hirabayashi and Ogawa (25) with slowly cooled alloys agrees with the present work in indicating that for a given composition in the range 25-30 atomic % the α($\alpha + \alpha_2$) boundary is at a somewhat higher temperature than the work of Owen and Roberts suggests (fig.15).

The X-ray films of alloy 34.14 has shown that the primary solid solution extends up to this composition at about 620° to 630°C. The thermal analysis results gave a peritectic horizontal at 627°C which terminates at about 34.5 atomic % cadmium (fig.13) in good agreement with the X-ray films.

Table 6

HIGH-TEMPERATURE X-RAY RESULTS FOR THE α BOUNDARIES.

AT.% Cd.	HRS.	TEMPERATURE, °C	RESULTS.
23.17 *	2	347 ± 4	f.c.c. tetragonal.
	½	365 ± 3	" "
	1	388 ± 3	" " splitting decreased.
	1	403 ± 2	f.c.c.
25 *	2	364 ± 4	f.c.c. + trace c.p.h.
	1	417 ± 2	f.c.c. + c.p.h.
	1½	455 ± 3	" "
		496	f.c.c. + trace c.p.h.
26	½	355 ± 5	f.c.c. + c.p.h.
	1	387 ± 2	" "
	2	412 ± 2	" "
	3	455 ± 2	" "
	120	310 + 2	" "
	40	533 ± 2	f.c.c. + trace c.p.h.
	1½	552 ± 2	f.c.c.
	1½	560 ± 2	f.c.c.
27 *	2	355 ± 4	faulted c.p.h.
	2	405 ± 5	" "
	2	450 ± 3	" "
32 *	4½	601 ± 2	f.c.c. + ? trace c.p.h.
	1	605 ± 2	f.c.c.
34.14 *	½	607 ± 3	f.c.c. + trace c.p.h.
	¾	617 ± 3	f.c.c.

Numbers in second column represent annealing time in hours immediately before exposure.

* Films were taken consecutively without cooling specimen to room temperature.

(c) Sharp and Diffuse Reflections in α_2 Films.

Several films of the α_2-phase showed reflections which were broadened and weakened (fig.2). The phenomenon was most marked on the gold-rich side, about 27 to 29 atomic % where the films, at first sight, showed no resemblance to a c.p.h. pattern. The results have been interpreted in terms of irregularly distributed growth stacking faults. It is likely that the faulting effect which introduces an f.c.c. stacking into the c.p.h. sequence was responsible for the twins observed in some α_2 alloys under the microscope.

An accurate measurement was made of the sharp lines of one high-temperature film of alloy 27 at 355°C which showed faulted c.p.h. Plots of the a parameter against the Nelson-Riley function were obtained for several values of c/a. Taking a linear variation of a with the extrapolation function as the criterion, then the optimum value of c/a is 1.6422 and a, by extrapolation, is 2.9230 kX. The extrapolation value of c is 4.8003 kX : the curve was almost but not quite linear. The c/a value is consistent.

Table 7

s = strong, m = medium, w = weak, d = diffuse,

H.T. = High-temperature, Q = Quench.

Composition / hkℓ	27(H.T.355)	27.5(Q.453)	29.63(Q.453)	34.14(Q.451)
10.0	?absent	d	v.s.	s
00.2	s	v.s.	v.s.	s
10.1	d	d (v.broad)	d	v.s.
10.2	absent	absent	w	s
11.0	m	s	s	s
10.3	absent	absent	d	s
20.0	absent	absent	v.w.	v.w.
11.2	s	s	v.s.	s
20.1	d	w + d	w + d	s
00.4	m	w	s	w
20.2	absent	absent	v.v.w.	w
10.4	absent	absent	v.v.s.	w
20.3	absent	absent	w + d	s
21.0	absent	absent	v.w.	v.w.
21.1	d	v.w.		s
11.4	v.s.	s	s	s
10.5	absent	absent	absent	s
21.2	absent	absent	absent	w
20.4	absent	absent	absent	w
30.0	v.w.	w	w	w
21.3	absent	absent	absent	s
00.6	s	w	w	w
30.2	s	s	s	s

The α_1-Phase

Three alloys of composition 23.17, 25 and 26 atomic % cadmium were investigated by the high-temperature method and it is with the results from these alloys with which this section is mainly concerned. As in the case of the α and α_2 alloys at 451°C and above, a microscopical identification of the α and α_1 phases was not possible in specimens of composition range 18.84 to 29 atomic % cadmium, annealed at 240°C for six to seven weeks.

The specimens intended for high-temperature work in the range 23-27 atomic % had been lump-annealed for eleven weeks at 351 ± 2°C and the filings prepared from the lumps were then strain-annealed for one week at the same temperature and water-quenched. In a few cases powders were prepared from the microscopical specimens for X-raying at room-temperature. The X-ray results are described below for each alloy (see also Table 6).

Alloy 23.17

The high-temperature films showed intense sharp lines. The pattern, by inspection, could be identified as tetragonally distorted f.c.c. Thus the (222) reflection did not split apart from resolution into the doublet for Cu Kα_1, and Cu Kα_2 radiation. The (400) and (331) reflections, on the other hand, to the high and low angle side respectively, of the (222) reflection were each split in three. The fact that only three out of the four possible reflections were visible may be attributed to coincidence of the CuKα_2 reflection from one plane with the CuKα_1 reflection from another. The behaviour of the (222) reflection confirms the conclusion that the film is an f.c. tetragonal pattern and not a mixture of two f.c.c. phases of slightly different dimensions.

The sharpness of the f.c. tetragonal reflections in the high-temperature films was a contrast to the rather diffuse reflections in the room-temperature film of the same specimen taken

before the high-temperature exposures. Here the pattern was diffuse f.c.c.

No superlattice lines were found in any film of this alloy whether at room temperature after quenching from 351°C or at high temperatures or after slow-cooling from high-temperatures. Films taken after slow cooling were f.c. tetragonal but diffuse.

The high-temperature exposures were taken at successively higher temperatures from 347°C upwards. The specimen was found to be f.c.c. at 403°C (Table 6) but f.c. tetragonal at lower temperatures. The exposure at 388°C indicated that the c/a ratio was closer to unity than at 365°C and below and that the c/a ratio approached unity with increase of temperature. The specimen was not allowed to cool down at any time until after the f.c.c. region had been reached at 403°C and after two exposures had been made at approximately 390°C and 395°C to confirm the reappearance of f.c. tetragonal structure. It is concluded that for this alloy the phase boundary is between 403° and 388°C.

Alloy 25

A film of a powder sample quenched from 240°C showed diffuse f.c.c. reflections one line identified as the f.c.c. (100) superlattice reflection and some sharp extra lines identified as c.p.h. The high-temperature films of another sample from the same ingot (Table 6) showed no superlattice lines and gave sharp reflections.

The film of alloy 25, taken after quenching from 351°C and before the high-temperature exposures, was found to be f.c. tetragonal though here the lines were more diffuse than in the films of alloy 23.17.

It is concluded from the high-temperature films of alloy 25 that the alloy is two-phase, f.c.c. + c.p.h. between 364° and 496°C.

Alloy 26

This alloy was very similar to alloy 25 but the c.p.h. reflections were stronger.

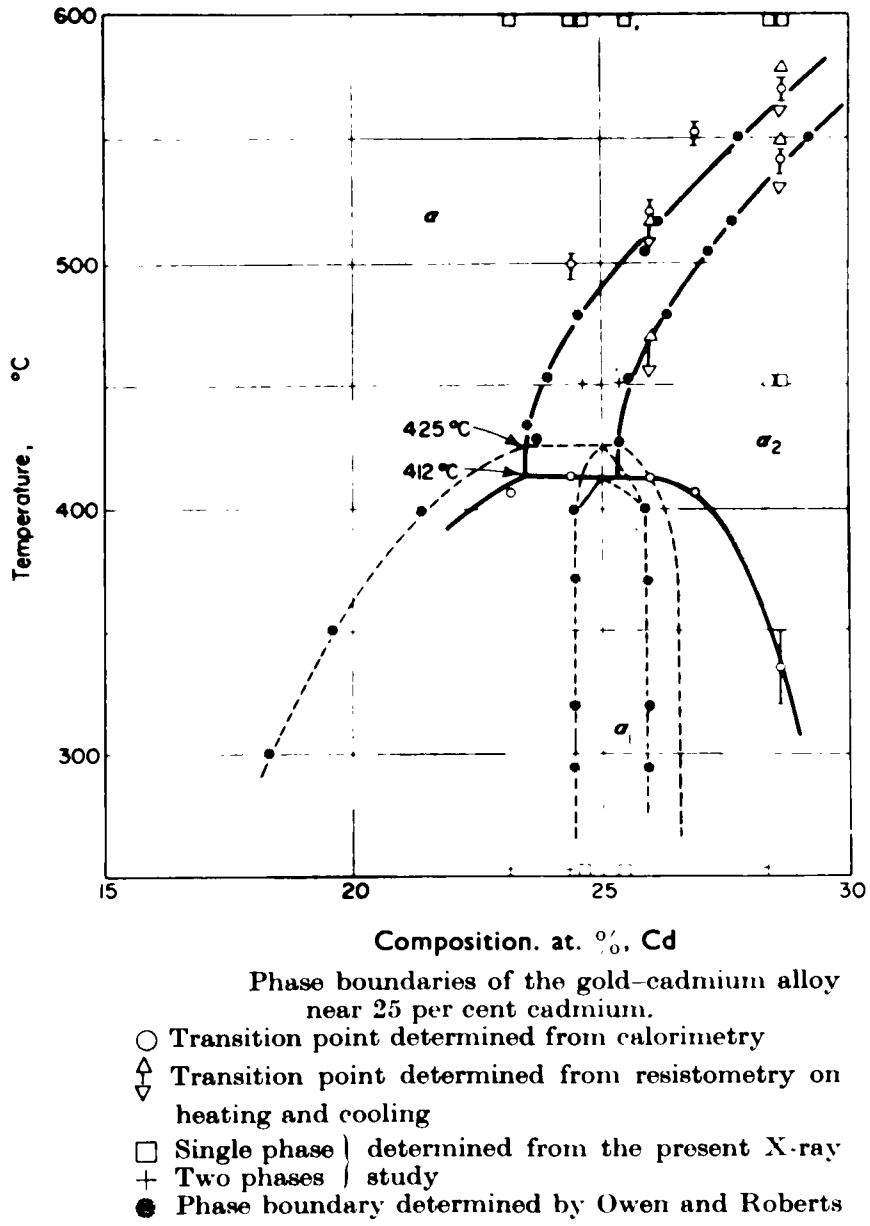

Phase boundaries of the gold–cadmium alloy near 25 per cent cadmium.

○ Transition point determined from calorimetry

△ ▽ Transition point determined from resistometry on heating and cooling

□ Single phase } determined from the present X-ray
\+ Two phases } study

● Phase boundary determined by Owen and Roberts

Fig.15. Hirabayashi and Ogawa, 1961.

(a) The Boundaries of the α_1-Phase

The results from alloy 23.17 place the α/α_1 boundary below 403°C. This is 15°C below the boundary drawn by Owen and Roberts (fig.14).

No evidence was found in any of the films of alloy 23.17 for a two-phase region $\alpha + \alpha_1$. The spacings of α and α_1 are very close (7, 9) and it is therefore possible that the reflections from the two phases may coincide. As far as the evidence available from the present work is concerned, a definite choice between the two possibilities cannot be made. The sharpness of the (222) reflection makes it reasonable to assume that the f.c. tetragonal films were one-phase. Therefore, in fig.14, the $\alpha(\alpha + \alpha_1)$ and $(\alpha + \alpha_1)\alpha_1$ boundaries are drawn close together and parallel to one another between 403° and 388°C.

The appearance of an f.c.c. phase at 25 atomic % cadmium would suggest that the c/a ratio changes towards unity as the composition changes from 23.17 to 25 atomic % cadmium. This interpretation was given by Byström and Almin (9) who claimed that the diffuseness in their f.c.c. patterns at 25 atomic % cadmium concealed f.c. tetragonal splitting. Owen and Roberts (7) report definite f.c. tetragonal patterns at 25 atomic %. Moreover, their lattice parameters do not extrapolate to $c/a = 1$ at 25 atomic %.

(b) The α'-Phase

An alternative interpretation adopted in the present work is that the f.c.c. phase observed at 25 atomic % is not the α_1-phase where $c/a = 1$ but another α-phase. In this case there must be a two-phase region between 23 and 25 atomic %. The f.c.c. phase is denoted α' in figs.12 and 14.

The suggestion of a new α phase means that there must be a new horisontal in the region of 400°C. The high-temperature X-ray results from alloy 25 gave no evidence for any horizontal whether peritectoid or eutectoid. Alloy 25 was f.c.c. + c.p.h. until 496°C

where the c.p.h. lines had almost vanished.

Hirabayashi and Ogawa (25) carried out specific heat measurements on an alloy of composition 24.4 atomic % cadmium which was first annealed at 550°C and then slowly cooled to room temperature for a period of between one and two weeks. The sharp maximum suggesting an 'infinite' specific heat at 412°C is interpreted as the peritectoid reaction $\alpha + \alpha_2 \rightleftharpoons \alpha + \alpha_1$. The result is in good agreement with the effect observed at 415°C in elastic moduli/temperature curves for slow-cooled alloys (4). No evidence has been found for the 425°C peritectoid of Owen and Roberts.

In the new version of the Au_3Cd region using the results of the present work (Fig.14) the 412°C peritectoid of Hirabayashi and Ogawa is accepted. The α'-phase requires another horisontal and it is assumed to be at 407°C. (This temperature is chosen because of the specific heat peak at 412°C with an alloy at 26.9 atomic % cadmium interpreted as the reaction $\alpha_2 \rightleftharpoons \alpha_1 + \alpha_2$). At 412°C the reaction is $\alpha_1 \rightleftharpoons \alpha + \alpha_2$ and at 407°C it is $\alpha' \rightleftharpoons \alpha_1 + \alpha_2$. Alloy 25 is f.c.c. + a little c.p.h. at 364°C. Therefore the boundary $\alpha'(\alpha' + \alpha_2)$ must be slightly to the gold-rich side of 25 atomic % cadmium.

Alloy 26 is f.c.c. + c.p.h. from 412°C downwards and the intensity of the c.p.h. reflections is greater in proportion to the f.c.c. reflections than was found from alloy 25. Alloy 26 is therefore nearer the middle of the two phase field $\alpha' + \alpha_2$.

Alloy 27 is faulted c.p.h. between 450° and 350°C. The gold-rich limit of the one-phase α_2 field must be between 26 and 27 atomic % below 450°C. This is in exact agreement with Owen and Roberts.

No data are available for a two-phase region $\alpha_1 + \alpha'$ but the possible boundaries are sketched in fig.14 where it is assumed that the $\alpha_1(\alpha_1 + \alpha')$ boundary coincides with the $(\alpha + \alpha_1)\alpha_1$ boundary of Owen and Roberts.

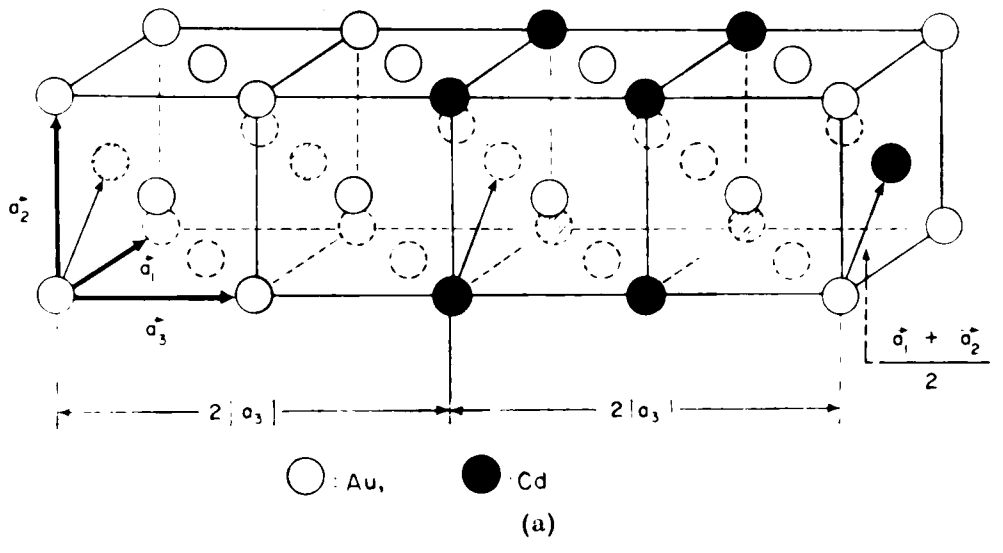

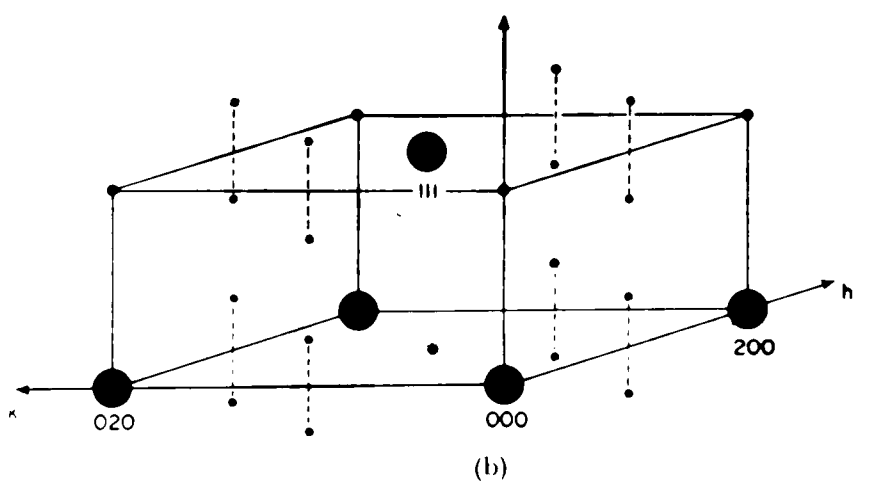

(a) One dimensional anti-phase domain structure of Au_3Cd. (b) Intensity distribution in reciprocal lattice corresponding to (a).

Fig.16. Unit cell of Au_3 Cd (Hirabayashi and Ogawa).

The diagram drawn in fig.14 must not be regarded as more than a speculative interpretation designed to reconcile the facts from this work and others. Not all the facts have been accounted for and discrepancies are discussed below.

(i) No peritectoid was detected in the high-temperature films of alloy 25. A possible explanation is that the α- and α'-phases are both f.c.c. with similar lattice parameters.

(ii) The 407°C horizontal is assumed because of the specific heat peak found at this temperature by Hirabayashi and Ogawa with an alloy of composition 26.9 atomic % cadmium. They interpret it as due to the reaction $\alpha_2 \rightleftharpoons \alpha_1 + \alpha_2$. The peak is very sharp but, unlike the peak at 412°C, is not an 'infinite' peak which would be expected for a peritectoid. On the other hand, high-temperature films of alloy 27 and quench films of alloy 27.5 were faulted c.p.h. and show (when compared with films of alloy 26) that the boundary is certainly a vertical boundary between 26 and 27 atomic %, from 400°C down.

(iii) It would appear that disagreement between Owen and Roberts and Bystrom and Almin over the question of ordering in the α_1-phase must be due to different quenching methods. The former workers used a special quenching furnace. The latter did not. The more rapid the quench the more likely the ordering reaction will be suppressed. But it was not found that superlattice lines appeared in films of alloy 23.17 after cooling slowly from about 400°C. Another puzzling fact is that Köster and Schneider (4) should have reported that the α_1-phase is stable up to 475°C. Although there is now good evidence that the α-phase transforms slightly, undergoing an ordering reaction, on quenching, no one else has reported similar results from quenching experiments.

(iv) Owen and Roberts and Hirabayashi and Ogawa agree in drawing an α_1-region centred about the composition Au_3Cd. The results of Bystrom and Almin and of the present work suggest an f.c.c. phase at Au_3Cd. Bystrom and Almin stated their films were diffuse.

The films of alloy 25 were reasonably sharp and did not mask tetragonal splitting.

(c) Ordering In The α_1-Phase

The absence of superlattice reflections in films of alloy 23.17 makes it certain that at high temperatures (from 350°C upwards) the α_1-phase does not show long-range order. The lines were strong and sharp and any superlattice reflections should have been easy to detect. The ordered unit cell reported by Hirabayashi and Ogawa (Fig.16) was obtained from quenched alloys. The one-dimensional anti-phase domain structure is similar to Au_3Zn and Ag_3Mg. A regular arrangement should produce superlattice reflections. Their absence means that the α_1-phase at high-temperatures is either (i) a simple disordered f.c. tetragonal structure or (ii) a series of domains each of which is highly ordered but which are too small for superlattice diffractions to occur.

It is known that ordering is often associated with tetragonal splitting of cubic reflections and the degree of splitting (i.e. the magnitude of the c/a ratio) has been suggested as a measure of the degree of ordering (37). Alloy 23.17 showed a change in the c/a ratio towards unity as temperature increased and this may be due to the increase of disorder due to increasing temperature. Therefore it is unlikely that the α_1-phase held at equilibrium e.g. at 350° is an ordered structure but with small irregular domains and no long-range order.

DISCUSSION

1. THE LIQUIDUS AND SOLIDUS

The liquidus and solidus of the gold-cadmium system may now be compared with those of other systems of the IB elements. The systems and components selected for comparison are denoted by their chemical symbols, e.g. Au-Cd, Ag.

Systematic comparisons of the liquidus and solidus and other comparisons to follow will require an estimate of the electrochemical factor and the choice of scale is discussed first.

(a) The Electrochemical Factor.

The electrochemical factor may be regarded as a measure of the difference in electronegativity of the components in a system of two or more components. This concept originated in the realisation that where an element, which is relatively electronegative, is dissolved in a metal, a stable intermediate phase, often analogous to a stoichiometric chemical compound, is likely to be formed at the expense of the primary solid solution (44). This effect, often described as the electronegative valency effect, may be used in interpreting alloy behaviour even when no markedly stable intermediate phases are present. A scale giving an estimate of relative magnitudes of the factor is therefore necessary in making such interpretations. The choice of scale is difficult because in most cases measured quantities do not refer directly to alloys.

Previous discussions have made an estimate of the electrochemical factor by reference to the standard electrode potentials of the elements (42, 49). This approach is open to the objection that, in effect, it is a comparison of the free energies of the elements in their standard states and in aqueous ionic solution. An independent scale, proposed by R.S. Mulliken, is the mean of the electron affinity and the first ionisation potential of the elements but it is handicapped by lack of data on the electron affinities. Another scale is due to Gordy and Thomas (27). Their

scale depends only on nuclear screening by the electron shells and on the atomic radius. An independent approach of this kind might appear promising but there are difficulties in estimating the exact screening in some cases.

Pauling's scale of electronegativities is calculated by applying simplifying assumptions to bond energy date. The bond energies are regarded as being ionic or covalent in origin, the proportion of the ionic contribution depending on the difference in electronegativity. A scale of electronegativities has been derived for all the elements (26) which agrees well with their general chemical properties. Similar results for nearly all the elements have been obtained by Haissinsky from bond energy data and are to be found in 27. The scale of Gordy and Thomas (27) is very similar but the discrepancies in Group VIII and the B sub-groups led the authors to believe their estimate of nuclear screening to be incorrect.

In metallic systems a large electrochemical factor results in a large ionic contribution to the total cohesive energy and therefore stabilises intermediate phases. This concept is analogous to the concept underlying the bond energies of chemical compounds. Therefore Pauling's values are adopted in the present discussion. But it must be emphasised that neither Pauling's scale nor other scales, described below and depending usually on chemical properties, can be wholly satisfactory as a measure of the electrochemical factor in alloys where the environment of an atom will be very different from that in a chemical compound.

With other methods (see ref.27) the test of reliability is still the Pauling scale. One, constructed from the photoelectric work function of elements, agrees well with the Pauling electronegativity values. Another is based on a relation between bond force constants, bond lengths and bond orders of hydride bonds and is also in good agreement with Pauling but several elements

diverge; gold is one puzzling exception with an electronegativity value of 3.1, rather higher than Pauling's value of 2.4.

For the purposes of the discussion the electrochemical factor is given by the difference in electronegativity, Δx, of the two components, i.e.

$$\Delta x = x_M - x_S$$

Here M = Cu, Ag or Au and S is the second component.

x values on Pauling's scale are sometimes sensitive to the valence states of the elements. The values selected refer to the group valencies of the elements concerned and are taken from ref.26, p.93.

Cu 1.9, Zn 1.6, Ga 1.6, Ge 1.8, As 2.0.

Ag 1.9, Cd 1.7, In 1.7, Sn 1.9, Sb 2.1

Au 2.4, Hg 1.9, Mg 1.2, Al 1.5.

Pauling gives no value for Sb (V) and accordingly Haissinsky's value (27) has been adopted. Pauling considers his values to be reliable to 0.1.

(b) The Liquidus in Systems of Ag and Au

Fig.17 gives a reproduction of the liquidus throughout the whole composition range in the systems of Ag and Au with the solutes Mg, Hg, Cd and Zn. The Δx value for each system is included in this figure.

It has been pointed out previously (42) that there is a much greater tendency for b.c.c. 3/2 electron compounds to be ordered in Au systems than in Ag systems. Ordering has been attributed (i) to strain relief and (ii) to a high electrochemical factor. Since Ag and Au are 'full' metals with similar ionic and atomic diameters the second factor is probably the more important. The same authors also point out that the Au alloys usually show maxima, unlike Ag, and conclude that the increased ionic contribution to the cohesive energy is responsible for raising the temperature

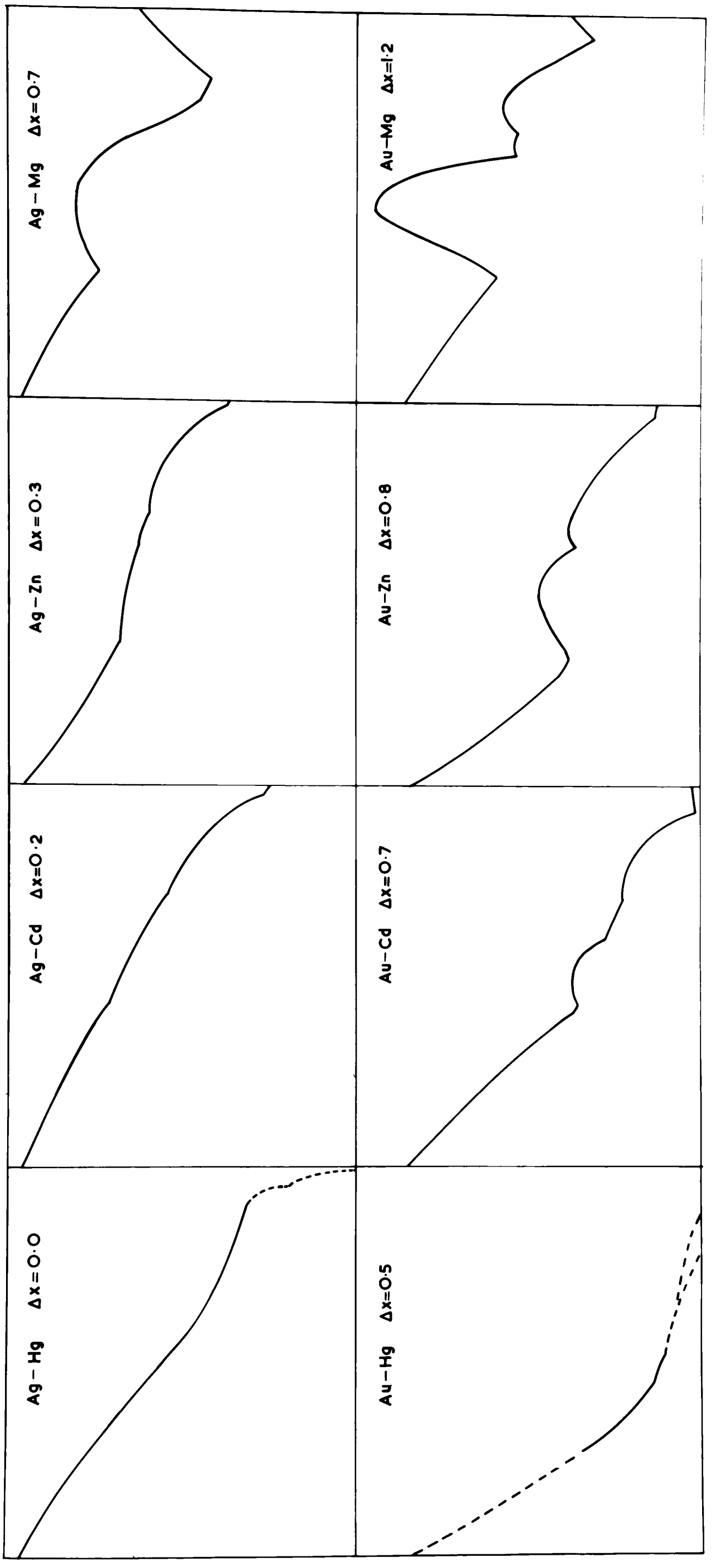

Fig.17. The liquidus in some binary systems of Ag and Au.

at which liquid is in equilibrium with solid.

The rows of diagrams in fig.17 illustrate this generalisation. In the Ag row, on going from left to right in the direction of increasing Δ x, it is evident that the liquidus tends to fall less steeply. It consists entirely of a series of peritectics in all systems except Ag–Mg, where a maximum appears.

The row of Au diagrams is very similar but because of the much larger electrochemical factor the maxima appear earlier in the sequence, at Au–Cd, and become more pronounced with increase of electrochemical factor. There are no maxima in Au–Hg, Δ x = 0.5, but the liquidus appears to fall less steeply than in AgHg, Δ x = 0. In Au–Cd the maxima can only just be observed. In Au–Zn and Au–Mg they become much more prominent, the β'-phase of Au–Mg melting 90° above the melting point of pure gold.

(c) The α-Liquidus in Some Gold Systems.

The α-liquidus of the gold-cadmium system, plotted against the electron : atom ratio, is compared with the α-liquidus of Au–In, Au–Sn and Au–Sb in fig.18 and with the α-liquidus of Au–Zn, Au–Mg and Au–Hg in fig.19. The curves are taken from Haneen, the readings being accurate to $\pm$5°C. Since the Au–Sn liquidus is incomplete and conflicting curves have been drawn for Au–Hg the plots in figs.18 and 19 for these systems are only approximate.

A plot of the liquidus curves for the systems Au–Cd, Au–In, Au–Sn and Au–Sb against atomic % solute shows that for a given amount of solute the liquidus depression increases in the order Cd, In, Sn and Sb. If the curves are plotted against the electron : atom ratio, obtained by assigning the components their group valencies, then as fig.18 shows, the curves for Au–In, Au–Sn and Au–Sb are almost superposed while that of Au–Cd slopes more steeply. It is clear that in dilute solutions, at least,

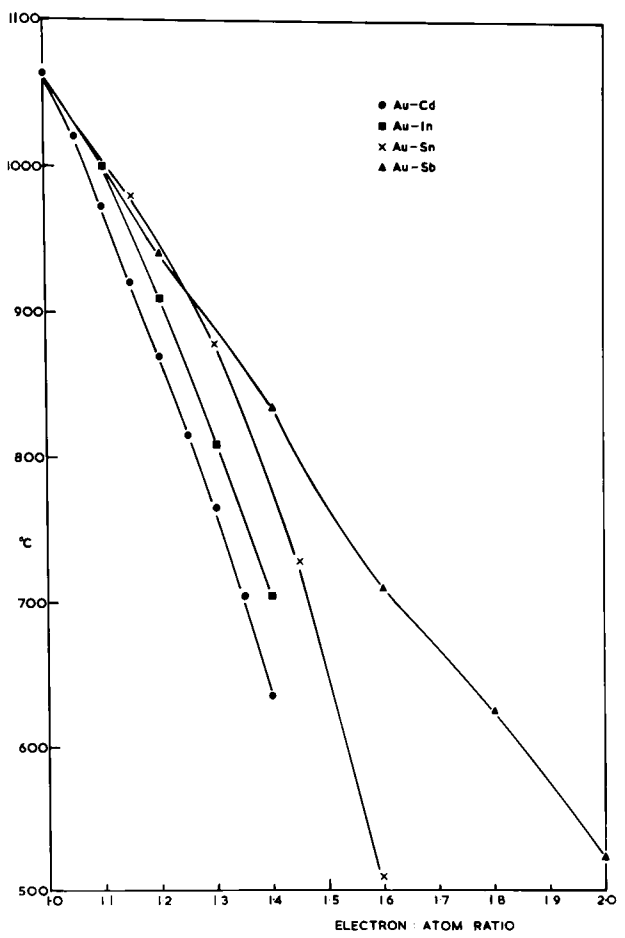

Fig.18. The α -liquidus in binary Au-systems with solutes from Groups IIB to VB.

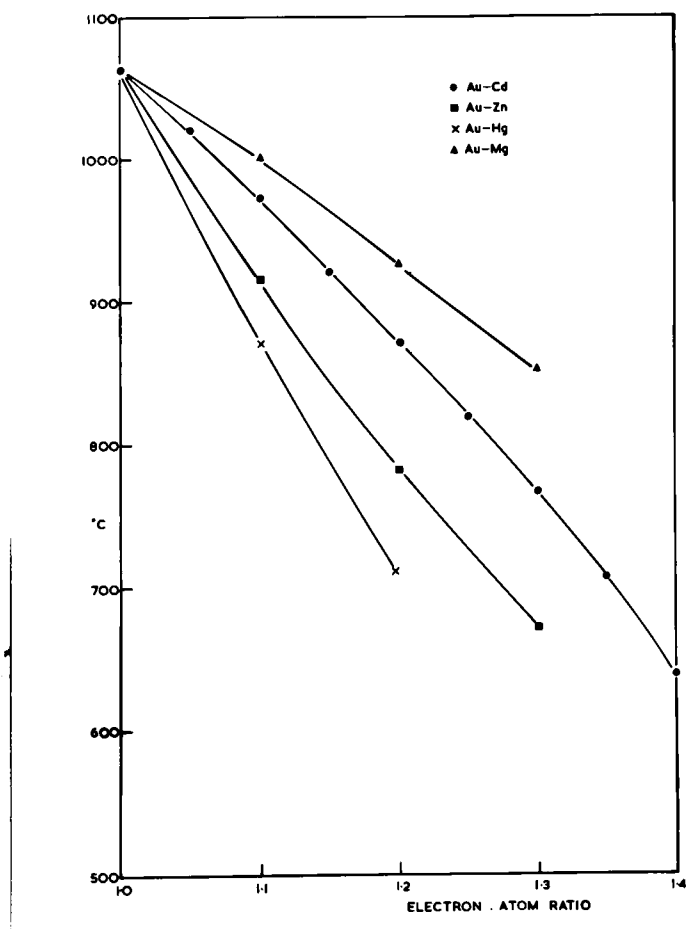

Fig.19. The α -liquidus in Au-systems with divalent solutes.

the electron concentration is the controlling factor in determining the extent of depression of the liquidus by the solute.

In fig.19 the liquidus curves for the divalent solutes are seen to be widely spaced with no tendency to become superposed. The liquidus depression by a given amount of solute decreases in the order Hg, Zn, Cd and Mg.

Table 8 gives the Δ x values for the above systems, the size factors calculated from the Goldschmidt diameters of co-ordination number 12 and the observed mean lattice distortions of the Au solvent at 18°C. The spacings for the Au solid solutions were taken from refs.28 and 29. The atomic proportions of solute required to give a constant electron : atom ratio are as 12: 6: 4: 3 for Groups II to V.

Table 8.

System	Δ x	size factor	Lattice Distortion per at.% solute	Lattice Distortion at constant e/a
Au-Cd	0.7	5.7	0.0017	0.0204
In	0.7	9.1	0.0027	0.0162
Sn	0.5	9.8	0.0037	0.0148
Sb	0.3	12.1	0.0050	0.0150
Au-Mg	1.2	11.1	(no data)	
Zn	0.8	-4.5	-0.0018	
Hg	0.5	7.7	0.0024	

Previous work on copper and silver alloys by Hume-Rothery and Burns (30) shows a very similar tendency for the liquidus curves to be superposed and the deviations from superposition may readily be correlated with the lattice distortion at constant electron concentration. The greater the distortion the greater the liquidus depression. A comparison of fig.18 with Table 8 shows that this generalisation is confirmed.

Au-In, Au-Sn and Au-Sb have liquidus curves which are nearly superposed at low electron concentration but it is possible to distinguish Au In from the other two. Au-Sn and Au-Sb have identical lattice distortions while that of Au-In is somewhat larger. The curve of Au-Cd shows no tendency to superpose at any solute concentration and falls more steeply. The lattice distortion is correspondingly larger.

The physical meaning of this relation is clearly the strain on the solvent lattice imposed by the solute. The greater the strain the more the free energy of the solid will be increased relative to that of liquid. The melting point will therefore be lower, resulting in a liquidus curve which falls more steeply.

Another generalisation due to Hume-Rothery and Burns (30) is the relation between the slope of the liquidus curves, plotted against the electron : atom ratio, and the electrochemical factor. Since the electrochemical factor has an influence on the bonding of the metal lattice and therefore on the heat of fusion, it is possible that a correlation may be found with the behaviour of the α-liquidus. It has been stated (30) that the greater the factor the greater the liquidus depression at constant electron : atom ratio. As before, this generalisation is based only on the Cu and Ag alloys with Group B solutes belonging to the same period as the solvents. From Table 8 it can be seen that the Δ x values are consistent with this generalisation.

A simple correlation with the Δ x values or lattice distortions is not possible for the divalent solutes in fig.19. The relative positions of the curves for Au-Cd and Au-Hg may be accounted for if it is assumed that the greater lattice distortion in Au-Hg outweighs the greater electrochemical factor in the former. It is also necessary to argue that the

contraction of the Au lattice by Zn has a less unfavourable effect on its stability than an equivalent expansion would have. But the behaviour of the Au–Mg liquidus cannot be interpreted in this way. Unfortunately no lattice spacing data are available for the solid solution of Mg in Au but the large positive value of the size factor, whether calculated from Goldschmidt diameters or interatomic distances, makes it unlikely that lattice distortion would be less than for the other divalent solutes under consideration. With the largest Δ x value in the series the Au–Mg curve is above all the other curves in Fig.19. This is probably associated with the fact that Mg belongs to a different part of the Periodic Table and may be due to the absence of a d-shell.

(d) α-Solidus : α-Liquidus Equilibria.

The data available are insufficient for a systematic comparison of solidus : liquidus equilibria in gold alloys. The above relationships for the solidus are found to be the same as for the liquidus in Au–Cd, Au–Zn and Au–Sn where data for the solidus are available.

A calculation of the latent heat fusion of Au has been made from the liquidus and solidus results for Au–Cd, using the equation corresponding to ideal conditions, i.e. infinite dilution: $\Delta S/\Delta T - \Delta l/\Delta T = L_f/RT_m^2$. Here ΔS = change in solidus curve, Δl = change in liquidus curve for a given change ΔT in temperature, and T_m the melting point of pure gold. The calculated value of L_f the latent heat of fusion is about one third of that reported in the literature. This result is hardly unexpected considering that the solidus and liquidus in Au–Cd were not investigated below 10 atomic % solute, a solute at which deviations from ideal mixing may become significant. If the α-liquidus and α-solidus inflect towards one another

at the melting point of pure Au then the slopes of the tangents to the two curves at infinite dilution will give a value of L_f corresponding to the known values in the literature.

It was found empirically (30) that $\bar{x}/T$ curves in the series Cu (Zn, Ga, Ge, As) and Ag (Cd, In, Sn, Sb) are controlled mainly by the electron concentration and that deviations were very closely related to the lattice distortion at constant electron concentration, increased distortion depressing the curve. Here $\bar{x}$ is defined as $\frac{1}{2}(x_s - x_l)$ where x_s and x_l are the atomic fractions of solid and liquid at temperature T on the solidus and liquidus. Exceptions to the general rule are Cu-Ge and Cu-As where marked depression of the $\bar{x}/T$ curve occurred without being accompanied by high lattice distortions. Cu-As showed the steeper fall and it was inferred that a high electrochemical factor will depress the curve. On Pauling's scale the electrochemical factors are as follows.

Cu-Zn	Cu-Ga	Cu-Ge	Cu-As
0.3	0.3	0.1	-0.1

The factor actually decreases from Cu-Zn to Cu-Ge and is negative for Cu-As. It is interesting to note that from the scale depending on the photoelectric work function of the elements the Δ x values are now respectively 0.3, 0.2, -0.1 and -0.3. This suggests that when the solute is negative with respect to solvent the $\bar{x}/T$ curve will be depressed, and that the greater the negative value of Δ x, the greater the depression for a given electron concentration. The following prediction may then be ventured, that when a complete set of data is available for Au alloys in the series Au-Cd to Au-Sb there will not be a marked $\bar{x}/T$ curve depression in the series, since no marked lattice distortions are found and the Δ x values are positive, whether on Pauling's scale or on any of the others mentioned above.

2. INTERMEDIATE PHASES

The Au-Cd system has five intermediate phases besides the terminal solid solutions. Three are known to have low-temperature modifications. All but one, the α_2-phase, fit into the general pattern of electron compounds set by systems of the IB elements.

The γ - and ϵ - phases belong to the groups of electron compounds found at an electron : atom ratio of 21/13 and 7/4 respectively. No information on the lattice spacings or on the nature of the different high-temperature modifications of the γ -brass structure seems to be available. It is stated (28) that ϵ is c.p.h. According to Westgren and Phragmén (31) an alloy containing slightly more than 75 atomic % cadmium (electron : atom ratio 7/4) is similar to γ " Au-Zn with 90 atoms to the unit cell, but this is unlikely; the cadmium content of the alloy was probably lower than 75%.

The results for the Au-rich alloys are discussed below in detail. Au-Tl, Au Pb and Au-Bi are not included. The diagrams are simple eutectic-type diagrams with very restricted solid solubility and no intermediate phases. It is thought that incomplete ionisation, known to be characteristic of their chemical compounds (Tl(I), Pb(II) and Bi (III)) is responsible, giving very unfavourable size factors.

(a) The Au Cd β'-phase.

The β'-phase is narrow at low temperatures about 4 atomic % wide. The range more than doubles with increase of temperature, reaching a maximum of 9 atomic % at about 620°C. At all temperatures investigated by high-temperature X-ray techniques the structure is ordered b.c.c. Long range order persists up to at least 5 degrees below the melting point, 629°C. The two low-temperature equilibrium modifications postulated by Birnbaum (15ii) below 100°C are also b.c.c. with slightly different dimensions.

An account of various effects recorded by dilatometry and electrical resistance measurements at about 300° to 270°C has been given in the Introduction. These effects are not understood though they have been wrongly associated with the transformation to the metastable orthorhombic and tetragonal phases and with an order-disorder change. The transformation temperature is now known to be below 100°C and the β'-phase is certainly ordered up to about 624°C.

From the high-temperature film of alloy 47.71 at 620°C it is calculated that the alloy is about 90% ordered. This result should be compared with Kubaschewski's calorimetric measurements of a 50 atomic % Au-Cd alloy (11). He found the entropy of melting to be 2.38 ± 0.14 cal./degree/g.m.atom. This figure differed from the sum of the entropies of melting of the pure metals by + 0.01 ± 0.25 cals/degree/gm.atom. It was concluded that the contribution of the entropy of ordering to the entropy change on melting the β'-phase was zero, i.e. the liquid is in equilibrium with disordered b.c.c. Kubaschewski's result would appear to be incorrect in view of the X-ray results with alloy 47.71 and the high degree of order at 620°C. It is possible that there is a rapid decrease in the degree of ordering between 620° and the melting point, 629°C (a co-operative change), giving disordered b.c.c. just below the melting point. However, it is more probable that the liquid is in equilibrium with ordered b.c.c.

Kubaschewski was able to detect an entropy of ordering in the melting entropy of β'-Au-Zn. The difference between the results for Au-Cd and for Au-Zn is probably due to the smaller electrochemical factor in the former system.

The greater stability at high temperatures of the b.c.c. β'-phase in Au-Cd and in many other systems is illustrated by the increase in composition range with increased temperature and sometimes by the appearance of a low-temperature close-packed

modification. Zener's interpretation in terms of the entropy factor (32) is as follows. The β -phase in Cu-Zn is known to have a high elastic anisotropy between the two lattice directions $[111]$ and $[100]$. The amplitudes of thermal vibration in the (110) plane and the $[\bar{1}10]$ direction are large. The entropy contribution from this source to the free energy of the b.c.c. phase will be large at high temperatures but as temperature is lowered, the $T\Delta S$ term in the expression for the free energy $\Delta G = \Delta H - T\Delta S$ will be less important. Consequently, as temperature falls, the free energy of the b.c.c. phase will rise relative to that of the adjacent α- and γ-phases and the common tangents to the respective free energy curves will give the β-phase a narrower composition range.

Zirinsky (33) has shown that at equivalent temperatures and compositions the degree of elastic anisotropy is greater in β'-Au-Cd than in β-Cu-Zn. The importance of the entropy as a factor contributing to the stability of the β'-phase at high temperatures will then be correspondingly greater. It has been suggested that this is the reason for the fact that it is impossible to retain the b.c.c. Au-Cd phase to room temperature on water-quenching at a cadmium content lower than about 50 atomic % (34).

The ordering of the Au-Cd β'-phase and the β'-phase of other Au systems is not so easy to reconcile with the above outline. The lower entropy associated with a superlattice means a larger free energy at any one temperature, compared with the disordered b.c.c. phase. It seems likely that while disordered b.c.c. structures at high temperatures may owe their stability to a high entropy the lower energy of the superlattice may play a more important part in the stability of the ordered b.c.c. structures.

(b) The α_2-Phase

(i) Stacking Faults

In the present work many of the α_2 alloys gave X-ray films in which a large proportion of the fundamental c.p.h. reflections were broadened, weakened or almost entirely absent. Similar effects have been reported for the α_2 phase in refs. 9, 23 and in the recent work of Hirabayashi and Ogawa (24).

Table 7 gives details of the behaviour of the α_2 c.p.h. reflections and typical films are reproduced in fig.20. It is known that line-broadening can be a result of small crystal size. But in Table 7 it can be seen that only some lines are affected and broadening cannot be interpreted in terms of crystal size. Thus if it is considered that the crystals are elongated in the c direction but are of very small dimensions in the other directions this would explain the persistence of sharp 00.l diffractions. However, the 11.4 reflections are also strong and sharp which would not occur if crystal size were the explanation (9). A similar objection can be made to the suggestion that the broadened lines were due to segregation. Another interpretation of weakened lines is preferred orientation. Given crystals of a characteristic shape it is possible for powder specimens, prepared either by rolling a glass fibre in the powder or by filling a silica capillary, to give films in which some reflections are strengthened and others are weakened or even entirely absent. But this effect would not produce very broad lines as was the case with the α_2 alloys.

The clue to the interpretation of the phenomenon was its marked sensitivity to composition, both in high-temperature and in room-temperature films. At 34 atomic % cadmium a normal c.p.h. pattern was found. As the cadmium content decreased certain lines

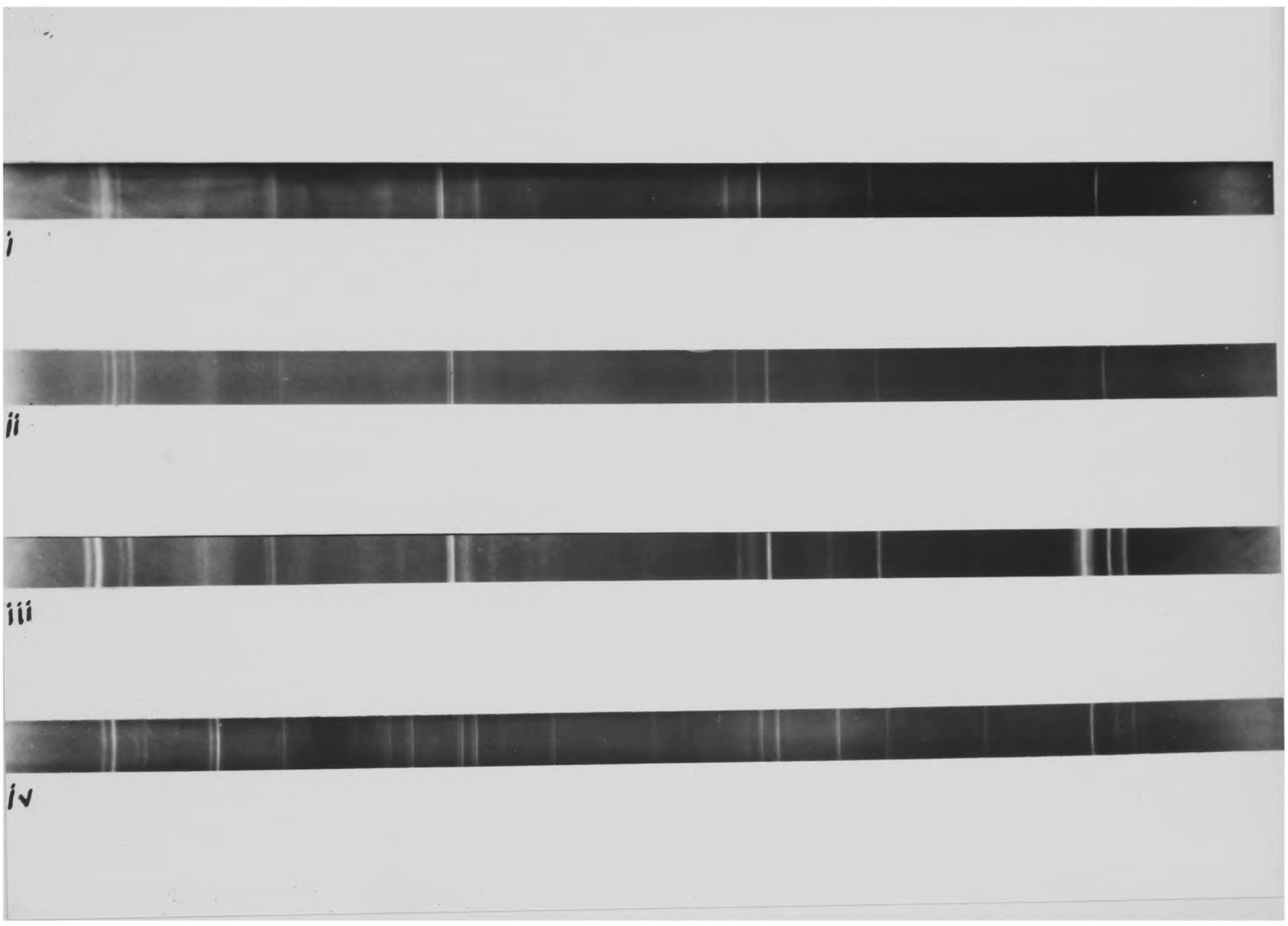

Fig.20. X-ray films of the α_2-phase.

(i) Alloy 26. High-temperature, 355°C. f.c.c + c.p.h.

(ii) Alloy 27. High-temperature, 355°C. faulted c.p.h.

(iii) Alloy 29.63. Quenched from 453°C. faulted c.p.h.

(iv) Alloy 34.14. Slow-cooled from 594°C. after high-temperature exposure. c.p.h.

became progressively weaker and broadened until at 27 atomic % a pattern was found which, at first sight, resembled an f.c.c. pattern with the (200) reflection missing and a strong high-angle extra line. It was found that on passing from 34 to 27 atomic % cadmium at temperatures from room-temperature to 450°C the X-ray films show a change from the normal c.p.h. pattern to a pattern in which many c.p.h. lines have become very weak, but there is no such effect on increasing the temperature of exposure of alloy 34.14.

Bystrom and Almin were the first to interpret the behaviour of the α_2 c.p.h. reflections in terms of the stacking fault theory originally developed for cobalt (35). According to the theory these reflections for which h-k = 3n where n is any integer, including zero, are sharp. All 00.l lines are sharp. Table 7 shows that these requirements are fulfilled by the films obtained in the present work. The interpretation was confirmed by Massalski (23) (who obtained continuous intensity data) and carried a stage further by the single-crystal work of Hirabayashi and Ogawa (24). They showed that in an alloy of composition 25.5 atomic % cadmium, water-quenched from 450°C, the α_2-phase (co-existing with α) was faulted. Those c.p.h. reflections where h-k = 3n were sharp while reflections with h-k not equal to 3n were drawn out into long streaks parallel to the 00.l rel-axis. The α-phase was also considered to be faulted because of the occurrence of streaks associated with the α-phase reflections.

The single-crystal results of Hirabayashi and Ogawa gave a unit cell for the α_2-phase where c is twice the length given by other workers but a is unchanged. The spacings given for the alloy containing 25.5 atomic % cadmium are:

$a = 2.910$ Å $c = 9.558$ Å

and from the intensity distribution in reciprocal space the atom positions are found to be :

$$2a : \quad 0\,0\,0, \qquad 0\,0\,\tfrac{1}{2}.$$

$$2c : \quad \tfrac{1}{3}\,\tfrac{2}{3}\,\tfrac{1}{4} \qquad \tfrac{2}{3}\,\tfrac{1}{3}\,\tfrac{3}{4}.$$

where Au and Cd atoms are distributed at random. The unit cell may be described as a structure in which stacking faults in the c direction appear regularly after each two close-packed planes of atoms, i.e. ... A B A C A B A C ... But from the broadening of reflections Hirabayashi and Ogawa conclude that the real crystal has some irregular faulting.

The unit cell of the α_2-phase as drawn by the above workers has been used in an attempt to index the extra lines observed in the α_2 films in the present work, but without success. Schubert and Wegst (25) have reported superlattice lines in quenched α_2 alloys but they have not been confirmed.

(ii) Energy Considerations And Stacking Faults

The faulting effect has been reported for other alloy systems and also in crystalline solids like graphite and the micas where the cohesive forces between basal planes are weak (36). When the two structures f.c.c. and c.p.h. have very nearly equal free energies in a given system then it is to be expected that the appearance or otherwise of one phase or the other will be very sensitive to the slight energy variations associated with the details of specimen preparation. Pure cobalt is an example. The transition point for the transformation c.p.h. $\rightleftharpoons$ f.c.c. is uncertain being about 400 to 450°C and both phases co-exist over quite a wide range of temperature. The apparent contradiction to the Phase Rule has been accounted for by reference to the fact that the two phases are nearly equal in free energy: the c/a ratio of the c.p.h. phase is 1.623, quite close to the ideal of 1.633 for the f.c.c. structure. The similarity of the two stackings has a second consequence, the appearance of stacking faults.

The stacking sequences for the f.c.c. and c.p.h. structures are as follows.

f.c.c.	c.p.h.
... A B C A B C A B C ...	... A B A B A B ...

The symbols A, B and C represent the close-packed layers stacked in the c direction. When the free energies of the two stacking sequences do not differ much mistakes in the c direction may be expected thus :

f.c.c.	c.p.h.
... A B C A B C B A C B A ...	... A B A B A C A C ...

The insertion of a single fault into the f.c.c. layers will convert the stacking sequence into two sequences, one of which is the mirror image of the other, i.e. the stacking is twinned on the fault plane(arrowed). The twinning effect cannot appear in the c.p.h. layers and the stacking sequence is altered from ... A B A B ... to ... A C A C ... The likelihood of a fault being inserted into a sequence will depend on the lattice toleration; faulting, as in cobalt, will be frequent when the two structures are similar in free energy. While there is one fault in each of the sequences given above, several appear in the following sequence

... A B A B A C A B A C A C A B A C ...

The f.c.c. stacking is not easily distinguished from c.p.h. stacking in this case.

Previous treatments of the faulting effect in alloy systems (37) illustrate the dependence of faulting on composition by reference to hypothetical free energy - composition curves such as those sketched in fig.21(i) for the f.c.c. and c.p.h. phases. At composition C_1 the c.p.h. phase has a much lower free energy than the f.c.c. phase and is unlikely to tolerate mistakes in the c.p.h. sequence. With change of composition from C_1 to C_4 the free energies approach one another and the probability of faulting increases.

The behaviour of the Au-Cd α_2-phase may now be interpreted with the help of this diagram: If compositions C_1 to C_4 correspond to alloys 34.14, 29.63, 27 and 26 respectively at temperature 450°C, it is clear how the faults should be undetectable in alloy 34.14 and increase in density through alloys 29.63 to 27.

(iii) The Peritectic-Eutectic Reaction

It is of interest to compare the free energy relationships suggested above for α_2 and α with the relationships which would be indicated by the observed equilibria at the melting points of the α and α_2 phases. The peritectic melting point is 627°C where the reaction is α + liquid $\rightleftharpoons \alpha_2$. The eutectic melting point is 626.5°C, half a degree below the peritectic and the reaction is $\alpha_2 + \beta' \rightleftharpoons$ liquid. This curious result, with two horisontals almost coincident, seems to have no parallel in other known phase systems. It was also accompanied by the appearance of unidentified reflections at 629°and 634°C. It may be interpreted by sketching hypothetical free energy curves as before. The α- and α_2- phases must have free energies close to one another. For a eutectic or a peritectic reaction the common tangent must be in contact with three curves at one temperature, i.e. at 627°C it is in contact with α, α_2 and liquid and at 626.5°C the curves are α_2, β' and liquid. The liquid in both reactions will be of nearly the same composition. If α and α_2 do not differ much in free energy a small change in the relative positions of the free energy curves with a small change of temperature will be sufficient to fulfil the requirements for a peritectic or eutectic reaction.

The above interpretation is supported by the very narrow composition range over which the eutectic-peritectic equilibria were observed. Another interesting confirmation is found in the work of Ölander. His diagram, based on E.M.F. measurements,

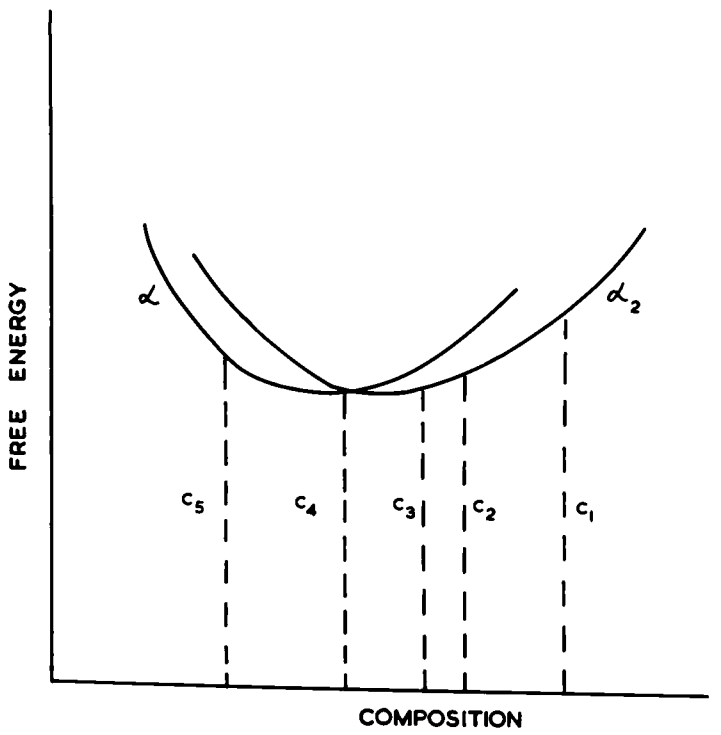

(i) gold-cadmium.

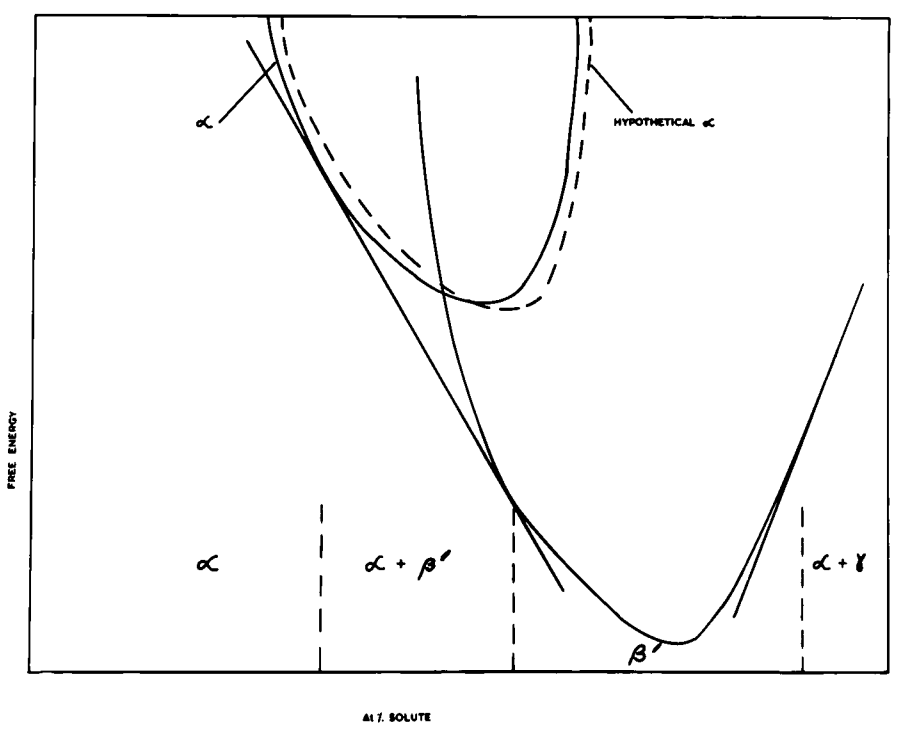

(ii) gold-zinc.

Fig.21. Free energy relationships.

showed the α- phase to be in equilibrium with β' at all temperatures (fig.2). Since Ölander did not detect the α_2-phase by the E.M.F. technique it is quite possible that this would be due to the α- and α_2- phases having free energies too close to one another for a distinction between the two phases to be made.

(iv) Stacking Faults and the $(\alpha+\alpha_2)\alpha_2$ Boundary

The above picture of faulted α_2 is in agreement with the current theory of the appearance of stacking faults on f.c.c./c.p.h. boundaries (37). But it does not account for all the facts observed in the present work. The faulting effect as shown by visual comparison of films is independent of the way in which the films were taken and appear just as readily in room-temperature as in high-temperature films. The effect is also independent of the temperature of specimen anneal. But it is not independent of composition, increasing gradually from alloy 34.14 to alloy 27. According to the above interpretation of the faults, this is because alloy composition is approaching the solvent-rich boundary of the c.p.h. phase (fig.20). If this were the only criterion of the appearance of faulting then one would expect faulting in the Au-Cd α_2-phase at any composition along the $(\alpha+\alpha_2)\alpha_2$ boundary at any temperature up to the 627°C peritectic. This has not been found to be the case in the alloys investigated. High-temperature films of alloy 34.14 were found to have normal c.p.h. patterns at 590°C, close to the $(\alpha+\alpha_2)\alpha_2$ boundary and were f.c.c. at 617°C. This would suggest that the use of free energy curves for α and α_2 as above may be misleading as an interpretation of faulting in Au-Cd and that it may be incorrect to relate the faulting problem to the eutectic-peritectic equilibria. Faulting is obviously very dependent on composition but not on temperature nor on the proximity to the $(\alpha+\alpha_2)\alpha_2$ boundary.

If the latter were a sufficient condition for faulting, one would expect alloy 34.14 to become faulted at about 590° and the faulting density to increase with temperature as the $(\alpha + \alpha_2)\alpha_2$ boundary is approached. Instead, whatever the temperature of exposure, the faulting effect has been observed only when composition changes from 34.14 atomic % cadmium to 27 atomic %.

All that can be said at present is that faulting in the α_2-phase is due to the c.p.h. stacking being so similar to the f.c.c. stacking but the f.c.c. stacking is not necessarily nearly identical with the α-phase with which α_2 is in equilibrium. It was found that at low temperatures there is a genuine though narrow f.c.c. + c.p.h. two-phase region. There is a marked change from alloy 27, faulted c.p.h. to alloy 26 f.c.c. plus c.p.h. while alloy 25 was f.c.c. plus trace c.p.h. In theory a two-phase region must always be present but in practice the difficulty of preparing equilibrium samples may introduce a faulting effect in which f.c.c. may change gradually into c.p.h. as was the case for cobalt. The fact that difficulties of this kind were not encountered in the work with Au-Cd and that present and previous work agrees in drawing a narrow $(\alpha_1 + \alpha_2)$ or $(\alpha' + \alpha_2)$ region at ca.25 to 27 atomic % cadmium, constitutes good evidence for the view that α_1, α' and α_2 though they may be quite close to one another in free energy are not so close as to pose the special problem found with cobalt.

(v) Cavities in α_2-Alloys.

Massalski (23) obtained continuous intensity data of α_2 alloys with a Geiger diffractometer. Besides observing the faulted c.p.h. patterns he also noted 'side-bands' which were

attributed to pre-precipitation of some other phase at about the composition Au_2Cd. Evidence of this phase was produced in the form of a photomicrograph in which dark material in a light matrix is seen (23). Similar micrographs in this composition range were obtained - see Plate 6, and as explained on previous pages the dark material was considered to be nothing more than cavities. Their appearance is attributed to segregation. When a quenched melt of gold-cadmium segregates on passing through the freezing range α or α_2 plus liquid, the resulting ingot may contain dendrites richer in gold than the surrounding melt, the dendrites having frozen first. During subsequent anneals cadmium can be expected to diffuse into the dendrites faster than gold will diffuse out and as a result cavities may appear between the dendrites. This model is analogous to the well-known Kirkendall effect demonstrated with a copper block with a brass core (38). The zinc can be shown to diffuse out of the core more rapidly than copper diffuses in the reverse direction and this may be associated with core shrinkage.

Direct evidence for such an effect in the Au-Cd system has not been found. The diffusion coefficient of cadmium in silver is greater than that for gold in silver. No figures are available for the diffusion of cadmium in gold. Geguzin states from a study of the self-diffusion and mutual diffusion in non-homogenous porous bodies that the diffusion is 'unipolar' in character, i.e. due largely to the metal having the smaller latent heat of evaporation (39). The figures in the case of Au and Cd are respectively 84 and 27 k.cal/mole. Geguzin found cavities in the brass section of a copper _ brass _ copper combination. The cavities varied in cross-section from grain to grain but appeared to be cubic in shape. Inspection of Plate 6 shows that the traces of cavities suggest, in parts, the original cast ingot. It is considered, therefore, that Massalski's conclusion that a

new phase is present at Au_2Cd seems to be wrong. Apart from the cavities no other evidence of a new phase has been found except for a few very faint unidentified extra lines at 29.6 atomic % cadmium quenched from 453°C. The side-bands in Massalski's intensity charts are believed to be due not to pre-precipitation but to the segregation which resulted in cavities. Should this interpretation of the cavities be proved correct a similar effect is to be expected in other phase systems but, so far as is known, it has not been observed.

(c) 3/2 Electron Compounds in Gold Alloys.

(i) Ordering In The b.c.c. Phase.

A b.c.c. phase is known in the following Au systems: Au-Cd, Au-Zn, Au-Mg, Au-Al, and possibly in Au-Ga. Only in those systems where the second component is divalent is the β-phase extensive in composition and temperature range. In Au-Al and Au-Ga high-temperature phases of very restricted composition and temperature range are found at compositions Au_4Al and Au_3Ga, i.e. at electron : atom ratios of about 1.41 and 1.60 respectively. In all cases where the structure is known, a superlattice can be detected, with the exception of Au_4Al. The Au-Al phase has been shown by high-temperature X-ray work to be disordered b.c.c. at 500°C (40). The structure of Au_3Ga is reported as c.p.h. but others noted a complex pattern in quenched specimens (28). The possibility of decomposition of Au_3Ga must therefore not be ignored. In Cu and Ag systems where the electrochemical factor is smaller, ordering is less common and occurs only at low temperatures.

The appearance of a disordered b.c.c. structure in Au_4Al is interesting. The superlattices in Au-Cd, Au-Zn and Au-Mg have been attributed to a high electrochemical factor. The factor of Au-Al, as measured by the Δx scale, is higher than that of either Au-Cd or Au-Zn.

Au-Cd	0.7	Au-Mg	1.2
Au-Zn	0.8	Au-Al	0.9

A probable explanation of the absence of a superlattice is the low size-factor of Au-Al. The size factor calculated from interatomic distances is -0.7% to -2.7% (depending on the exact values chosen for aluminium). A favourable size factor will minimise the strain relief due to ordering and make it less probable that a superlattice will be found. It must then be concluded that the effect of a

high electrochemical factor in Au-Al is offset by the favourable size factor. It has been noted (42) that in spite of the high electrochemical factor Au_4Al does not have a maximum in the liquidus, unlike the other Au alloys where a superlattice is found, but this is not understood.

The appearance of superlattices in the ζ -phases in IB systems has not been investigated systematically and it is not known whether there is a preference for ordered c.p.h. in Au alloys as compared with alloys of Ag and Cu. What is known of the ζ -phases suggests that ordering is less frequent and that the factors underlying the distribution of superlattices among the IB systems will be less clear-cut than for the b.c.c. structure. The same remarks apply to the other intermediate phases in IB series of electron compounds, i.e. γ- and ϵ -structures. But Section 1(b) has shown that the behaviour of the liquidus in Ag and Au systems with divalent solutes suggests a general increase of stability of all the intermediate phases with respect to liquid phase as the electrochemical factor increases (fig. 17), and not only of the β -phase. The β -phase is however the most sensitive to this effect.

(ii) ζ -Phases.

Previous discussions of 3/2 electron compounds (42) have set out the conditions which favour the formation of ζ- and ζ' -phases. The μ (β -manganese type) structure is found to be subject to the same stability restrictions as ζ and ζ'. They are as follows.

(i) Increasing valency will favour ζ or β' (ordered or disordered) at the expense of β or β'.

(ii) Decreasing temperature favours ζ or μ.

(iii) Increasing size factor favours β or β' at the expense of ζ or μ.

The meaning of the valency relation is not known. The effect of temperature may be interpreted in terms of the entropy effect as in section 2(a). The effect of size factor is regarded as showing that the b.c.c. structure is more likely to tolerate lattice strains than the close-packed c.p.h. lattice. Raynor and Massalski (43) have added a rider to the third generalisation on the basis of the lattice spacings of the ternary Cu-Ge-Ga system. Along lines of constant electron : atom ratio in the ternary ζ -phase the value of c/a remains almost constant. The smaller Ge atom is believed to favour a wide binary Cu-Ge ζ -phase while the larger Ga atom results in a narrow field for the binary ζ_1- and ζ_2-phases. Fermi surface lattice distortion effects, responsible for the variation of c/a with variation in the electron : atom ratio, may be opposed by size-distortion effects, i.e. size distortion may make impossible the c/a ratios required by the Fermi surface effect. Therefore when size factors are large, c.p.h. may be displaced by f.c.c., b.c.c. or ϵ -brass which are all cubic, $c/a = 1$ at all compositions.

A comparison of 3/2 phases for Ag and Au gives the following range of structures.

Ag:-

System	Ag-Mg	Ag-Zn	Ag-Cd	Ag-Hg
Phase	β'	β / ζ	β / ζ	γ / ζ

Au:-

System	Au-Mg	Au-Zn	Au-Cd	Au-Hg
Phase	β'	β'	ζ, β'	ζ'

In Au-Cd the ζ -(i.e. the α_2-) phase and β' -phase co-exist from low temperatures to the eutectic temperature. In Ag-Cd the β -phase and ζ -phase are respectively high and low-temperature modifications of the 3/2 electron compounds. The Au-Cd c.p.h. structure is, however, very similar to the other ζ -phases found in Au systems. Massalski and King (52) have shown that the ζ -phase lattice

parameters of Au-Cd, Au-Sn, Au-In and Au-Hg vary in the same way with variation of the electron : atom ratio (see Section 3). There is, on going from Ag to Au in the systems listed above a definite tendency for c.p.h. to replace b.c.c. This tendency cannot be accounted for entirely by the size factor generalisation of Hume-Rothery et.al (42) since Au and Ag have atomic diameters which are nearly identical. This tendency is paralleled by other systems in which the solute is from Groups III to V. Another point to note is that the ζ-phases in Au systems invariably occur at electron : atom ratios lower than the theoretical 3/2 ratio, and are to be found at values from 1.25 to 1.35, as compared with 1.4 to 1.5 in Ag alloys.

(iii) The Occurrence of the Au-Cd α_2 Phase.

The Au-Cd system is something of a curiosity among the IB systems on account of the α_2-phase. While other systems may have both a c.p.h. and a b.c.c. phase in the range of electron : atom ratios 1.2 to 1.5 the b.c.c. phase is usually restricted to high temperatures and is of limited range. The Au-Cd system is alone in having both a b.c.c. and a c.p.h. phase stable from low temperatures to the melting point.

In the Au-Zn and the Au Mg systems an α/β equilibrium is found with no c.p.h. phase at any temperature in the Au-rich part of the diagram. In Au-Hg the equilibrium is α/ζ the ζ-phase being centred round the composition Au_3Hg.

An answer to the question why no c.p.h. phase, analogous to the Au-Cd α_2-phase, is found in Au-Zn or Au-Mg may be made in terms of the electrochemical factor. The factors on Pauling's scale are listed in Table 8. If an α_2-phase were found in Au-Zn and Au-Mg then, by analogy with Au-Cd, it may be expected that it would not differ very much from the primary solid solution in free energy. In that case a free energy curve may be drawn for the

hypothetical α_2-phase of Au-Zn, fig.21(ii). From the discussion on previous pages the β'-phase has been shown to be very stable as a result of the high electrochemical factor and it is likely that its free energy curve will be as sketched in fig.21 (ii). The sketch shows that a common tangent cannot touch both the hypothetical α_2 and β' curves. Therefore no α_2-phase is seen in Au-Zn.

The same interpretation will apply to Au-Mg where the electrochemical factor is even larger than in Au-Zn. The lower electrochemical factor in Au-Cd means there is no marked displacement of the β' curve such as that drawn in fig.21(ii) and that a peritectic reaction α + liquid $\rightleftharpoons \alpha_2$ is possible. Au-Hg is not strictly comparable with the other systems since there is no b.c.c. phase but the appearance of a c.p.h. structure in the first intermediate phase in equilibrium with α is consistent with the interpretation.

The theory of the γ-phases to the solute-rich side of the b.c.c. structure may be compared with the above outline for the ζ-phases. In Au-Zn a γ-brass structure is found at an electron : atom ratio higher than the ratio 21/13. This phase has been shifted to higher solute content as a result of stabilisation of the β'-phase: The more stable the β'-phase is the lower its free energy curve will be and consequently the higher the solute content at which the common tangent is in contact with the γ-phase free energy curve. The γ-phase in Au-Zn, by analogy with the γ-phase structures in Cu-Al and Cu-Ga, is believed to be a defect lattice in which atoms have been dropped out to maintain the fundamental electron to unit cell ratio 88 electrons per unit cell (41). In Au-Mg there is no γ-phase. Electrochemical stabilisation of the β'-phase is believed to have shifted the γ-phase to a composition at which even a defect γ-brass structure is unstable.

3. SOLID SOLUBILITY IN GOLD ALLOYS

The primary solid solutions of many B elements from the later Periods, and of A elements like AC and Mg, in the IB elements Cu, Ag and Au have been known for a long time to show regularities when the maximum solid solubilities are expressed in terms of the electron : atom ratio. One necessary condition is, of course, that the size factors, measured in terms of interatomic distances, shall be within the favourable zone, i.e. less than 13-15%. Before discussing the possible significance of the critical electron : atom ratios, some of the limitations of the size factor concept in predicting solid solubility or otherwise should be described. For the purpose of the present discussion the limitations are considered under three headings, (a) the difference between ionic and atomic radii, (b) the electrochemical factor and (c) the intermediate phase or phases in equilibrium with the primary solid solution.

The following series of solid solubilities, expressed in terms of the electron : atom ratio is observed in Cu, Ag and Au.

Cu :-

System.	Cu-Cd	Cu-In	Cu-Sn	Cu-Sb
Solid Solubility.	1.14	1.21	1.27	1.24

Ag :-

System.	Ag-Cd	Ag-In	Ag-Sn	Ag-Sb
Solid Solubility.	1.43	1.40	1.33	1.29

Au :-

System.	Au-Cd	Au-In	Au-Sn	Au-Sb
Solid Solubility.	1.34	1.25	1.20	1.04

The size factor in Cu-Cd is large and positive which predicts limited solid solubility, as is the case. But it will also predict decreasing solubility from Cu-Cd to Cu-Sb, which is not

found. To interpret this a distinction is made between the ionic and atomic radii in the alloys. Cu is a 'full' metal and there is little difference between the ionic and atomic radii. But from Cd to Sb there is a rapid decrease in ionic radius associated with the higher valency and the resulting high nuclear charge. As a result there is an increase in the solid solubility from Cu-Cd to Cu-Sb (44).

The Ag series has a favourable size factor in each system Ag-Cd to Ag-Sb; the solubility limit decreases from left to right. In the Au series the size factor is always within the favourable zone but the electron : atom ratio is smaller than the maximum of 1.4 observed in Ag. This is typical of the Au systems. No case is known where there is solubility limit of 1.4 in Au systems but many have been found in Cu and Ag systems. A detailed comparison (44, 45, 46) has shown that the electron : atom ratios cluster around certain critical values, as 1.35 to 1.40 in Cu and Ag and 1.2 to 1.34 in Au. The close correlation of solid solubilities with the electron : atom ratio is unlikely to be fortuitous. But a satisfactory theory that will interpret it and will also predict the systematically lower solid solubilities in Au has still to be devised. As described later, the Jones theory (47) was held to explain solubilities in Cu and Ag. The deviations in Au were attributed (i) to the fact that Au might (as its chemical behaviour suggests) have a valency greater than unity (ii) the high electrochemical factor in Au alloys which may stabilise the intermediate phases at the expense of the terminal solid solutions (46).

In the series of Au alloys with divalent solutes the following solid solubilities are found.

	Au-Hg	Au-Cd	Au-Zn	Au-Mg
Solid solubility	1.20	1.34	1.31	1.25
Δ x	0.5	0.7	0.8	1.2

The electrochemical factor may interpret the series in three of the four systems but the fourth, Au-Hg, does not fit the sequence. Since the size factor is probably very favourable it is possible that the low solid solubility may be due to Brillouin Zone effects. But the f.c.c. phase in Au-Hg is in equilibrium with a c.p.h. intermediate phase. In Cu and Ag the intermediate phase is frequently b.c.c. while in most Au systems it is c.p.h. Also, with the exception of Au-Al all Au b.c.c. phases in equilibrium with f.c.c. are ordered and consequently have been stabilised at the expense of f.c.c. It would seem therefore that any electronic theory of solid solubilities in Cu, Ag and Au must take account of the intermediate phases when comparing solid solubilities in the three metals.

The original Jones theory of solid solubility limits, in which a spherical Fermi surface (FS) is assumed, has been generally accepted for many years (47(i)). Of the various contributions to the free energy of the solid solution only the electronic contribution is believed to change markedly with composition. According to calculation the spherical FS will touch the $\{111\}$ planes of the first Brillouin Zone (BZ) at an electron : atom ratio of 1.36, surprisingly close to the experimental value of 1.4 for copper and silver. The rather lower solid solubilities in gold, 1.20 to 1.35 and never 1.4, was, as explained above, attributed to the greater electrochemical factor in gold alloys and to the likelihood of a higher valency than one in gold.

In 1957 the anomalous skin effect in pure copper indicated that the FS is either touching, or very close to, the $\{111\}$ planes of the first BZ, i.e. it is not spherical in the pure metal (45). This result confirmed a calculation by Jones himself, based on the optical properties of Cu, that the first peak of the N(E) curve must occur at an electron : atom ratio

of 1.0 (47(ii)). This calculation, though made in 1937, went almost unnoticed for a long period.

Attempts by Cohen and Heine (49) to adjust the electron theory of Cu alloys so as to take account of the aspherical FS, led to a general interpretation of the solubilities in Cu, Ag and Au. The main feature of their theory of solubilities is that the FS of pure IB metals is not necessarily spherical and that the distortion from a sphere may vary with composition in alloys. The effect of alloying on the shape of the FS is predicted from the s - p excitation energies of the free atoms. In the pure metal, at the centre of the zone face in the first BZ of the f.c.c. structure the electrons are either 's-like' or 'p-like' in energy, but not a hybrid of both. The band gap Es-Ep at the zone face is obtained from the s-p excitation energies, Δ sp, in free atoms. For Cu E_s-E_p is positive for Au it is negative and in Ag it is very close to zero. The distortion of the FS, deduced from E_s-E_p, is shown to be marked for Cu and Au but not for Ag. The effect of alloying on the distortion is found from an examination of Δ sp values in the B elements. They increase on going from top to bottom and from left to right in the periodic table, i.e. in the IB systems Δ sp is always greater for the solute than the solvent. Therefore in alloys E_p is always raised relative to E_s. In Cu solutions the FS must become more spherical with increased solute content, while in Au the reverse is the case. Two effects may then be expected: when the electron concentration in Cu alloys is increased (i) the FS pulls away from the zone face becoming more spherical (ii) the FS expands until the $\{111\}$ planes are touched once more. In Au the distortion of the FS is increased on alloying and lower solid solubilities than in Cu will result. Since E_s-E_p is nearly zero in pure Ag the FS of Ag should be nearly spherical and this may account for maximum solid solubilities being higher than in Au.

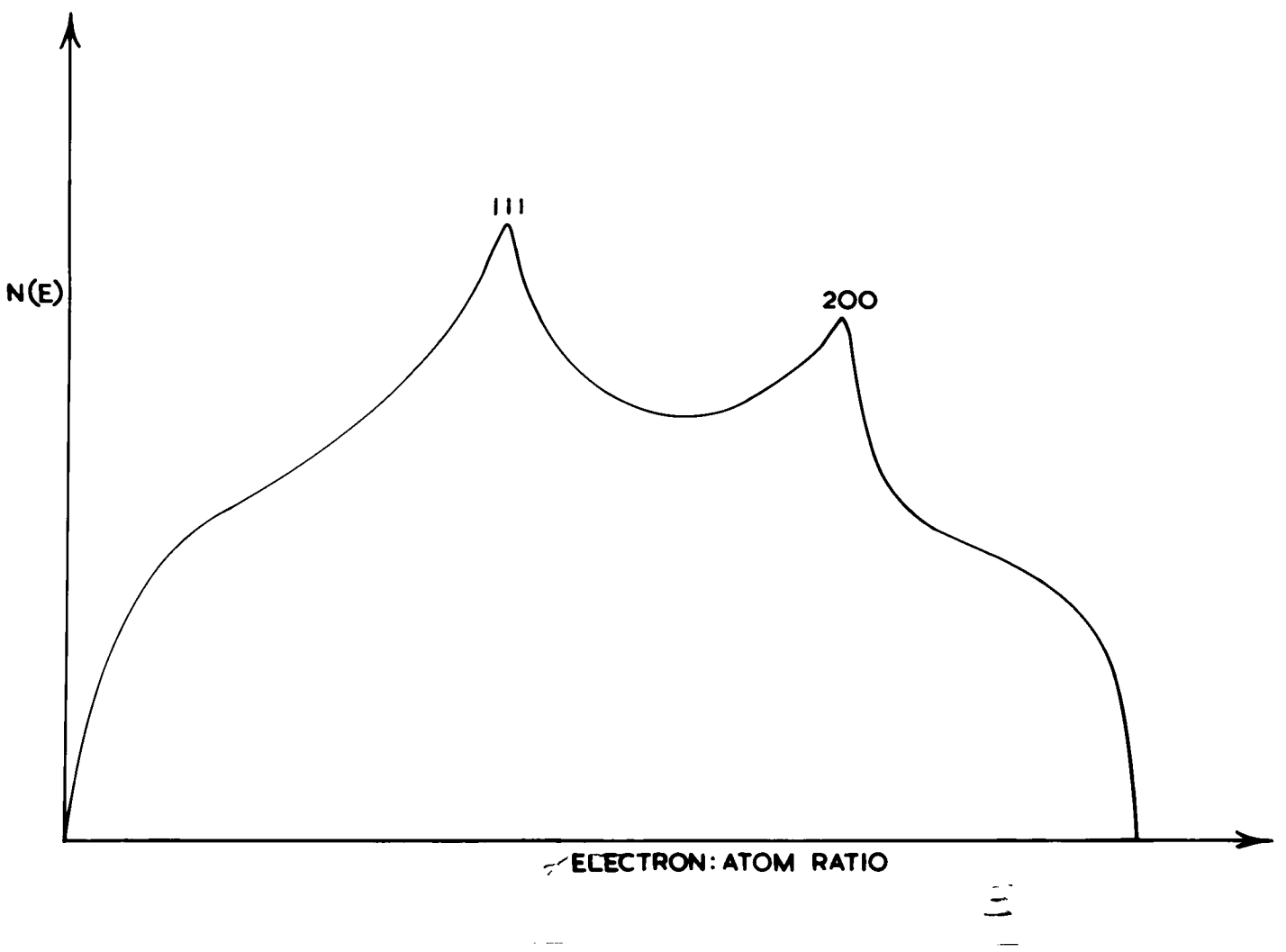

Fig.22. Suggested N(E) curve for primary solid solutions in gold.

It is now known from experiments on the de Haas-van Alphen effect in the pure metals that the FS is touching the $\{111\}$ planes in all three IB metals (50). Therefore the Cohen and Heine picture (49) would seem to be incorrect for Ag at least. A recent suggestion (51) has been made that while the first peak of the N(E) curve may occur in the pure metals with the FS in contact with the $\{111\}$ planes, contact with the $\{200\}$ planes is the critical point at which there will be a rapid rise in the energy of the f.c.c. solid solution. For a spherical FS the first peak is at 1.36 and the second at 1.88. When the FS is distorted sufficiently the first N(E) curve peak is at 1.0 while the second may be found in the range of electron : atom ratios corresponding to the observed maximum solid solubility limits, but the values of these ratios will then depend on the chosen distortion of the FS (see fig.22).

Two recent papers by Massalski and King (52, 53) give an interesting interpretation of the lattice spacing variations in ζ-phases found in systems of Ag and Au by means of FS distortion effects. The α- and ζ-phases were compared for a number of systems of the IB elements by assuming the α-phases to have hypothetical c.p.h. parameters c' and a', calculated from the a parameters of the cubic lattice by the relations $a' = a/\sqrt{2}$ and $c' = 1.633\, a/\sqrt{2}$. The ideal value of the c/a ratio, 1.633, for a c.p.h. phase, corresponding to the f.c.c. lattice has been used.

In the case of Au four systems, Au-Cd, Au-Hg, Au-In and Au-Sn are compared (5). Fig.23 shows typical results. The values of the volume per atom in the α- and ζ-phases plotted against electron : atom ratio fall on a straight line. The typical variations in lattice parameters are also given in fig.23 and may be divided into four stages on going from low to high electron : atom ratio (c/a).

1. c increases markedly on passing from α to ζ at $e/a \simeq 1.3$.
2. a decreases at the same e/a as in 1.
3. a increases gradually the slope becoming steep at $e/a \simeq 1.36$.
4. c decreases at the same e/a as in 3.

Plots for Cu-Ge and Cu-Ga show that the decrease in a is almost undetectable at onset of the ζ-phase at an electron : atom ratio of about 1.36. The subsequent increase in a occurs at about 1.40. In a number of Ag systems (53) the results are similar to Au. Stages 1 and 2 are small but measurable and take place at an electron : atom ratio rather higher than in Au.

Massalski and King first suggested in their paper on the gold systems (52) that the four stages could be interpreted by FS interaction and overlap with the first BZ of the c.p.h. structure takingplace. According to the Goodenough theory interaction between the approaching FS and the BZ may take place before there is actual contact and may result in a change of lattice parameter with change of composition (54). In the Au ζ-phases interaction with the $\{00.2\}$ planes of the first BZ takes place, resulting in an expansion of c on passing from α to ζ (stage 1). The decrease in a (stage 2) is attributed to the tendency to keep the volume per atom constant. The subsequent increase at a higher electron : atom ratio is associated with overlap of the FS across the $\{10.0\}$ faces which takes place at an electron : atom ratio of about 1.35 to 1.36. Following Cohen and Heine it was inferred that FS distortion effects are involved in the differences between the ζ-phases of Au, Ag and Cu. Since then the published data on the FS of the three metals (50) made it necessary for Massalski and King to modify their picture. Their new interpretation is given in their paper on Ag alloys (53). The Goodenough interaction effect is abandoned. It is argued that in Au ζ-phases FS contact with the $\{00.2\}$ faces is responsible for

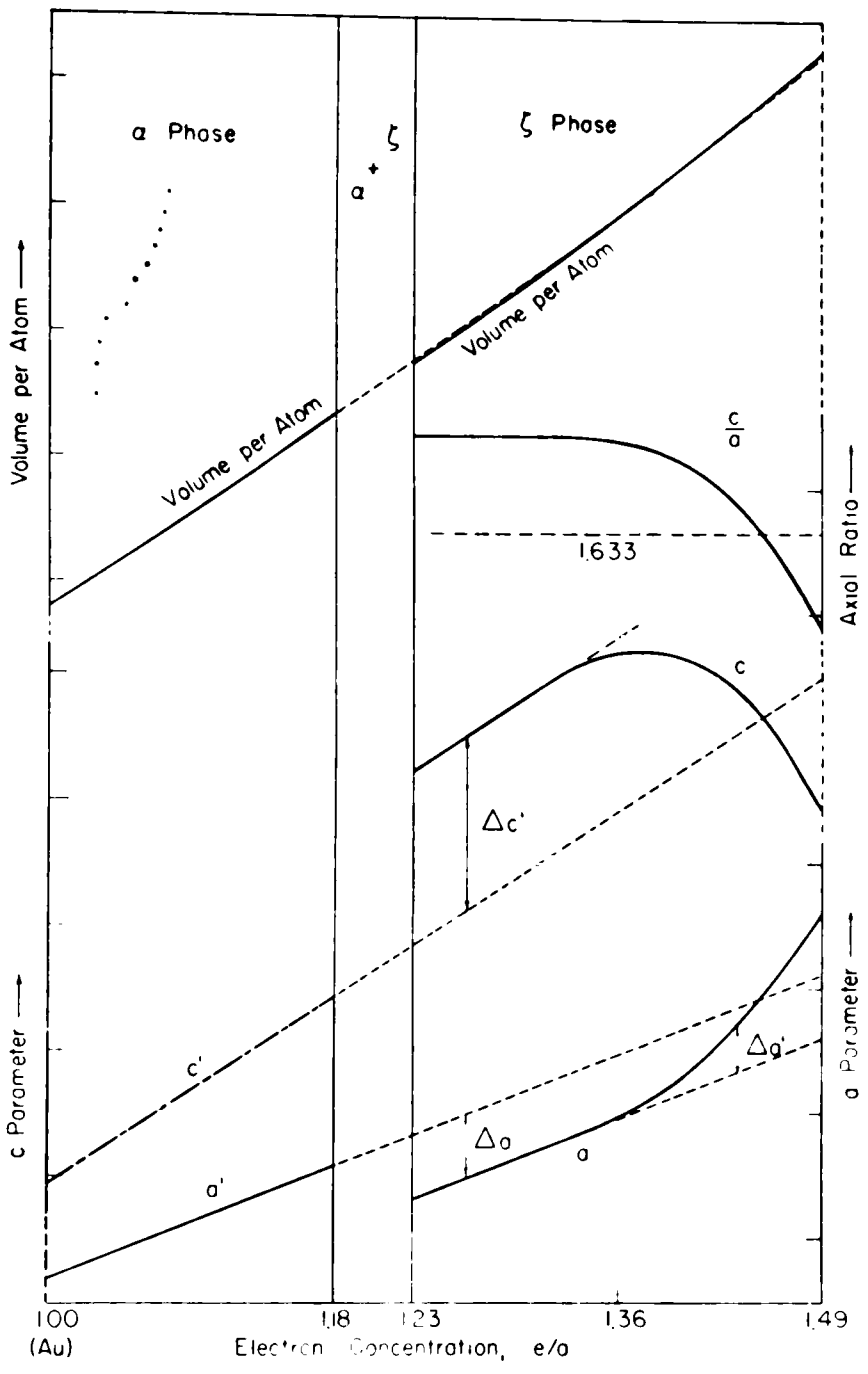

Fig.23. Typical lattice spacing variations of the ζ -phase in gold systems. Massalski and King, 1960.

the higher than ideal c/a values observed in these alloys. Taking the deviation from the ideal 1.633 as a qualitative measure of the amount of FS contact, it is concluded that in the Ag alloys the FS is nearly spherical (i.e. does not 'bulge') in the $\langle 00.2 \rangle$ directions, since at the onset of the ζ -phases the c/a ratio is only slightly larger than ideal. A similar deduction is made for Cu where axial ratios are again slightly greater than ideal at ζ -phase onset. It is concluded that $E_s > E_p$ for Ag as for Cu. Therefore when Ag is alloyed the FS distortion must decrease according to the Cohen and Heine method outlined above, just as for Cu.

Returning to solid solubilities, it is possible that the Cohen and Heine theory can be reconciled with the recent suggestion (51) that solid solubilities may be associated with the $\{200\}$ rather than the $\{111\}$ planes. On the other hand the importance of the intermediate phases must be emphasised. When the intermediate phase in equilibrium with the primary solid solution varies in structure from one system to the next it is not to be expected that solid solubility limits will be the same in all cases. The Au-Cd system illustrates this point. The maximum solid solubility is at an electron : atom ratio of 1.34 at 620°C but decreases markedly with decreasing temperature. The maximum value is not much smaller than the value found in Cu and Ag systems. It is quite possible that the deviation can be interpreted, at least in part, by a stable c.p.h. phase interposing between the f.c.c. and bc.c. structures. There are no other Au systems with c.p.h. and b.c.c. phases in equilibrium with each other from low temperatures to the melting point but in Au-Sn, Au-In and Au-Hg the appearance of a stable c.p.h. phase at electron : atom ratios of 1.22 to 1.35 may be one reason for the lower solid solubilities. In general, the tendency is for an intermediate c.p.h. phase to appear in the order Au > Ag > Cu and the lower solid solubilities in Au can very probably be attributed, in part, to this fact.

APPENDIX.

APPENDIX

THE ANALYSIS OF GOLD-CADMIUM ALLOYS

In the determination of the various phase boundaries of the gold-cadmium system critical specimens were sent away for analysis as a matter of routine. The analyses were carried out by Johnson Matthey & Co.

Cooling Curve Ingots.

All ingots were analysed for gold and in five cases cadmium was determined as well. The results (pages33-4) were satisfactory, showing only a slight cadmium loss. In some cases the samples analysed were ingot sections weighing five to ten grams; in other cases the whole ingot (excluding sawdust) weighing about twenty grams was analysed. In the batch of five where both metals were determined the weight per cent total came to 100.23 for one sample and varied between 99.90 and 99.96 for the remaining four.

Microscopic Specimens from Quenching Experiments.

The analysis results for the specimens prepared in the annealing and quenching experiments are quite different from those for the cooling curve ingots. The alloys were prepared by the sealed-tube method as described in the experimental section. Weight changes after quenching the melt were usually very small; a weight loss of less than 0.05% was observed in most cases. The specimens showed a negligible weight change on annealing. It was therefore concluded that precautions against cadmium loss were satisfactory. As the analyses of small specimens showed, the possibility that gold was being lost by reaction with silica during melting had to be considered, but this was never confirmed by the analyses of large specimens. Moreover it was extremely unlikely that weight changes would then have been so small.

Thus it was expected that the bulk composition of the ingots would be very close to synthetic composition. To test for inhomogeneities in the ingots, two were selected for analysis. Thin slices were taken from the top, middle, and bottom of each ingot and analysed for cadmium. The results, together with the weight of each sample are collected in Table I at the end of the Appendix.

One ingot, of composition 27.48 weight % cadmium had been subjected to the usual homogenising treatment. The other had not. The results were regarded as reasonable and hence this method of preparing ingots was used in the present work.

Tables 2 to 4 show the analysis results for the critical specimens on the solidus, the α_2 $(\alpha_2 + \beta')$ and the $(\alpha_2 + \beta')\beta'$ boundary. The weights of the specimens are also given. It is clear that in these tables there is no instance when a sample gives a lower analysis value for cadmium than predicted by the synthetic composition. If inhomogeneities were responsible for the analysis results coming too high in cadmium, then one would expect that, in some instances at least, cadmium content would be too low. The results on plotting gave reasonable curves for the solidus and the $(\alpha_2 + \beta')\beta'$ boundary but the figures for the α_2 $(\alpha_2 + \beta')$ boundary were clearly useless (Table 3).

In all cases where analyses were carried out for gold as well as cadmium the totals appeared to be so close to 100.0 as to remove any doubt about the accuracy of the analytic method. However as evidence accumulated of cadmium coming higher than expected it was decided to test the effect of size as follows. A five-gram ingot was prepared in the usual way. The composition was 34 atomic % cadmium 22.7 weight %. Table 5 summarises the results. The ingot sections were prepared as illustrated in the sketch.

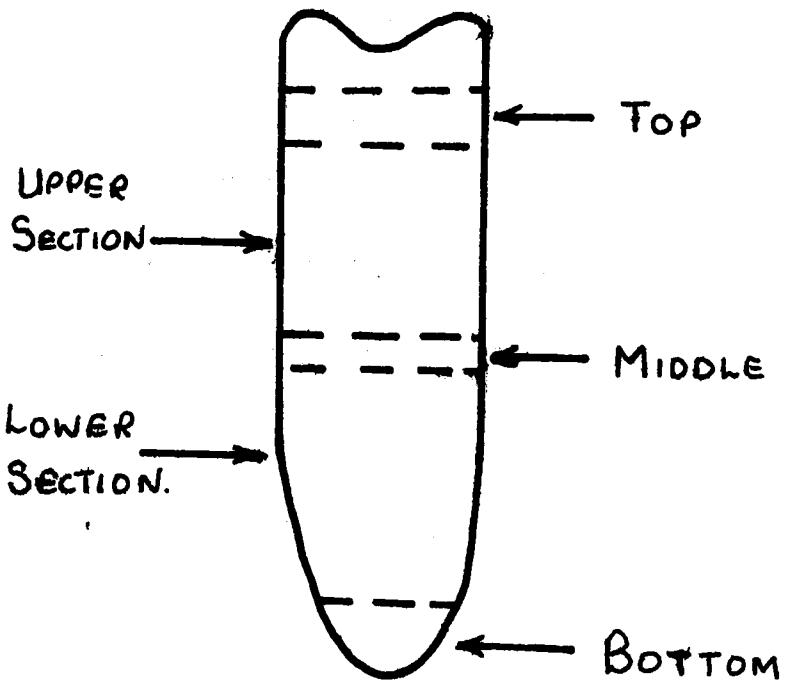

A definite dependence on weight is revealed, the results coming higher than expected in cadmium for the small samples and lower for the large samples. Microscopic examination in transverse section showed the ingot to have annealing twins in the central grains but not on the periphery. Annealing twins did not appear when longitudinal surface of the ingot was examined. It thus appears that the ingot may possibly have been segregated, having mainly f.c.c. grains with a few c.p.h. (α_2) grains at the circumference, but it is difficult to see how this kind of segregation could have produced the results recorded in Table 5.

Johnson Matthey independently undertook the following experiment. Gold and cadmium were mixed in the proportion of 5 to 1. Then using the analytic technique employed for alloys the results were as follows.

	Weight taken (gms)	Weight Cd SO_4 recovered (gms)	Weight Cd gms.
1.	0.1000 (Au) 0.0200(Cd)	0.0372	0.0200
2.	1.0000 (Au) 0.2000 (Cd)	0.3698	0.1994

They also checked some of the results by a polarographic method, obtaining good agreement. Thus it appeared that the small size of the samples alone could not be responsible for the discrepancies.

The method used by Johnson Matthey is described in outline below.

The sample is dissolved in aqua regia. Excess nitric acid is removed by evaporation with hydrochloric acid. The solution is diluted and the gold precipitated by passing a stream of sulphur dioxide through the solution. The gold is filtered off and weighed. The filtrate is then evaporated to a low bulk, a small amount of sulphuric acid is added and evaporation continued to dryness, followed by ignition at 590°C. The residue is weighed as $CdSO_4$.

In reply to the suggestion that incomplete precipitation of gold might lead to some gold being weighed as cadmium sulphate and therefore to the observed analysis results, Johnson Matthey state that tests on the sulphate never showed traces of gold.

A fresh effort to solve the problem was made by calling in a

referee analyst (D.C. Griffith & Co.). The following procedure was adopted after consultation with the British Non-Ferrous Metals Research Association. A five-gram ingot was prepared by the sealed-tube method. From the weights of the metals taken the synthetic composition is

32.07 atomic % cadmium; 67.93 atomic % gold

21.20 weight % " ; 78.80 weight % "

The loss in weight on quenching the melt was 0.0067 grams or 0.13 weight %. The ingot was not homogenised. A powder was prepared from the ingot by filing down to as small a lump as possible with a fine clean file. The powder was allowed to fall on a large sheet of glazed paper, separated from iron filings with a strong magnet, transferred to a bottle, then washed with carbon tetrachloride, alcohol and ether and dried. It was then shaken up for ten minutes.

Two batches of the powder were prepared for analysis. One batch was sent to Johnson Matthey and one to Griffiths & Co. the referee analysts. Both metals were determined. Table 6 gives the results. It is seen that the two analysts agree very closely. For the small samples weighing about 0.1 gm., nos.1 and 2, the results are too high in cadmium and too low in gold as with the microscopical specimens. For the large samples, about 1.0 gm the results are reasonably close to the synthetic values.

Griffiths & Co. used a method very similar to that of Johnson Matthey. The samples were dissolved in aqua regia, converted to chloride and the gold precipitated with sulphur dioxide, the precipitate was filtered off, ignited, again dissolved and re-precipitated as before to ensure complete removal of cadmium. The gold was then collected, ignited and weighed. The combined filtrates from the gold were evaporated and converted to sulphate, gently ignited in a tared crucible and weighed. After weighing the cadmium sulphate was dissolved, filtered and any residue weighed and deducted. The resulting solution was examined for any further gold.

The referee analysts stated that they preferred duplicate tests for this type of material, if only available in one gram quantities or less. Accordingly samples 1 to 4 weighing 0.1 and 0.3 gms were sent. Table 7 gives results. With the exception of no.1, they are now quite close to

the synthetic value for cadmium, but as in Table 6, they are too low in gold. No.1 is similar to nos.1 and 2, Table 6, in having too high a value for cadmium, too low for gold, with a total appreciably larger than 100.0. It may be significant that for most small powder specimens the % totals came out a little larger than 100.0, while those for the large specimens were closer to 100.0. In this connexion the % totals in Table 7 are interesting. For no.1 it is 100.30, and no.1 was similar to the specimens in Table 6. The remaining specimens nos.2 to 4 in Table 7 all show a % total less than 100.0 by about 0.5 wt.%; as pointed out above, the cadmium figures are good but the gold is too low. It is suggested that the referee analysts dealt with the specimens in Table 7 in the order given (nos.1 to 4) and that they managed to remove a source of error in the cadmium determination but not in the determination of gold.

It should be noted that the small specimens for microscopical work did not show a tendency to give % totals larger than 100.0. Johnson Matthey objected to the method of sampling the powder. They claimed that if the filings were of varying size, simply shaking up the powder in a bottle was insufficient to produce homogeneity. There seems to be no way however in which this would give a dependence on the weight of sample. In addition, the similar effects found with the small microscopical specimens would be free of this sampling error.

In conclusion it appears, though no definite proof has been obtained, that the analyses are unreliable for small specimens. Enough evidence has been accumulated to make it undesirable to use the analysis results in the present work except where the weights of samples were 1.0 gm or more.

TABLE 1.

Section of Ingot	Weight (gms)	Analytic weight % Cadmium
1.	19.35	synthetic weight % cadmium
Top	0.1267	19.25
Middle	0.1535	19.73
Bottom	0.0951	19.85
2.	27.48	synthetic weight % cadmium
Top	0.1598	27.95
Middle	0.0990	27.55
Bottom	0.0972	27.80

TABLE 2.

Solidus specimens, weight %. Weights 0.2024 gms or less

Synthetic		Analytic		
Cadmium	Gold	Cadmium	Gold	Total
5.84	94.16	7.30	92.82	100.12
"	"	6.63	93.3	99.93
12.93	87.07	13.46	-	-
"	"	13.80	-	-
20.11	79.89	20.79	-	-
"	"	20.29	-	-

TABLE 3.

The α_2 (α_2 + $\acute{\beta}$) boundary

Weight of specimen (gms)	Synthetic weight %		Analytic weight %		
-	Cadmium	Gold	Cadmium	Gold	Total
-	22.81	77.19	23.68	-	-
-	"	"	23.25	-	-
-	"	"	24.24	75.70	99.94
0.0290	21.26	78.74	24.79	75.18	99.97

TABLE 4.

The $(\alpha_2 + \beta')_{\beta'}$ boundary

Weight of specimen (gms)	Synthetic weight %		Analytic weight %		
	Cadmium	Gold	Cadmium	Gold	Total
0.1437	30.75	69.25	31.18	-	-
0.1125	"	"	31.58	68.50	100.08
0.2602	"	"	30.90	-	-
0.4320	30.82	69.18	31.07	-	-
0.4285	"	"	31.30	68.63	99.63
0.2760	32.66	77.34	33.05	-	-
0.2752	"	"	33.48	-	-
0.1884	34.21	65.79	35.18	-	-

TABLE 5.

Synthetic composition 22.7 weight % cadmium

Section of Ingot	Weight (gms)	Analytic weight % cadmium
Top	0.1240	23.72
Middle	0.2380	23.03
Bottom	0.1109	23.46
Upper Section	1.5390	22.04
Lower Section	1.5336	22.22

TABLE 6.

Synthetic composition: 21.2 weight % cadmium, 78.8 weight % gold.

Weight of specimen (gms)	Analytic weight %		
	Cadmium	Gold	Total
0.1			
1. Johnson Matthey	21.8(6)	78.3(6)	100.2(2)
2. Griffiths & Co.	21.94	78.31	100.25
1.0			
3. Johnson Matthey	21.35	78.69	100.04
4. Griffith & Co.	21.24	78.74	99.98

TABLE 7.

Synthetic composition: 21.2 weight % cadmium, 78.8 weight % gold.

Weight of specimen (gms)	Analytic weight %		
	Cadmium	Gold	Total
1. 0.1	21.89	78.41	100.30
2. 0.1	21.26	78.26	99.52
3. 0.3	21.35	78.07	99.42
4. 0.3	21.12	78.49	99.61

PURITY OF MATERIALS

The gold, lent by Messrs. Johnson Matthey & Co.Ltd., was stated to be 99.99 + % pure.

The cadmium was kindly donated by the Imperial Smelting Company. The spectrographic analysis of samples gave the following results.

Lead, Copper	not greater than 0.0001%
Zinc, Thallium, Other Elements	not detected.

REFERENCES

1. M. Hansen, Constitution of Binary Alloys, 1958.
2. P.J. Durrant, J.Inst.Metals, 1929, 41, 139.
3. A. Ölander, J.Amer.Chem.Soc., 1932, 54, 3819.
4. W. Köster and A. Schneider, Z. Metallkunde, 1940, 32, 156.
5. P. Ya Saldau (i) Intern.Z.Metallog., 1915, 7, 3.
   (ii) J.Russ.Phys.Chem.Soc., 1917-19, 49, 449
   (iii) J. Soc. Chem. Ind., 1923, 42, 609A.
6. A. Ölander, Z.Krist, 1932, (A), 83, 145.
7. E.A.Owen and E.A. O'Donnell Roberts, J.Inst.Metals, 1940, 66, 389.
8. E.A. Owen and W.H. Rees, Ibid., 1941, 67, 141.
9. A. Byström and K.E. Almin, Acta Chem. Scand., 1947, 1, 76.
10. L. Muldawer, Acta Metallurgica, 1954, 2, 555.
11. O. Kubaschewski, Z. Phys. Chem., 1943, 192, 292.
12. (i) T.A. Read and L.C. Chang, Trans. A.I.M.E., 1951, 191, 47.
    (ii) L.C. Chang and T.A. Read, J. Metals, 1951, 3, 47.
    (iii) L.C. Chang, Acta Cryst., 1951, 4, 320.
    (iv) D.S. Liebermann, M.S. Wechsler and T.A. Read, J.Appl.Phys. 1955, 26, 473.
13. C.W. Chen, Ph.D. thesis, Columbia University, 1954.
14. (i) L.C. Chang, T.A. Read and M.S. Wechsler, Acta Cryst., 1953, 6, 567.
    (ii) M.S. Wechsler, J.Appl.Phys., 1957, 28, 1509.
    (iii) M.S. Wechsler, Acta Metallurgica, 1957, 5, 150.
15. (i) M.S. Wechsler and T.A. Read, J.Appl.Phys., 1956, 27, 194.
    (ii) H.K. Birnbaum, Trans. A.I.M.E., 1959, 215, 786.
16. A.J.C. Wilson, J.Inst.Metals, 1944, 70, 543.
17. D.J. Moore and H.R. Thornton, J.Res.Nat.Bur.Standards, 1959, 62, 127.

18. W. Hume-Rothery, J.W. Christian and W.B. Pearson, Metallurgical Equilibrium Diagrams, 1952.

19. A.L. Sutton, D.Phil. thesis, Oxford, 1955.

20. R.G. Ross, Private Communication.

21. W. Hume-Rothery and P.W. Reynolds, Proc.Roy.Soc., 1938, A.167, 25.

22. E.A. Owen and E.W. Roberts, Phil.Mag., 1939, 27, 294.

23. T.B. Massalski, Acta Metallurgica, 1957, 5, 541.

24. M. Hirabayashi and S. Ogawa, Acta Metallurgica, 1961, 9, 264.

25. J. Wegst and K. Schubert, Z.Metallkunde, 1958, 49, 533.

26. L. Pauling, Nature of The Chemical Bond, 3rd Edition, 1960.

27. W. Gordy and W.J.C. Thomas, J. Chem. Phys., 1956, 24, 439.

28. W.B. Pearson, Handbook of Lattice Spacings and Structures of Metals, 1958.

29. H.W. Rayson and L.D. Calvert, J.Inst.Metals, 1958-9, 87, 88

30. W. Hume-Rothery and J. Burns, Phil.Mag., 1957 (viii), 2, 1177.

31. A. Westgren and G. Phragmen, Phil.Mag., 1925, 50, 339.

32. C. Zener, Phys.Rev., 1947, 71, 846.

33. S. Zirinsky, Acta Metallurgica, 1956, 4, 164.

34. T.B. Massalski and C.S. Barrett, Journal of Metals, 1957, 9, 455.

35. O.S. Edwards and H. Lipson, Proc.Roy.Soc., 1942, A180, 268.

36. S. Anantharaman, D.Phil. Thesis, Oxford, 1955.

37. C.S. Barrett, Structure of Metals, 2nd Edition, 1952.

38. E.O. Kirkendall, Trans A.I.M.E., 1942, 143, 104.

39. Ya E. Gegusin, Doklady Akad. Nauk, S.S.S.R, 1955, 100, 255. Translation: A.E.R.E. Lib/Trans 615.

40. V.G. Kusnetsov and V.I. Rabezova, Doklady Akad.Nauk., S.S.S.R, 1951, 81, 51.

41. W. Hume-Rothery, J.O. Betterton and J. Reynolds, J.Inst.Metals, 1951-2, 80, 609.

42. W. Hume-Rothery, P.W. Reynolds and G.V. Raynor, J.Inst.Metals, 1940, 66, 191.

43. G.V.Raynor and T.B. Massalski, Acta Metallurgica, 1955, 3, 480.

44. W. Hume-Rothery and G.V. Raynor, The Structure of Metals and Alloys, 3rd Edition, 1954.

45. W. Hume-Rothery, Atomic Theory for Students of Metallurgy, 3rd Edition, 1960.

46. G.V. Raynor, Prog.Met.Phys., 1949, 1, 1.

47. H. Jones (i) Proc.Roy.Soc., 1934, A144, 225.
(ii) Proc.Phys.Soc., 1937, A49, 250.

48. A.B. Pippard, Phil.Trans.Roy.Soc., 1957, A250, 325

49. M.H. Cohen and V. Heine, Advances in Physics, 1958, 7, 395.

50. D. Schoenberg, Phil. Mag., 1960, 5, 105.

51. W. Hume-Rothery and D.J. Roaf, Phil.Mag., 1961, 6, 55.

52. T.B. Massalski and H.W. King, Acta Metallurgica, 1960, 8, 677, 684.

53. H.W. King and T.B. Massalski, Phil.Mag., 1961, 6, 669.

54. J. Goodenough, Phys.Rev., 1953, 89, 282.

LIST OF FIGURES

		PAGE
Fig.1.	Hansen, 1958.	2
Fig.2.	Ölander, 1932.	6
Fig.3.	Owen et.al. 1940, 1941.	6
Fig.4.	Bystrom and Almin, 1947.	9
Fig.5.	The Au-Cd β'-phase below 100°C.	9
Fig.6.	Thermal analysis crucible assembly.	16
Fig.7.	Examples of cooling and heating curves.	18
Fig.8.	Section of the modified Unicam high-temperature camera	23
Fig.9.	Temperature control unit of the Unicam camera.	25
Fig.10.	Thermocouple circuit.	27
Fig.11.	High-temperature camera calibration curve.	29
Fig.12.	The gold-cadmium system. Results of present work.	35
Fig.13.	Results of present work in range 33-47 atomic % cadmium.	39
Fig.14.	Results of present work in range 22-34 atomic % cadmium.	67
Fig.15.	The α_1-region, Hirabayashi and Ogawa, 1961.	74
Fig.16.	Unit cell of Au_3Cd (Hirabayashi and Ogawa).	77
Fig.17.	The liquidus in some binary systems of Ag and Au.	83
Fig.18.	The α-liquidus in binary Au-systems with solutes from Groups IIB to VB.	85
Fig.19.	The α-liquidus in Au-systems with divalent solutes.	85
Fig.20.	X-ray films of the α_2-phase.	94
Fig.21.	Free energy relationships.	99
	(i) Gold-cadmium.	
	(ii) Gold-zinc.	
Fig.22.	Suggested N(E) curve for primary solid solutions in gold.	113
Fig.23.	Typical lattice spacing variations of the ζ-phase in gold systems. Massalski and King, 1960.	116

LIST OF PLATES. (pages 46-50)

PLATE 1. 54.22 at.% Cd. Cooling curve ingot. Widmanstatten precipitation of γ -phase in β' matrix. Electropolish. X 100.

2. 39.14 at.% Cd. Cooling curve ingot. α_2 + eutectic. Mechanical polish. Etch in aqua regia. X 385.

3. 41.79 at.% Cd. Cooling curve ingot. α_2 + eutectic. Mechanical polish. Etch in aqua regia. X 200.

4. As 3. Electropolish. X 2500.

5. 30.64 at.% Cd. Solidus specimen, annealed at 676 $\pm$ 1°C. Traces of liquid at boundaries of f.c.c. α matrix. Heavy twinning. X 100.

6. 32.14 at.% Cd. Annealed seven weeks at 240°C. α_2-phase, possibly with traces of β'. Cavities in α_2 due to segregation. Electropolish.

7. 45.97 at.% Cd. Annealed eight months at 150°C. β' matrix with traces of α_2 at grain boundaries. Fine structure in grains. X 1100.

8. 47.71 at.% Cd. Annealed eight months at 150°C. β' -phase with markings due to b.c.c. $\longrightarrow$ orthorhombic. transformation on quenching. Electropolish. X 550.

9. 35.67 at.% Cd. Annealed eight months at 150°C. Mainly α_2 with islands of β'. No etch. Mechanical polish. X 1100.

10. As 9. Annealed seven weeks at 240°C. α_2 with a little β'. Fine structure in grains. Electropolish. X 550.

LIST OF TABLES

		PAGE
1.	Thermal Analysis Results.	33-4
2.	Microscopical Results With Cooling Curve Ingots.	41
3.	The α-Solidus.	45
4.	The $(\alpha_2 + \beta')\beta'$ Boundary.	53
5.	The α_2 $(\alpha_2 + \beta')$ Boundary.	62
6.	High-Temperature X-Ray Results For The α Boundaries.	69
7.	X-Ray Reflections In α_2 Alloys.	71
8.	Δ x Values, Size Factors And Lattice Distortions In Some Gold Systems.	86

APPENDIX TABLES, pages 123-125.

ACKNOWLEDGMENTS

The author must record his gratitude to Professor W. Hume-Rothery, O.B.E., F.R.S., for patient supervision and great help throughout the course of the work.

Thanks are due to Dr. A. Hellawell for generous helpfulness, without which the work would never have reached its present form.

Dr. J.W. Christian must be thanked for several valuable discussions. Messrs. J.C. Chaston and F.M. Lever of Johnson Matthey Ltd., must also be thanked for their care and attention in dealing with the problems arising from the chemical analysis of the alloys.

The main part of the work was carried out during the tenure of a Research Studentship from the Department of Scientific and Industrial Research and was completed at the Fulmer Research Institute. The author is indebted to the Institute staff for much help in the preparation of the thesis.